8-2015

A Study of DAS delays and their Impact on the Wireless Channels with Application to Indoor Localization

Ahmed Sallam Mohamed Ibrahim
asi5989@rit.edu

A Study of DAS delays and their Impact on the Wireless Channels with Application to Indoor Localization

by

Ahmed Sallam Mohamed Ibrahim

A Thesis Submitted in Partial Fulfillment of the Requirements for the Degree of Master of Science in Electrical Engineering

Supervised by

Dr. Muhieddin Amer
Department of Electrical Engineering
Kate Gleason College of Engineering
Rochester Institute of Technology
Dubai, UAE

August 2015

Approved by:

Dr. Muhieddin Amer
Primary Advisor – R.I.T. Dept. of Electrical Engineering

Dr. Ali Raza
Secondary Advisor – R.I.T. Dept. of Electrical Engineering

Dr. Boutheina Tlili
Secondary Advisor – R.I.T. Dept. of Electrical Engineering

Acknowledgements

I would like to express my deepest gratitude to Dr. Muhieddin Amer and the committee. This work would not have been completed without their continuous support. A special thanks to TE-Connectivity and Consultix for enabling the measurement setup and access to simulation software.

Abstract

This research evaluates the Distributed Antenna Systems (DAS) introduced delays and their effects on the indoor channel in simulcast situations where the effect of delays is most prevalent. Different simulcast cases that form the basic building blocks are analyzed to form an understanding of the problem. Two case studies of important indoor environments are presented. Importance of improving ray tracing simulations to include propagation and DAS delays is highlighted.

The paper also introduces a DAS element representation and delay mapping model and explores techniques of engineering DAS delays to optimize location estimation by ranging and RF fingerprinting to achieve E911 mandated accuracy.

A brief description is introduced for a Software Defined Radio (SDR) implementation of a Correlation Channel Sounder and the possible application of channel sounding for indoor DAS. The paper suggests procedures to produce a full DAS delay profile and ways to optimize it for location estimation.

Table of Contents

List of Figures

List of Tables

Glossary

BER	Bit Error Rate
BTS	Base Transceiver System
CDMA	Code Division Multiple Access
CIR	Channel Impulse Response.
CPICH	Common Pilot Channel
DAS	Distributed Antenna System.
DDDAS	Distributed Delay DAS.
EIRP	Effective Isotropic Radiation Power
GSM	Global System of Mobile communications.
PDP	Power Delay Profile.
RBS	Radio Base Station
STDCC	Swept Time Delayed Cross-Correlation channel sounder
TOA	Time of Arrival.
WCDMA	Wideband Code Division Multiple Access.

Chapter 1 Introduction

1.1. Motivation

Being in the wireless industry for the last 9 years I have observed a need for a test equipment and design tools that predict and estimate the final performance of a deployed Distributed Antenna System (DAS) site. With Data technologies advancing from GPRS, EDGE, HSPA and LTE, the demand to predict final throughput was deemed critical from there being no way to address this demand without full deployment of the project. My initial hypothesis about such tool was a high resolution channel sounder to collect Path Loss values and indoor multipath information. A considerable amount of time was spent building a Software Defined Radio (SDR) channel sounder to prove the concept. Channel sounder researches and literature were surveyed in a quest for this ultimate indoor design verification tool. I noted that a very important part of the indoor channel was overlooked in these researches, the effect of the DAS design on the channel. The characterization of indoor channel was basically based on simple case of one transmitter. For the Distributed Antenna Systems, as the name suggests, the transmit antenna is actually a modified distributed version of standard antenna. The delays introduced by this distributed nature is much higher than the indoor multipath case for the intended coverage area. Although these delays are a direct result of the DAS design, delays are not considered in the DAS design process.

Based on these findings I decided to direct my effort to the understanding of the delay attributes of DAS systems on indoor wireless channels and possible applications for indoor localization and positioning.

1.2. Thesis Overview

In this thesis, our aim is to study the Delays introduced by different Distributed Antenna Systems types on an indoor channel. Our aim is to understand the sources of these delays and how to adjust them to improve indoor cellular coverage and possibly improve the indoor RF designs for location estimation.

Chapter 2 gives a background of DAS types and definitions, both active and passive DAS.

Chapter 3 evaluates sources of delays in DAS, analysis on the effects of absolute and relative delay for simulcast situations compared to indoor reflections, describes a general DAS model and delay mapping concept. Basic cases of simulcast transmission are analyzed and case studies are presented for important propagation environments

Chapter 4 examines practical delay adjustment techniques and introduces a design concept to optimize location finding. Fingerprinting for indoor positioning is briefly described in this chapter.

Chapter 5 sheds light on the Channel Sounding applications for DAS and introduces a testing procedure for optimizing DAS delays

Chapter 6 concludes with a list of possible future research related to indoor DAS delay adjustments.

Chapter 2 Overview of DAS systems

2.1. Introduction

Passive and active Distributed Antenna Systems (DAS) have been in the mobile industry for the past three decades as a means of delivering quality mobile services and public safety communications for indoor subscribers. The need for DAS has increased over the last decade with the introduction of new cellular standards and the exponentially increasing data demand. Often, the indoor channel characterization concentrates on the case of single transmitting antenna. In this paper, we will study DAS systems with emphasis on their delays specially in simulcasting deployment where multiple antennas transmit the same signal to the indoor environment. The available studies of the DAS introduced delays and their effects on the indoor channel properties are not sufficient. This paper examines also the effect of delays on the fading characteristics of the channel for different delay profiles.

DAS can be classified into two major categories: Passive DAS and Active DAS. A Passive DAS system utilizes a dedicated indoor Base Transceiver Station (BTS) to distribute its signal to multiple indoor antennas using a passive distributing network. The passive network is formed of Coaxial cables, equal and non-equal power splitters. On the other hand an active DAS system distributes the signal through amplification of the signal electronically on the Forward and Reverse path, utilizing optical fiber, network cables, and other types of low-loss physical media to deliver better signal with the target of achieving better quality of service. A combination of active and passive DAS is often referred to as Hybrid DAS.

An active DAS will solve mainly three coverage problems that legacy macro cellular, dedicated indoor BTS and Femto-cells cannot solve. An Indoor site with a low number of subscribers but with a wide coverage area requires more power than a typical dedicated BTS can provide is one example. A second example is to the other extreme; a high number of subscribers in a relatively small coverage area with limited space to host the required equipment for such high concentration. Finally some Active DAS equipment comes as a solution for a third problem where quick and easy deployment is required due to physical limitations and aesthetic considerations. DAS technology is becoming more

advanced every day promising better quality signal delivery for traffic hungry user equipment's (UE).

2.2. DAS Types and Architecture

The detailed comparison and classification of DAS equipment is outside the scope of this thesis. However, an overview of the commonly used transport media and topology will help us understand the sources of signal propagation delays.

2.2.1 Passive DAS

Passive DAS refer to the use of coaxial cables, power splitters and antenna to distribute the signal from the BTS, NodeB or eNodeB (hereafter referred to as Signal Source) in an indoor location to the antenna to deliver a signal to the subscribers. Passive, as opposed to Active, does not utilize any kind of electronic signal amplification at any

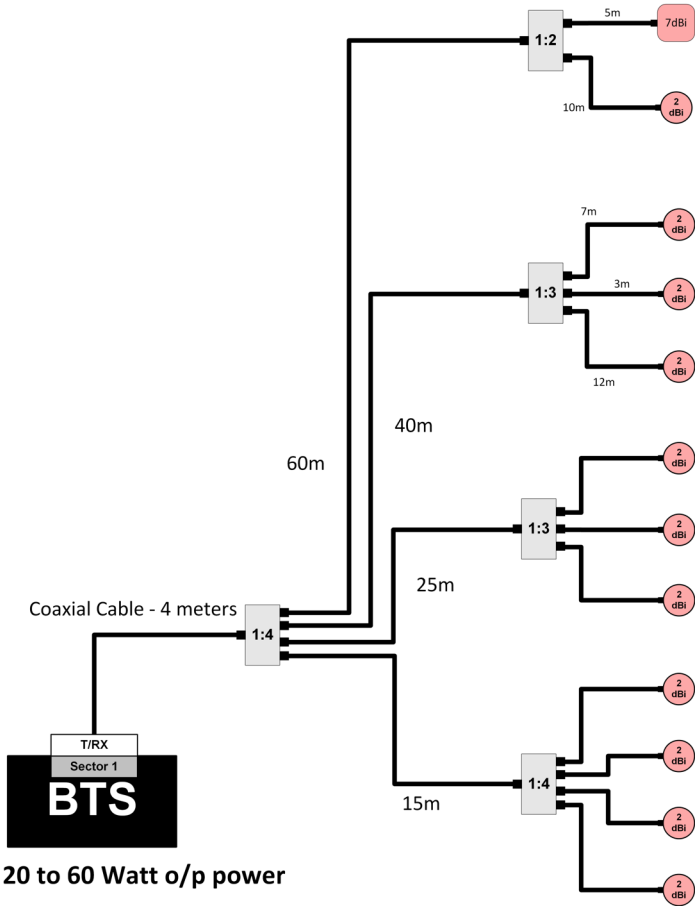

Figure 2-1 Sample Passive DAS Schematic representation

stage after the original signal source. The available power to distribute is limited to the signal source power Figure 2-1.

A Passive DAS design is characterized by high cable losses, is difficult to balance to provide the same output EIRP from each antenna, has a limited area span from the BTS room depending on the BTS power, and lower SNR on the uplink (reverse) path due to the initial attenuation of signal from mobile to the receiver amplifier.

2.2.2 Active DAS

An Active DAS system, on the other hand, solves the problem of limited available power at the signal source that is distributed to many indoor antennas. An active system distributes and amplifies the signal through several amplifiers, each feeding a group of antennas. In uplink, or reverse path, active DAS amplifiers pick up the signal as close as possible to the UE. Having the first amplifier stage closer to the user equipment enhances the Signal-to-Noise ratio (SNR) significantly. The main advantage of Active DAS is the use of a low intermediate frequency on different transportation media, (fiber, twisted pair or thin coaxial) to achieve lower losses than the RF signal on coaxial cables, thus carrying the signal longer distances and across wider coverage areas. The Active DAS then converts the signal back to the original RF Frequency.

There are various topologies and architectures for active DAS equipment in the market. Figure 2-2 shows a general representation of an Active DAS, mainly influenced by both the transportation medium and amplifier power. The main components are Head-end

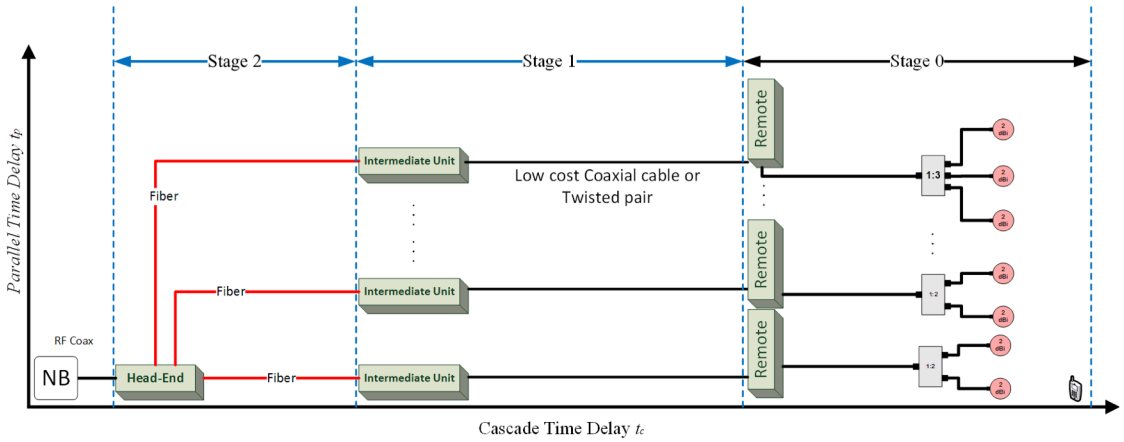

Figure 2-2 General 2-Stage DAS schematics

and Remote-end units. Some architectures have an additional unit between the front end and the head-end. Specific naming of these units depends on the manufacturer or vendor. Active equipment units are sometimes referred to as Main unit and Remote unit. Transport medium can be optical fiber, twisted pair or thin coaxial cables. With all active equipment sharing the same concept of distributing RF signal from a single point to multiple antenna, the topology depends mainly on the transport medium. For example, a product using twisted pair cables to transmit the signal and DC power to a remote amplifier has a low amplifier power, typically less than 1 watt. This type of amplifier in typical indoor deployment requires using several remote units in the same floor to achieve the required coverage levels. With power amplifiers below 1 watt feeding antennas, several amplifiers will transmit the same signal on the same floor with overlapping coverage areas. These overlapping coverage areas will receive a signal from different antennas with different arrival times. Such overlapping coverage areas can exceed 30% of a given floor layout.

2.2.2.1 Digital and Analog Active DAS

A Digital DAS system digitizes the signal source at very high speed through Analog to Digital Converters (ADCs) before transporting it to the remote-end. At the remote-End equipment, the signal is converted back to its original analog form using Digital to Analog converters (DACs) and then amplified to the rated amplifier power.

The use of data converters and digital transport technology minimizes the effect of loss and noise in transport medium thus achieving better signal quality in both the forward and reverse path. Additionally, the digital DAS system can digitally control the delay to each individual remote-end amplifier for multiple remote deployments.

On the other hand, active Analog DAS applies several amplifier stages with up and down converters to lower the signal to IF frequency on the transport cables. Any introduced noise on the system at any stage has a direct impact on the system output in both forward and reverse paths. Analog systems in the market do not have the ability to alter the delays to different remotes. The practical way to control delay is spooling extra cables to increase any required delay

2.2.3 Hybrid DAS

It is a common practice in DAS industry to identify an Hybrid DAS as an Active system utilizing high power amplifiers since Hybrid DAS has enough power to drive a large network of passive splitters and coaxial cables similar to the Passive DAS. While this definition is common, we observe that a hybrid system is better defined as the system where a passive distributing network is employed to deliver power RF power to one or more antennas in parallel to an active DAS of any Power rating. The Characteristics of delays of a Hybrid System defined in this way exhibits a specific pattern dissimilar to the common definition.

2.2.4 DAS RF Power

Typical values of head-end RF power range from 0.5 watt to 40 watts. For Middle East indoor DAS designs, an average EIRP varies between 5 to 10 dBm per channel due to the heavy use of concrete Middle Eastern building structures. For such environment, a low and medium power DAS equipment is connected to maximum of 1 to 5 antennas while a higher power remote-end can support up to 20 antennas depending on the design of the passive RF distribution network.

2.3. Simulcasting Concept

Simulcast in DAS refers to utilization of two or more head-end units to transmit the same signal from the same signal source. This concept is used to extend the coverage map of the cellular sector in areas where more coverage is required without adding more capacity to the system.

In simulcast configurations, the signals arrive at the receiver in an overlapping coverage area with relative power intensities but different delays. For public safety communications, design guidelines and delay limitations are well defined to provide a certain voice quality in indoor environments [15]. Clear guidelines for DAS design in relation to mobile communication standards are yet to be established. The lack of these guidelines can be attributed to the advanced equalization techniques in these standards that took care of the typical degradation so far. However, it is important to study the case of

DAS simulcasting in details to better understand the channel characteristic to optimize DAS designs and channel equalizers.

Chapter 3 DAS Delays

3.1. Sources of Delays in DAS Systems

To analyze the effect of DAS delays on the wireless channel, we first identify two different ways to measure the delay: Absolute delay and relative delay. The absolute delay is the time needed for the signal to travel through all the system components from the signal source to the UE taking the DAS RBS RF port as the reference of measurement. The relative delay on the other hand is the time of arrival relative to the first version of the signal.

3.1.1 Cable and filter Delays

Electromagnetic waves propagate in different mediums with different velocities. The velocity of Electromagnetic waves in fiber, copper and coaxial cables (non-magnetic mediums) depends on the dielectric constant ϵ or refractive index n of the cable. For Coaxial cables, *propagation velocity* is given by [17]

$$Vp = \frac{c}{\sqrt{\epsilon}} \tag{3.1}$$

where c is the speed of light in vacuum. Cable manufacturers quote the Velocity Factor VF for cables relative to c instead and is defined as the percentage of the velocity of electromagnetic signals in the cable to the velocity of light in vacuum. Hence VF in Coax is given by

$$VF = \frac{100}{\sqrt{\epsilon}} \tag{3.2}$$

For Optical fiber cables, the refractive index n is, by definition, the ratio of the speed of light in vacuum to the speed of light in the optical cable. Hence Velocity factor in fiber is given by

$$VF = \frac{100}{n} \tag{3.3}$$

Splitter and filter delays are assumed to be very small compared to cable delays and do not contribute to the relative delays.

Cable Property	Type of Cable			
	Braided Coax (RG-58A/U)	Foam Coax LDF4-50A	Optical Fiber	Twisted Pair CAT5E
Velocity Factor[a] (%)	66	88	67	74
velocity (m/s)	197863022	263817363	200860946	221846418
Propagati on Delay (ns/m)	5.054	3.791	4.979	4.508

[a.] Reference to speed of light in vacuum of 299,792,458 m/s

Table 3-1 Propagation Delay for Common DAS cables

Figure 3-1 presents the propagation delay values for common cables used for DAS. A typical value of 5ns/m for fiber and 3.8ns/m for common Coaxial cable (LDF4-50A) are used. To put this delay value in perspective, the chip duration for WCDMA is 260.4ns; hence a generic ½" coaxial cable of 68m introduces a propagation delay equivalent to one chip in WCDMA as exhibited in Figure 3-1

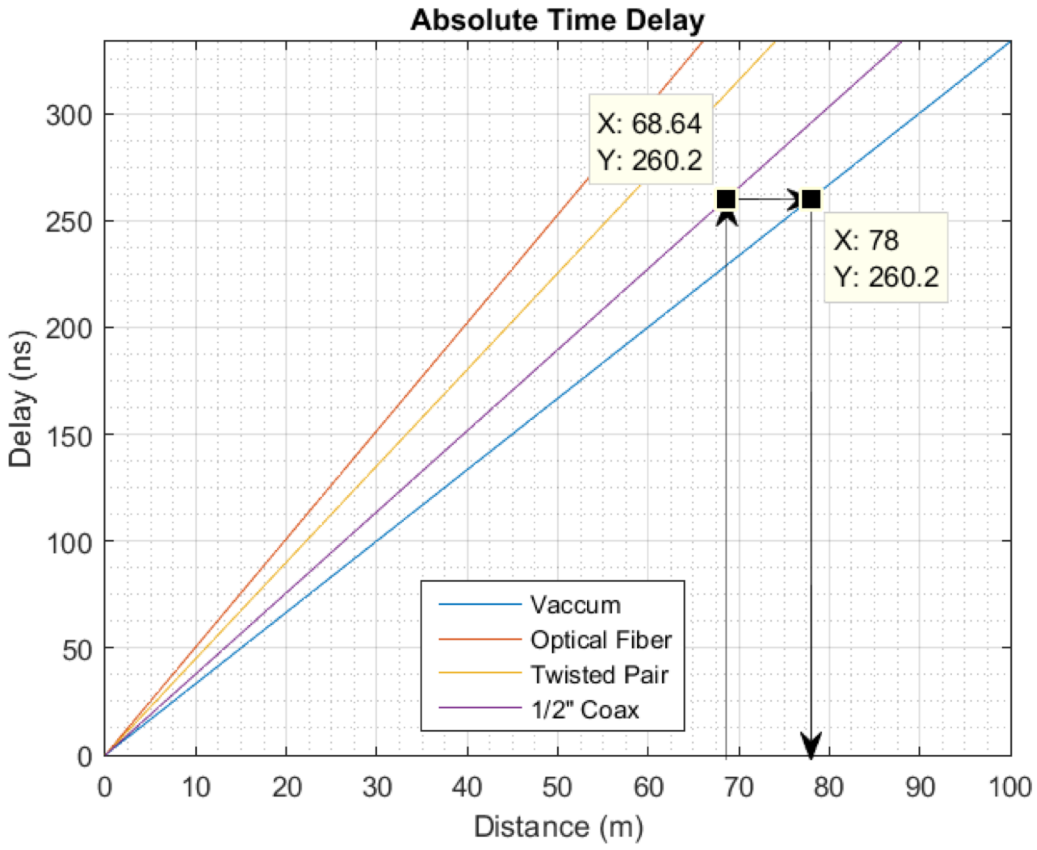

Figure 3-1 Propagation Delays for Typical DAS cables

3.1.2 Hardware Delays

Delays due to the electronic circuitry of active DAS are here referred to as Hardware delay. These delays are always constant for an individual active DAS product. It is very rare that two types of active products are used in the same indoor site to cover the same location, although it can be used in the instance of upgraded sites. Assuming single product usage, HW delays are consistent for all devices and add to the absolute delay. However, relative delays are only triggered by differences in cable lengths. Quoted value for the hardware delays for an Analog DAS product is less than 500ns and 12µs for the Digital DAS product [29] [31].

3.1.3 Generalized DAS model

To build a better understanding of the DAS delay and its effects we build a general DAS model that can represent all DAS types and products. The DAS can be divided into cascaded Stages numbered beginning from the antenna side and rising to the RBS. Stage-0 is an RF stage and is the basic stage for all active and passive DAS types. However, it can be as small as one antenna or as large as a full distribution network of splitters and jumpers, depending on the available RF power from the amplifier and the design

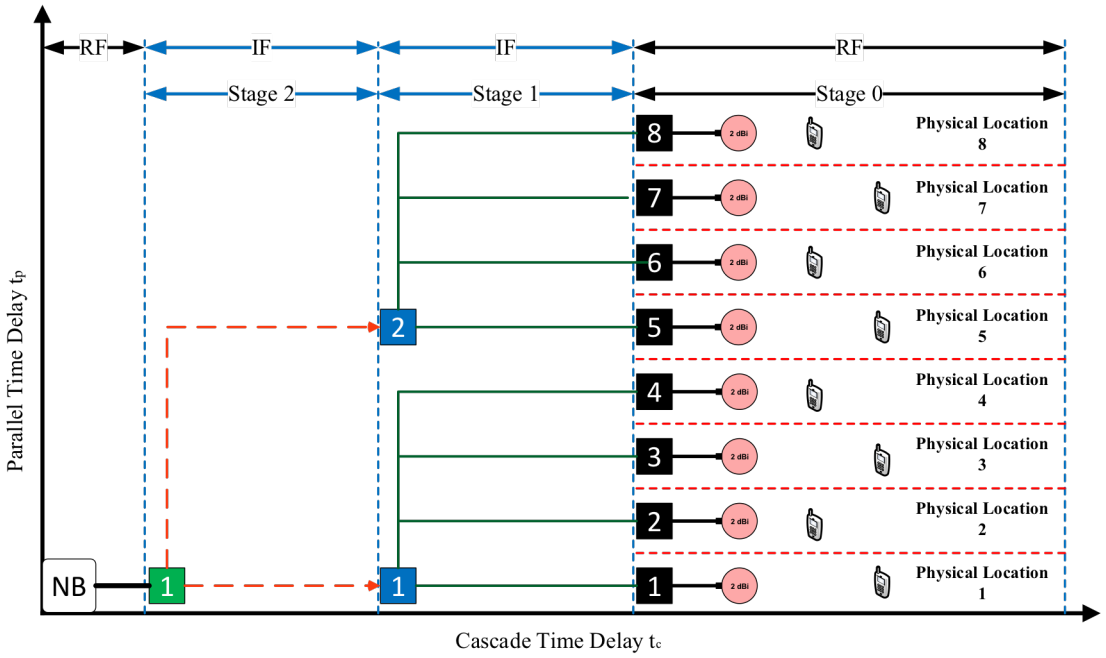

Figure 3-2 Generalized DAS model and propagation delay map

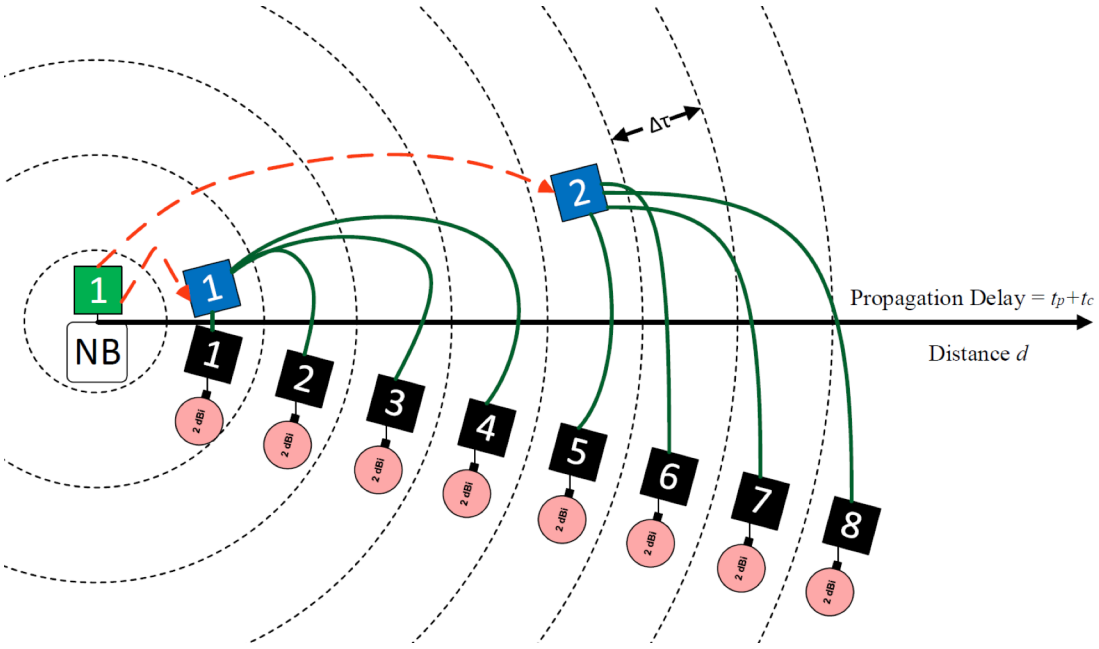

Figure 3-3 Radial Delay Map

requirements. A purely passive DAS will only have Stage-0. An Active DAS of a single star connection topology will have both Stages-0 and Stage-1. A double star topology will have Stage-0, Stage-1 and Stage-2 and so on for Cascaded DAS systems. Figure 3-2 depicts the general DAS model mapped on a Delay Map where no two equipment have the same absolute delay. Each box indicates an active equipment device. The boxes are marked with numbers labeling the corresponding device. The two axes have time dimensions and the absolute delay is the sum of the cascade delay component τ_c and parallel delay component τ_p .where cascaded and parallel subscripts refer to hypothetical direction of delay measurement.

3.1.4 Delay Mapping Concept

It is the industry standard to have Power budget and Antenna EIRP reports as the main design deliverables along with the indoor floor layouts. Recently, DAS software tools introduced specific reports to help deployment teams in their work by providing details on antenna orientation, cable routing and cross references. A very important yet missing concept in these deliverables is the calculation of delays from source to antennas and a mapping to their physical locations. The simplest form of such map can be a table with calculations and physical installation location. A more detailed representation can be as

presented in Figure 3-2 and Figure 3-3. The importance of a delay map will be clear in the discussions of indoor positioning information available from DAS. A single glance to a delay map should be sufficient to identify the possible locations and causes of ambiguity in indoor Time of Arrival (TOA) ranging. Such delay map should be added to the site database, planned at design and verified at commissioning stage.

3.1.5 Wall Penetration Delay

Penetration of walls on the path of the signal will introduce a delay equivalent to the time of propagation in material of a certain relative permittivity. The maximum penetration path is determined by Snail's law to avoid total internal reflection inside the wall. Table 3-2 shows the maximum delay for the wall material for a given thickness. Maximum penetration path accounts for the real path at the critical angle inside the wall.

	Stone Brick	Concrete	Wood	Glass	Fiberglass
Rel. Permittivity	4	6	1.8	6.7	5.2
Material Thickness (m)	0.15	0.2	0.1	0.01	0.01
Velocity factor	50.00	40.82	74.54	38.63	43.85
Propagation Delay (s/m)	6.67E-09	8.17E-09	4.48E-09	8.63E-09	7.61E-09
Critical angle (rad)	0.2527	0.1674	0.5890	0.1498	0.1935
Maximum Penetration Path (m)	0.1549	0.2028	0.1203	0.0101	0.0102
Maximum Penetration delay (ns)	1.034	1.657	0.538	0.087	0.078

Table 3-2 Estimated Wall Penetration Delays for simulation Materials

3.2. Effect of absolute delay introduced by DAS

The absolute delay of Active DAS system will be seen by the source as an offset to cell radius. The distance at which the UE is located away from the source is increased by an offset equivalent to the same delay in a vacuum. Figure 3-1 can be used to estimate the effective location of the UE as seen by the source. Depending on the specific technology, the signal source with feedback from the UE estimates the distance based on the propagation delay by assuming propagation in a vacuum (or any predefined propagation model). Methods like Time of Arrival (TOA) and round trip time (RTT) are used for ranging. A hybrid DAS signal source will see the subscribers' UEs as two groups. The first group is very close to the source communicating through passive DAS and a second distant group communicating through the active DAS with an offset in distance equivalent to the hardware and fiber delays. Figure 3-4 illustrates this effect where d_0 corresponds to maximum delay in passive DAS. d_1 equivalent to minimum active hardware and cable delays, d_2 is the distance of the farthest UE. It is important to carefully study and consider relative delays for indoor sites with a mix of passive and active DAS to avoid possible

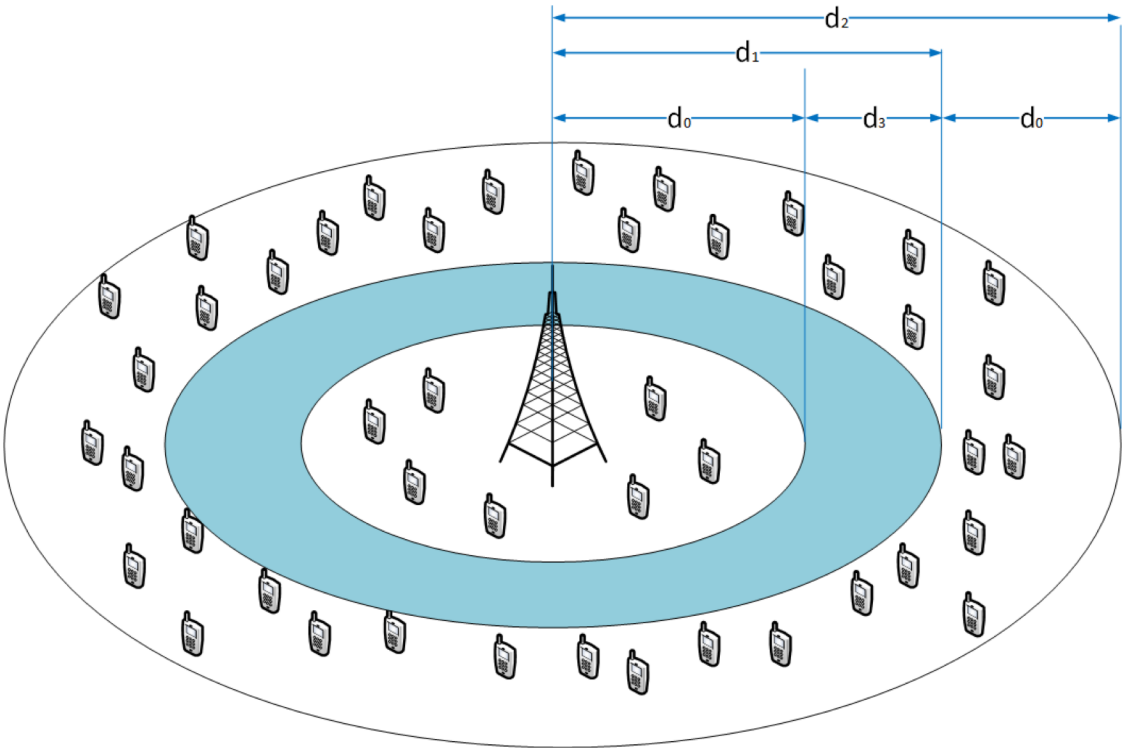

Figure 3-4 Effect of Absolute Delay on Subscribers' location for a Hybrid DAS

channel degradation and interference due to the relatively high hardware delays in overlapping coverage area.

3.2.1 Accumulated Propagation Delay

The accumulated propagation delay for a given antenna n is the summation of all delays accumulated over the signal path to this antenna according to the DAS model in Figure 3-2 and is given by

$$\tau_n = \sum_{i=0}^{I} k_i + (l_i \cdot Pd_i) \tag{3.4}$$

where n is the antenna number, i is stage number and I is the total number of stages, k_i is the active equipment hardware delay, l_i is the cable segment length and Pd_i is its propagation delay per unit length of the cable.

3.2.2 Manipulating DAS delay

The ability to manipulate DAS delays without affecting the RF output power can become handy in many applications such as indoor positioning and localization as it will be further discussed in Chapter 4. This is achieved without affecting the RF output power of the system at the IF stages by adding extra cable lengths and spooling fiber. Active DAS will compensate additional cable losses in the IF stage within the limits of the product specification. The introduction of delays at RF stages will have a direct impact on RF coverage, design parameters and cost of the deployment. It is also impractical to spool Coaxial cables compared to Fiber or thin coaxial cables of the IF stages. As will be discussed in section 4.1, Active DAS with low power amplifier is more suitable for the indoor positioning applications due to flexible to higher flexibility in defining the delay to individual antenna with smaller coverage areas. A Low power amplifier will have limited RF coverage and hence a limited area corresponding to each amplifier. Digital DAS have the ability to change the delay to each active unit individually without the need to add extra cables.

3.3. Effect of relative delays introduced by DAS on Channel Impulse Response

For the selected case studies and antenna deployments, the effect of indoor multipath can cause a negligible delay in the range of several nano seconds as in corridors to larger delays but with high reflection and propagation losses that minimize their effect on the channel characteristics. Thus it's safe to exclude these components from the study of power delay profile caused by the DAS. On the other hand, the relative delays caused by DAS can range from 80~300 with comparable power levels at significant percentage of indoor coverage area. To further justify this assumption, simulations of the first level of reflections using one transmitting antenna was conducted in the corridor and Open-Office room of Figure 3-5. Wall and ground reflection losses are assumed to be 6.5dB. The transmitting and receiving antennas are placed at coordinates (x_T,y_T,h_T) and (x_R,y_R,h_R). Image concept was used to calculate the length of the reflection path as in Figure 3-6. The number of images is 5 including the ground bounce for a rectangle room. For the corridor case it is assumed to be very long that only reflections from sidewalls and ground are present. The assumed corridor length is 30m and 3 m width. Antenna is placed 3m away from the start of the test path at $(x,y,z)= (3,1.5,2.5)$. The receiver is moved in 2m steps slightly off the center of corridor on the path ($x=1$). The frequency response of the channel along the test path at 1m steps is shown in Figure 3-7. Figure 3-8 and Figure 3-9 show the detailed frequency response with the PDP at the corresponding points. All power levels are relative to the strongest direct path. Simulation covered the frequencies from 800MHz to 2170MHz.

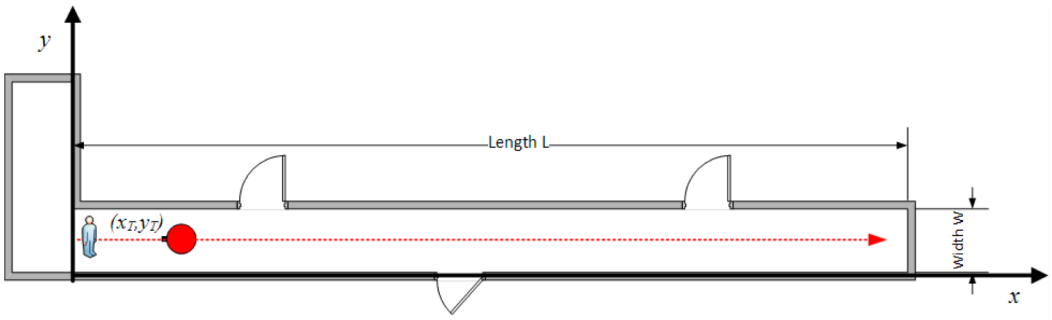

Figure 3-5 Test Cases of typical corridor

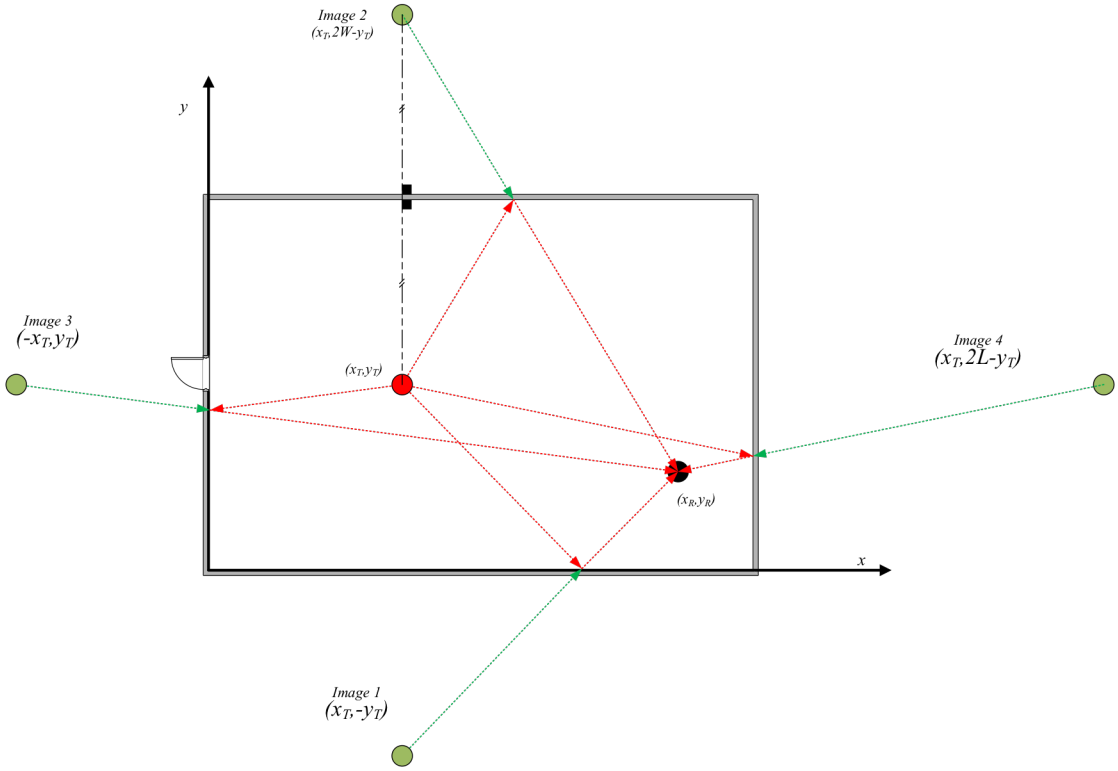

Figure 3-6 Images concept

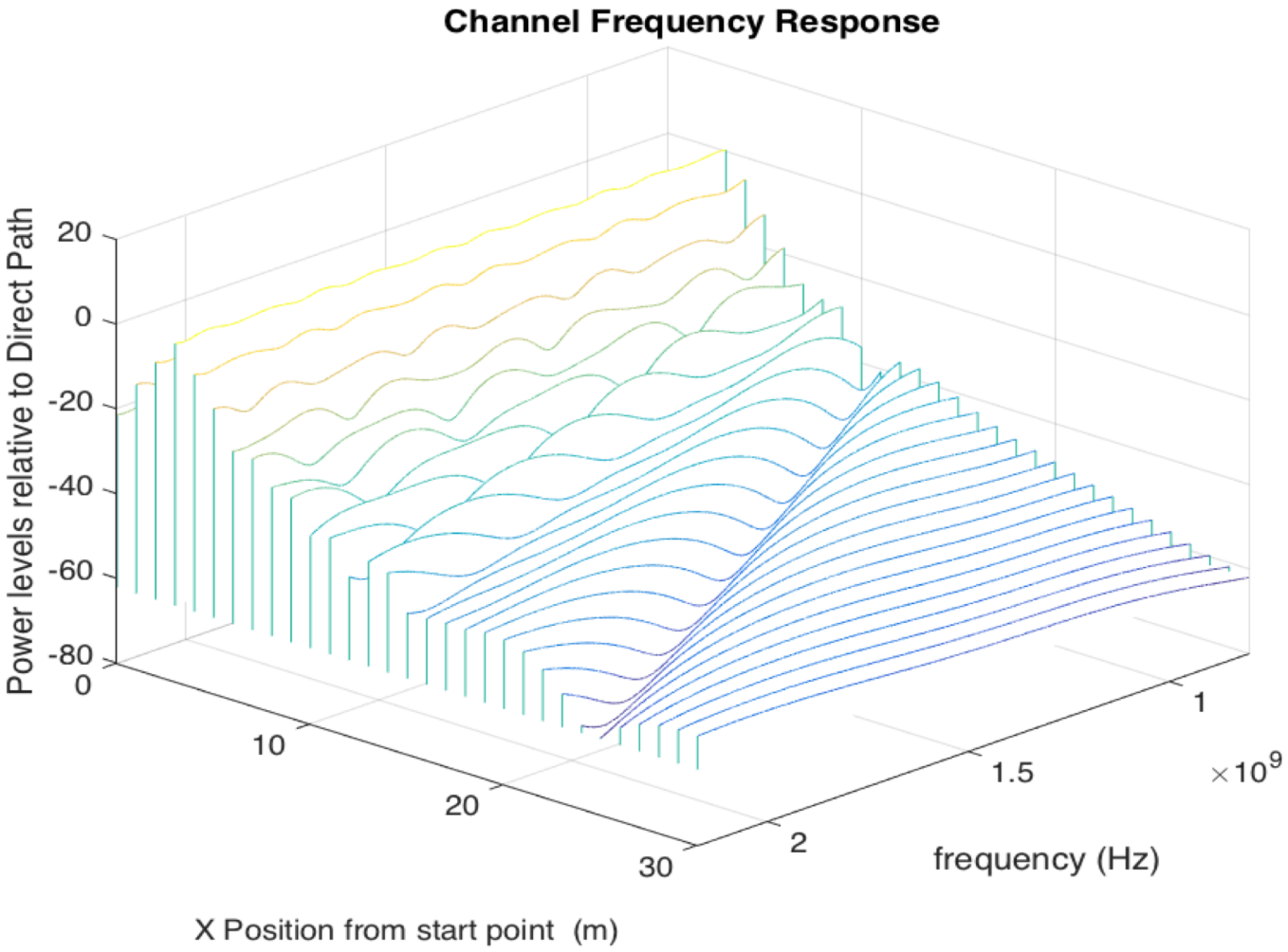

Figure 3-7 Simulated Frequency Response at different points along a corridor

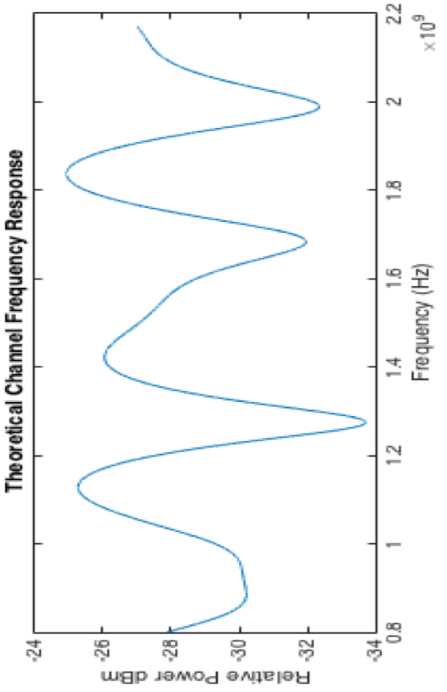

Figure 3-8 theoretical PDP and Frequency response at x=8

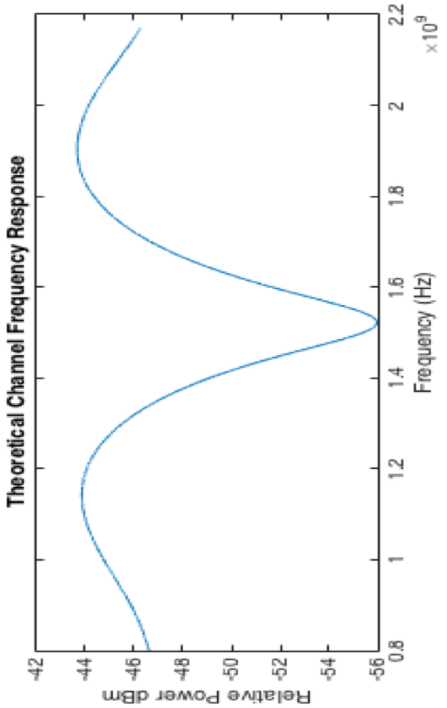

Figure 3-9 theoretical PDP and Frequency response at x=18

Comparing the result of single antenna with reflections taken into account against another two cases where two antennas are placed symmetrically across the corridor at *x=3* and *x=37m.* A relative delay of transmission from the antenna equivalent to a cable of 40m length is assumed. We can safely conclude that we can neglect the reflection components in channel merits related to delays in the presence of a DAS simulcast system. Figure 3-10 shows the RMS delay spread for the three different cases of the corridor example.

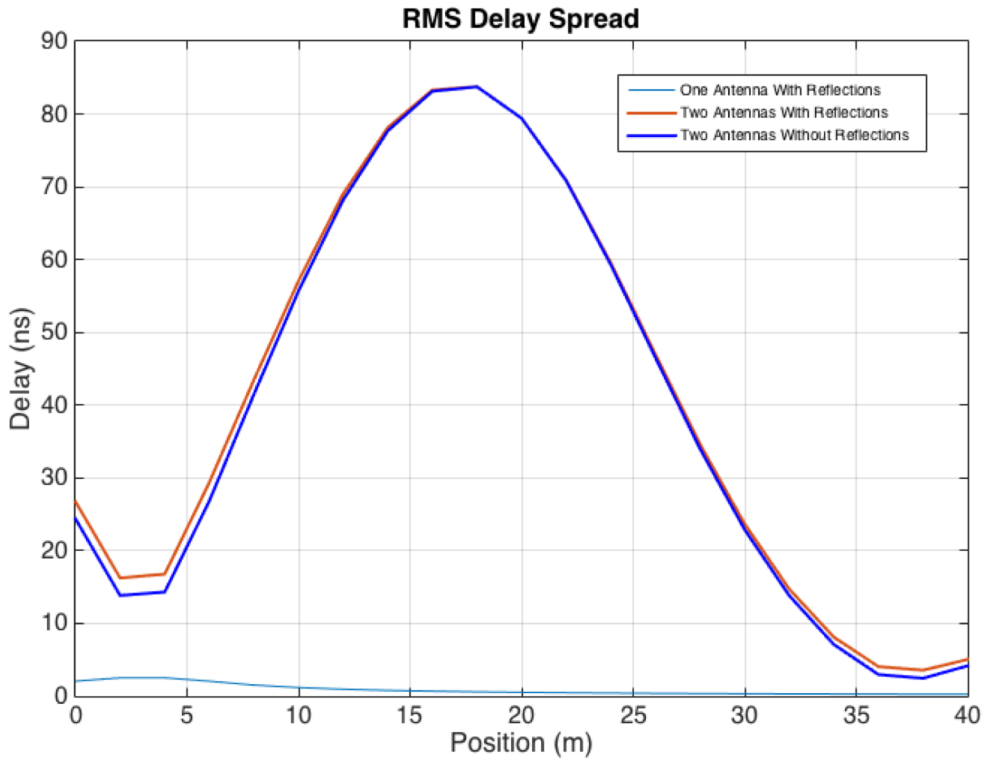

Figure 3-10 RMS Delay Spread for a Corridor for 3 different cases

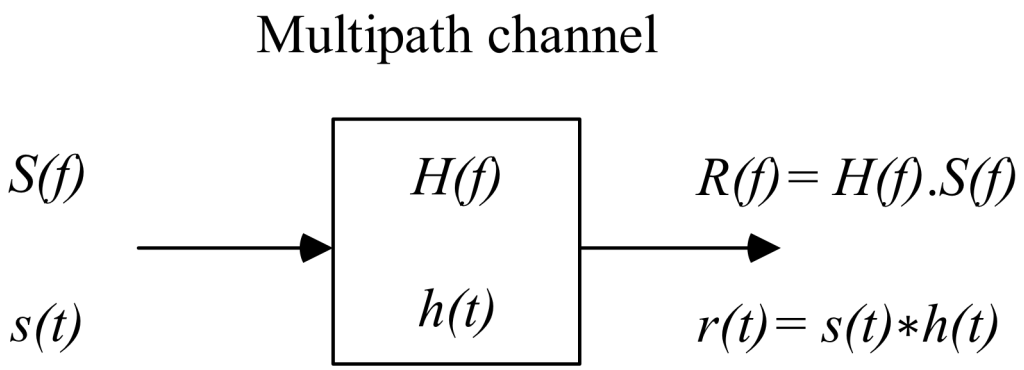

Figure 3-11 General Linear Channel Model

3.3.1 General formula for Simulcast DAS Channel delays

The simulcast channel model caused by DAS is identical to a multipath channel where delay between DAS antennas is the main cause of the multipath nature. Indoor locations receiving signals from more than one antenna can suffer from dispersive fading. This fading envelope can change the channel classification from wideband to narrow band, in addition to the introduction of inter-symbol interference caused by path delays.

The general formula governing multipath linear channel *h(t)* is given by corresponding to Figure 3-11 [7].

$$h(t) = \sum_{m=0}^{M-1} \alpha_m \delta(t - \tau_m) \tag{3.5}$$

$$H(f) = \sum_{m=0}^{M-1} \alpha_m e^{-j2\pi f \tau_m} \tag{3.6}$$

$$r(t) = \sum_{m=0}^{M-1} \alpha_m s(t - \tau_m) + v(t) \tag{3.7}$$

where

s(t) is the input signal,

H(f) and *h(t)* are the channel spectrum and impulse response, respectively

r(t) is the received multipath signal.

M is the number of multipath components,

$v(t)$ is a zero-mean white Gaussian noise random variable with power spectral density of No/2, and

τ_m is the m^{th} component delay.

We are interested in the study of the channel in simulcast scenarios discussed in the following section.

3.3.2 Simulcast deployment scenarios

3.3.2.1 Scenario I: Direct indoor with two antenna in an open area

A common deployment scenario in an indoor environment is where UEs are stationed in an open area and receive signals from two DAS antennas.. Such a case can apply to theaters, food courts and stadium seating where UEs are almost stationary. Corridors are another common situation with slowly moving UEs. The resultant channel is described by Fig.3 with frequency response equal to

$$H(f) = 1 + \alpha e^{-j2\pi f\tau} \tag{3.8}$$

Where τ is the relative delay between the two received signals and α is the relative amplitude of the delayed signal from the second antenna. For the worst case, this factor is assumed to be 1. Lower values of α will have a scaling factor equal to $\frac{1+\alpha}{1-\alpha}$ on the peak-to-peak amplitude of the sinusoidal channel frequency response pattern as in Figure 3-13. The resultant channel is a frequency selective fading channel with nulls at

$$f = \frac{(2n+1)}{2\tau} \tag{3.9}$$

where n is an integer ≥ 0.

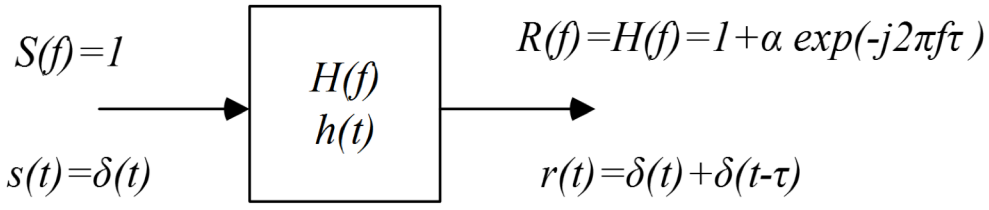

Figure 3-12 Channel Impulse Response of the two antenna case

A set of charts are produced to locate these nulls corresponding to certain cable length or delay τ (Appendix D). Figure 3-14 show an examples for 2110MHz band chart. Values of delay τ are limited to a certain range of interest for better appearance. The colored lines represent the location of nulls for different values of n. a vertical line intersects the colored lines at null locations. Sliding this line to the right or left gradually changes the null locations and separation corresponding to a moving receiver around the initial point.

Emulation of this channel in the lab for various cable lengths was conducted using the setup in Appendix E . A wideband pseudo-random sequence generator is used to excite the channel and a spectrum analyzer is used as a receiver. The testing results in Figure 3-15 Figure 3-14 confirm that the location of frequency fading nulls are consistent with the charts. The ratio of peeks to nulls were found to exceed 25dB with the spectrum analyzer set to RMS detector mode.

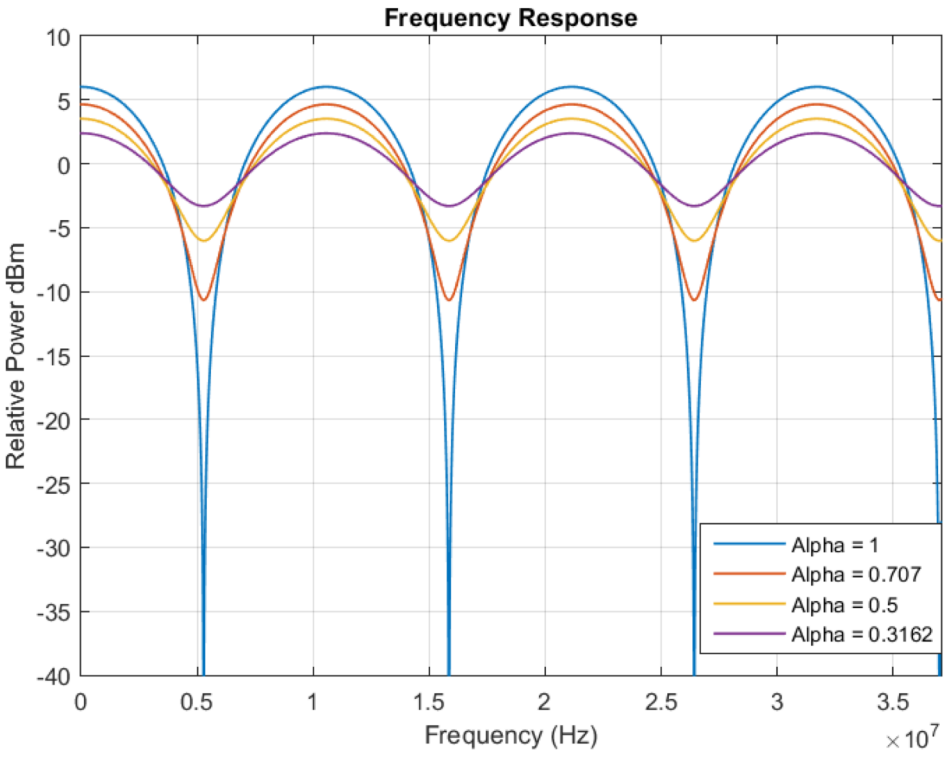

Figure 3-13 frequency Response for different values of α

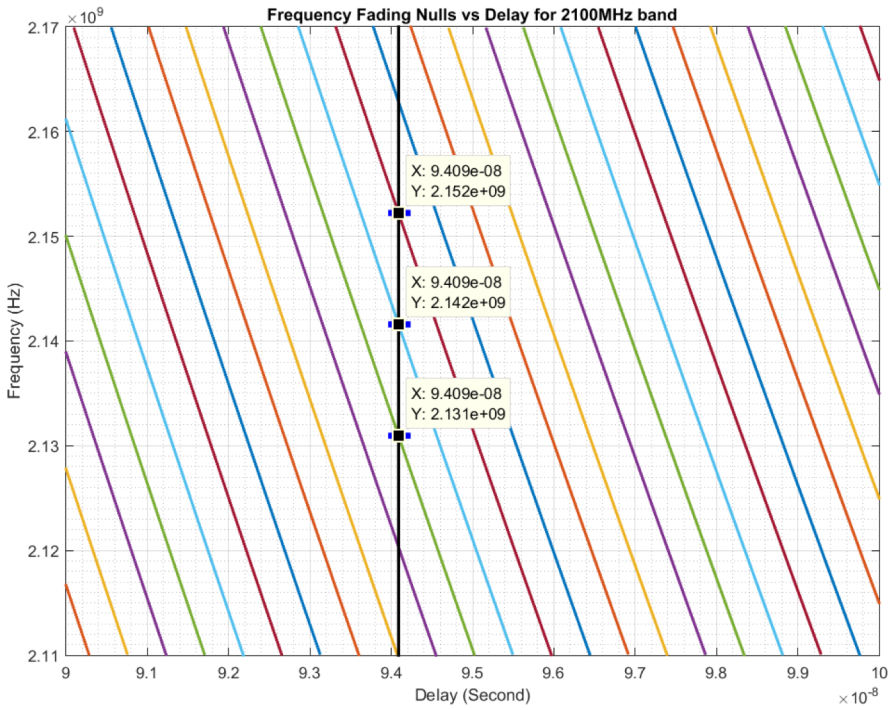

Figure 3-14 Dispersive Fading null chart for 2100MHz band (Zoomed)

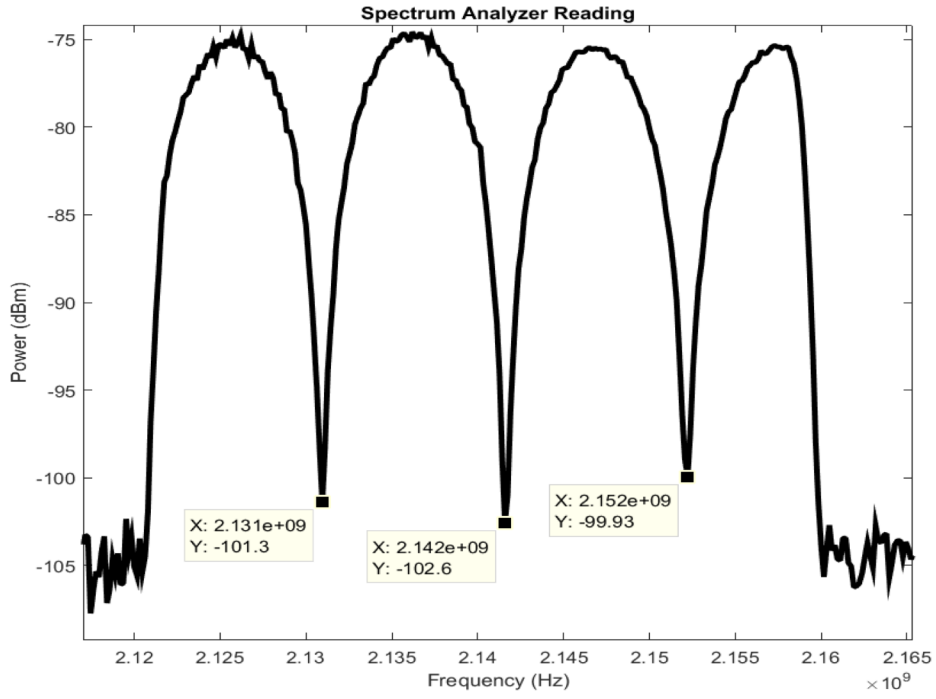

Figure 3-15 Measured Frequency response for a 2 antenna case.

3.3.2.2 Scenario II: Three Antenna in an Open Area

Another simulcast situation of interest is where the UE is in the coverage of three antennas. Typical examples of these environments include theaters and stadium seating. Mobile users are almost static in this case. So far, a widely accepted approach to cover high capacity stadium is to divide seating area into sectors of few thousand subscribers. To achieve high isolation between these sectors antennas are positioned on the edges of the sector radiating inwards (two on the sides and one at the back) to increase received signal levels and increase isolation relative to adjacent sectors. Effects of delays are not accounted for when designing for such situation. Similar to the two antenna case, the frequency response of this channel of three antennas is given by

$$H(f) = 1 + \alpha_1 e^{-j2\pi f\tau_1} + \alpha_2 e^{-j2\pi f\tau_2} \quad (3.10)$$

α_1 and α_2 equal 1 for the worst case where the 3 signals from the 3 different antennas are exactly equal in power. There are unlimited possibilities for the frequency responses for different combinations of α_1 , τ_1 , α_2 and τ_2 that can be accurately predicted by ray tracing simulations to obtain the frequency responses. Figure 3-17 exhibits that more than 60% of the area has a relative received power within 6dB which translates to α = 0.5 . For areas where one of the received signals rays is very weak (α is very small) presents the effects of a 2 antenna scenario. We can simplify the problem by considering a common *deployment* cases where $\tau_2 = \tau_1$ and $\tau_2 = 2\,\tau_1$ as shown in Figure 3-16.

The channel impulse responses for these cases are given by

$$H(f) = 1 + 2e^{-j2\pi f\tau_1} \quad (3.11)$$

$$H(f) = 1 + e^{-j2\pi f\tau_1} + e^{-j4\pi f\tau_1} \quad (3.12)$$

Figure 3-19 displays the frequency response for a given τ_1 for both cases. The frequency axis is normalized to τ_1. It is clear that an indoor RF designer should avoid the second splitting arrangement where the three antennas are connected with constantly progressive delays.

Simulation and testing results for emulated channel with cable lengths of 3m, 20m and 50m is shown in Figure 3-19. The simulated and measured power values were shifted to have the closest relative amplitude matching. In frequency domain, a shift of 1.2MHz was observed and attributed to extra delays in variable attenuators and connectors.

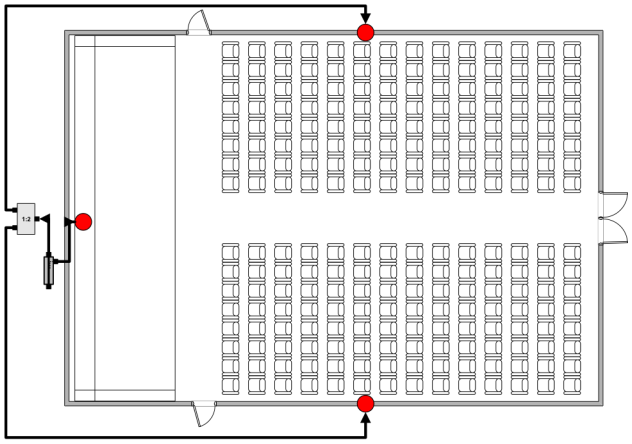

(a) $\tau_1=\tau_2$

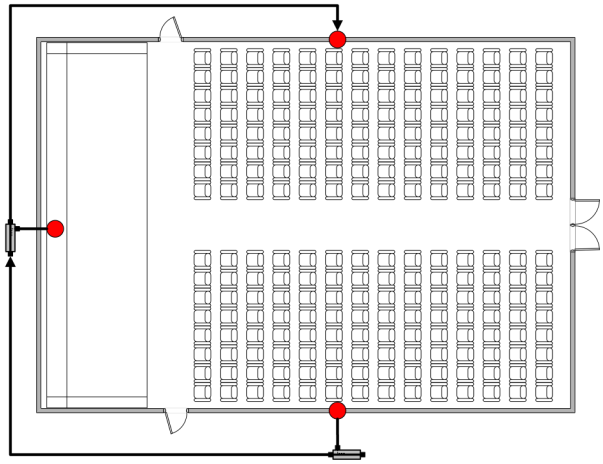

(b) $\tau_2=2\tau_1$

Figure 3-16 three antenna case with different DAS splitting arrangement

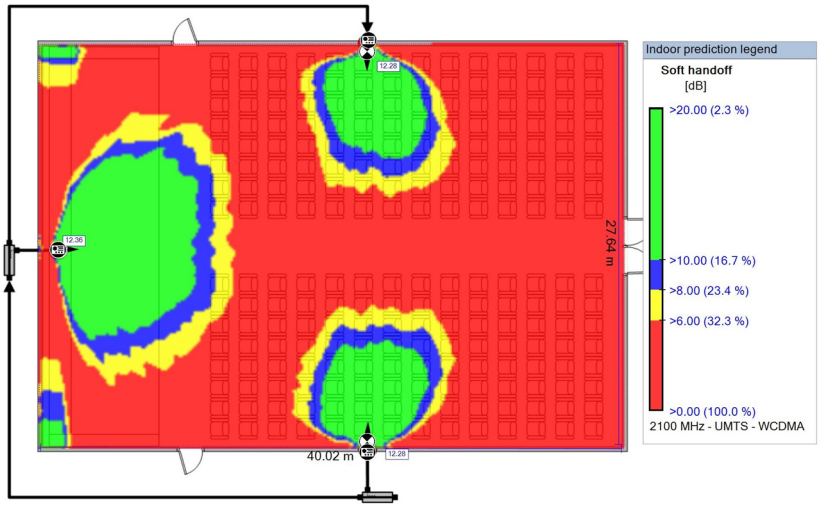

Figure 3-17 Soft Hand off simulation for 3 Antenna scenario

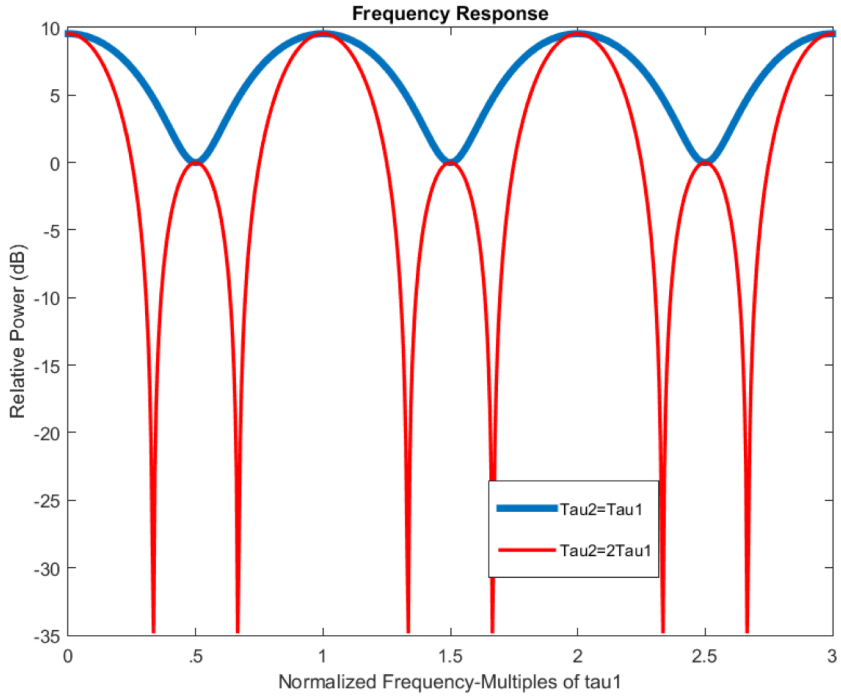

Figure 3-18 Frequency Response for 3 Ray Case

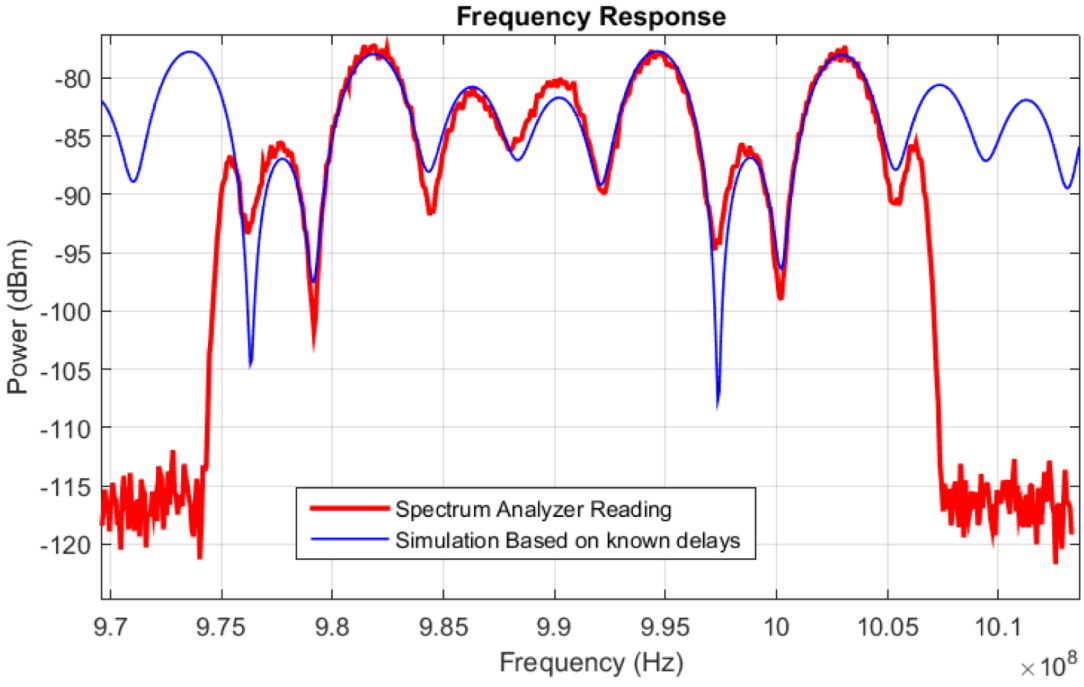

Figure 3-19 Simulation and Measurement of Three Antenna Case

3.3.2.3 Scenario III: Tunnels and Outdoor DAS

Outdoor DAS (sometimes referred to as Street DAS) refers to the deployment of Active DAS in outdoor environment for coverage extension or capacity enhancement. Outdoor DAS deployment is usually characterized by High Power Amplifiers, low numbers of antenna per remote equipment and longer distance span from head-end to remote-end equipment over optical fiber cables. Tunnels can have remotes placed at distances approximately 1km apart with hundreds of meters of radiating cables (cable antenna) to distribute the signal in the tunnel. Outdoor and street DAS are intended to cover large outdoor areas like college campuses, outdoor malls and outdoor exhibition venues. For overlapping coverage areas, relative delays will be contributed mainly by fiber optic delays in the order of few micro seconds. Such large delays should be eliminated and brought down to a value that the technology is capable of handling for simulcast cases and Handover between different sectors. Cable spooling or digital delay is used to balance delays. A State of the art digital DAS has a 1µs delay adjustment resolution over the fiber.

Moreover, the known effect of Doppler Shift caused by the relative motion of the transmitter and the receiver has a different effect in tunnels with DAS simulcast deployment. The receiver will be relatively moving away from a transmitter but at the same time approaching another transmitter. This will result in having a positive and negative frequency shifts at the same with one of these shifts is also delayed in time. Figure 3-20 represents a DAS in a tunnel showing the resultant signal smeared frequency.

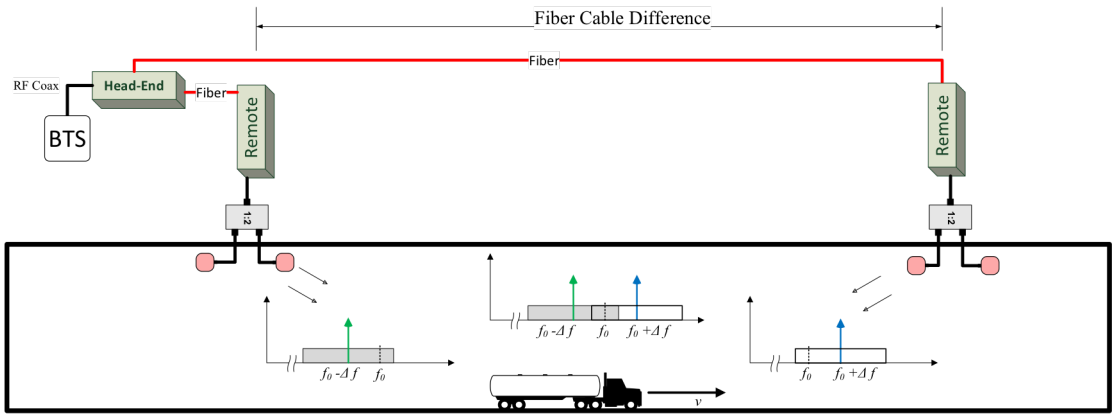

Figure 3-20 Doppler Shift in a DAS Tunnel deployment

3.3.3 Relative Delay Effects for Different Cellular Technologies

In addition to the dispersive fading effect on the channel, relative DAS delay in an indoor site causes delay spread and inter-symbol interference. This effect is most significant for WCDMA technology where the symbol rate (chip rate= 3.84MHz) is the highest in all existing cellular standards. The highest rate for EDGE is 325KHz while LTE has hundreds of subcarriers with a symbol rate of 15 KHz. Direct sequence spread spectrum systems like WCDMA have to rely on rake receivers and frequency domain equalization to untangle ISI [16] .In WCDMA, relative delays below one chip duration of 260.4ns will cause delay spread and inter-chip interference. The typical distance of 30m or less between indoor antennas causes a delay equal to half the chip duration which affects signal quality. RAKE receivers are able to resolve the second path only if the delay exceeds one chip period, or equivalently, antennas are separated over 68m apart. Unfortunately, this will impose harder constraints on the designer and might not be possible for all RF designs. A solution is avoiding two serving antennas in the same open area unless there is sufficient delay between them. Also assuring there is ample RF isolation for antennas in close vicinity of each other. i.e., avoid overlapping coverage areas of comparable power.

It is noteworthy to highlight that current RF prediction models and design tools do not take into account the effect of simulcasting or DAS delays. Software tools that use Ray Tracing prediction models can be improved by calculating delays to predict the exact channel impulse response for a given indoor location and, consequently, help predict BER performance and expected data throughput for any technology.

3.4. Case Studies

In this section we will study a specific cases and apply the analysis of DAS delays and their effect on the indoor channel.

3.4.1 Dense Indoor Environment with Corridors

One of the most challenging indoor propagation environments is hotel rooms. Most hotel owners restrict antenna installations in guest rooms, preferring to have the antenna out of sight of guests. Practically the only places left for installation are corridors and lift lobbies. This restriction imposes a great impact on the RF design, particularly the amount

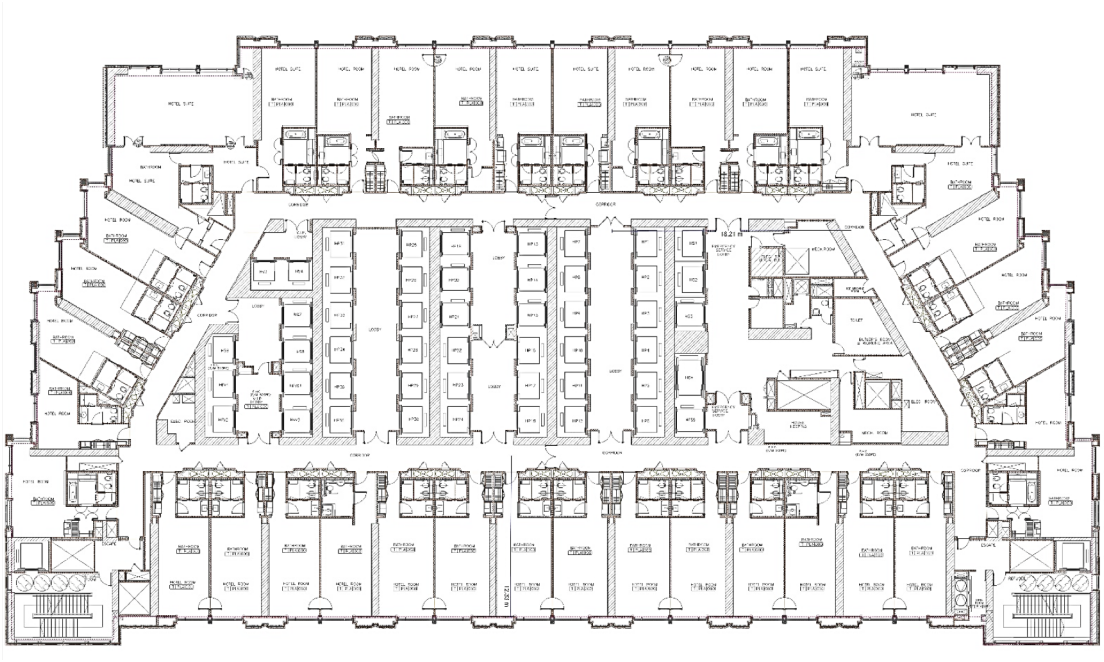

Figure 3-21 Dense Indoor Environment (High Rise Hotel).

of RF power and active equipment needed to generate enough power to penetrate the dense structure at the entrance of the hotel rooms (Toilets, Wooden closets, air ducts, etc.). Figure 3-21 presents a floor layout of the clock tower hotel in Makkah, KSA (the 3rd tallest building worldwide).

Delivering the required coverage levels at room edges is nearly impossible when coverage from nearby outdoor cellular sites is significantly high. Adding more indoor antenna to get the required coverage levels also adds more sources in a simulcasting configuration and changes the channel characteristics in the overlapping coverage areas. IBwave software is used to simulate the overlapped coverage area with its proprietary fast ray tracing algorithm. A very detailed 3D model of the building was developed using material types in AutoCAD files and matching IBwave material definition (Figure 3-22). Wall material parameters was calibrated using feedback from several CW tests and site surveys. The resultant 3D model includes effects of not only brick and concrete walls but also the false ceilings, large metal pipes in Electromechanical Risers, toilet wall partitions and wooden cabinets. All simulation were run with a resolution of 15cm at h_R=1.5m above ground applying a fast ray tracing algorithm. Table 3-3 shows the material parameters used in simulations antenna height h_T =2.5m.

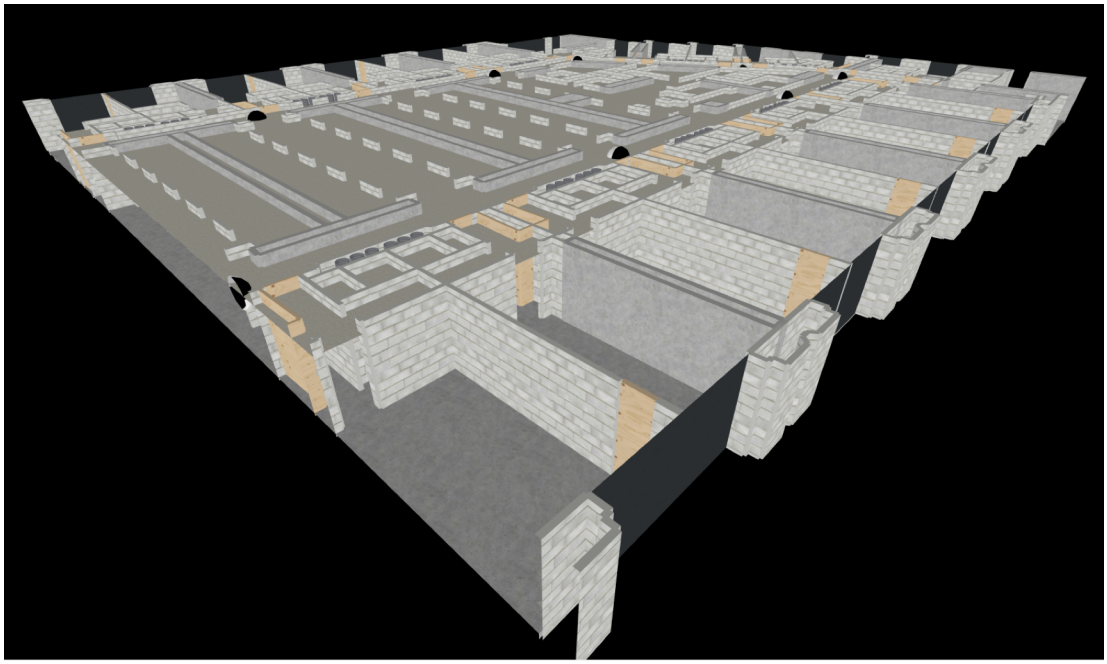

Figure 3-22 3D cross section of IBwave Floor Model for a Hotel

Cable lengths and distances measured on IBwave layout are in the x and y directions. To account for the direct path in the z dimension we use equation (3.13) corresponding to Figure 3-23 where l is the direct ray distance from Antenna to receiver and d is the horizontally measured value from IBwave. In our case, the difference between measured and actual path is very small for d >5m that it can be neglected.

$$l = \frac{d}{\cos\left(\tan^{-1}\frac{h_T - h_R}{d}\right)} \tag{3.13}$$

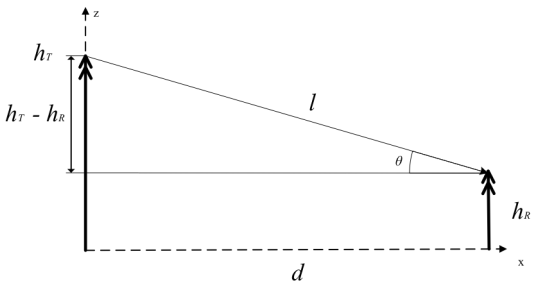

Figure 3-23 Geometry of antenna arrangement

To obtain an indication of coverage overlap, we examined three different prediction types for two proposed designs with 11 and 22 antennas respectively. Nature of path, service count and Soft handoff simulations were compared. The Soft hand off simulation is used to predict the relative coverage levels from each antenna. To accomplish this, we temporarily assign a different sector to each antenna for the purpose of simulation only. However, in Simulcast configuration, all antennas are connected to the same RF BTS sector thereby transmitting the same signal. The Soft Handover simulation calculates the relative signal levels at each point in the layout and calculates the percentage of area with certain limits. For this study we will concentrate on 8~10dB difference between the signals from different antennas. Figure 3-32 , Figure 3-30 and Figure 3-31 show soft handoff, service count and nature of path simulations respectively. Nature of path simulation indicates the type of dominant signal path which are either a Diffracted Ray, Direct Line of Sight (DLOS), Direct Non Line of sight (DNLOS) or multiple contributors. Since our main concern is in areas with relatively similar received power from more than one antenna, we

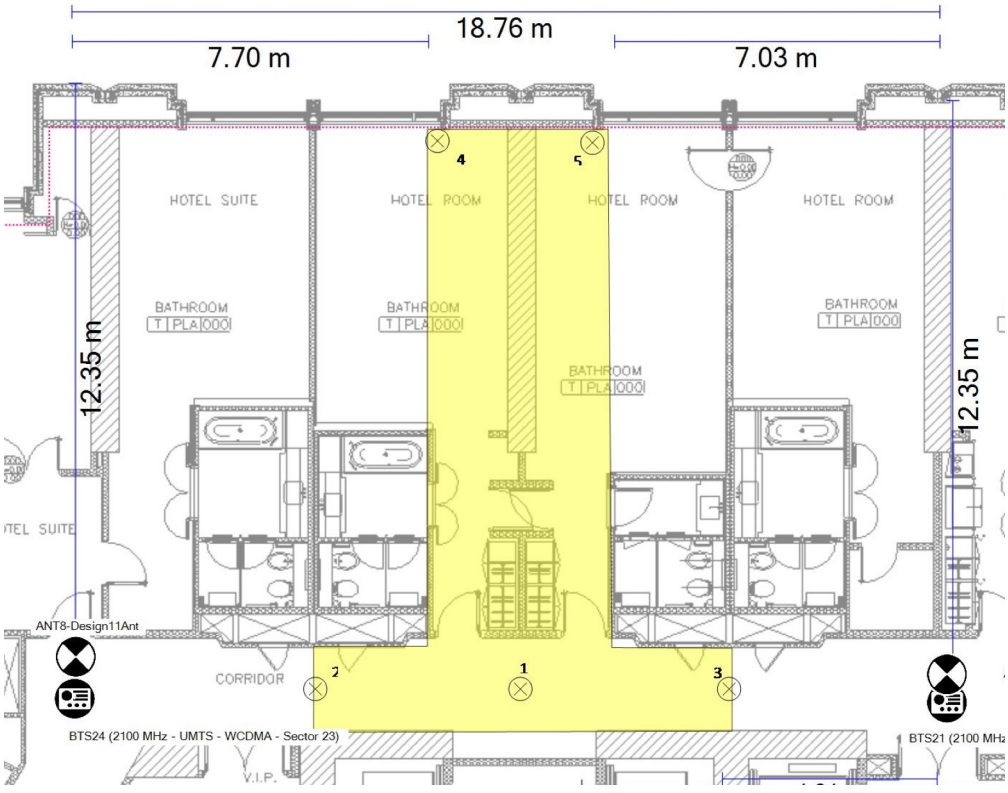

Figure 3-24 Multiple Contribution Zone

are concerned only with the multiple contribution zone in the nature of path simulation Figure 3-31.

A detailed analysis on the five points shown in Figure 3-24 is conducted. Wall penetration delays is assumed to be an exaggerated value of 5ns for all wall types. The increase from the values calculated in Table 3-2 accounts for wall thickness variations among different floors of the HI-Rise buildings. Concrete walls and columns are thicker in the lower floors compared to the top floors of the building. Table 3-5 shows the extracted values from different simulations from IBwave. For each of the five points, we have the received signal strength (Rx power), path length and the corresponding propagation delay. Moreover, we calculate the wall penetration delay based on a 5ns assumed wall penetration delay multiplied by the number of walls in the signal path from source to receiving point. For the given design, cable lengths of Active DAS are listed in Table 3-4 Assuming a cable with VF=84

	Type	Stone Brick	Concrete	Wood	Glass	Fiberglass	Metal sheet
Diffraction loss (dB)		20	19	22	17	20	20
Incident loss (dB)	Max	36	35	33	34	36	36
	Min	12	12	9	13	12	12
Reflection loss (dB)		9.52	7.51	16.2	7.08	8.17	0.05
Rel. Permittivity		4	6	1.8	6.7	5.2	1
Rel. Permeability		1	1	1	1	1	20
Conductivity (S/m)	2000MHz	0.04	0.08	0.03	0	0.03	11111.11
	2400MHz	0.05	0.09	0.04	0	0.03	13333.33
	interpolated for 2170MHz	0.044	0.084	0.034	0	0.03	12055.5535
Transmission Loss (dB)	2000MHz	4.48	12.08	4.24	1.9	1.62	951.94
	2400MHz	7.57	14.16	5.05	1.9	1.66	1014.73
	interpolated for 2170MHz	5.79325	12.964	4.58425	1.9	1.637	978.62575
Material Thickness (m)		0.15	0.2	0.1	0.01	0.01	0.01

Table 3-3 Wall Materials Simulation Parameters

Antenna #	ANT11	ANT 9	ANT 8	ANT 6	ANT 3	ANT 2	ANT 10	ANT 5	ANT 4	ANT7	ANT 1
Cable length (m)	26	44	44	63	12	30	21	20	8	63	25
Cable Delay (ns)	103.25	174.72	174.72	250.17	47.65	119.13	83.39	79.42	31.77	250.17	99.28

Table 3-4 DAS cable length to Antenna Units

	Point 1			Corridor		
Source ID	Rx Power (dBm)	Path length (m)	Pd (ns)	Penetrations	Type	Wall Delays
2	-75.20	19.63	65.5	1	DNLOS	5.00
3	-58.57	9.32	31.1	0	DLOS	0.00
5	-70.61	36.73	122.5	0	DLOS	0.00
9	-67.83	27.28	91.0	0	DLOS	0.00
11	-57.80	9.30	31.0	0	DLOS	0.00

	Point 2			Corridor		
Source ID	Rx Power	Path length (m)	Pd (ns)	Penetrations	Type	Wall Delays
3	-53.52	5.31	17.7	0	DLOS	0.00
4	-81.61	24.86	82.9	0	Diffracted	0.00
5	-71.55	41.91	139.8	0	DLOS	0.00
9	-69.25	31.94	106.5	0	DLOS	0.00
10	-75.87	24.50	81.7	0	Diffracted	0.00
11	-61.40	13.76	45.9	0	DLOS	0.00

	Point 3			Corridor		
Source ID	Rx Power	Path length (m)	Pd (ns)	Penetrations	type	Wall Delays
3	-62.06	14.25	47.5	0	DLOS	0.00
5	-69.44	32.14	107.2	0	DLOS	0.00
9	-66.14	22.62	75.5	0	DLOS	0.00
11	-52.31	4.71	15.7	0	DLOS	0.00

	Point 4			Guest Room		
Source ID	Rx Power	Path length (m)	Pd (ns)	Penetrations	Type	Wall Delays
2	-84.69	30.94	103.192	2	DNLOS	10.00
3	-84.2	13.87	46.252	4	DNLOS	20.00
11	-97.71	15.93	53.141	5	DNLOS	25.00

	Point 5			Guest Room		
Source ID	Rx Power	Path length (m)	Pd (ns)	Penetrations	Type	Wall Delays
2	-84	30.94	103.192	2	DNLOS	10.00
3	-98.9	15.79	52.675	6	DNLOS	30.00
11	-86	13.87	46.252	5	DNLOS	25.00

Table 3-5 Receive Points Analysis

Using the information about signal power and path delay we ran a series of MATLAB simulations to estimate the channel characteristics both in time domain and frequency domain. Simulation in time produces the Power Delay Profiles while the frequency simulation produces the channel frequency response for a given location.

3.4.1.1 Channel Power Delay Profile and Frequency Response

Figure 3-26 to Figure 3-29 show the Expected Power Delay profile of the channel as a result of the reception of the signals in Table 3-5 adjusted by delays of Active DAS Stage-1 cables in Figure 3-2.

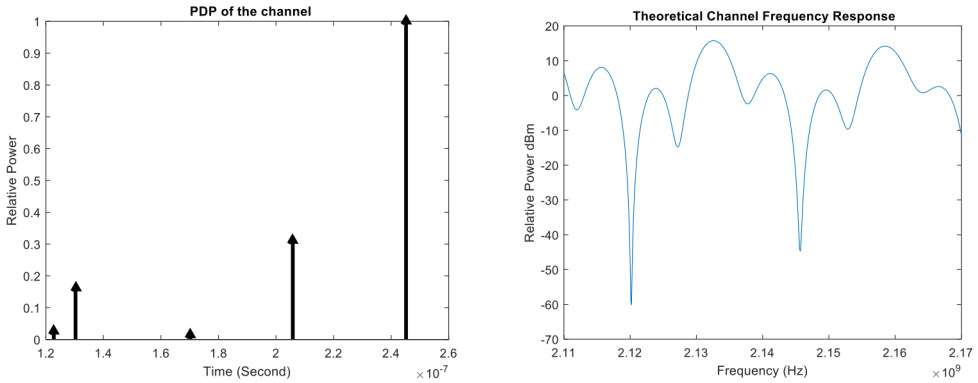

Figure 3-25 PDP and Frequency Response for Point 1

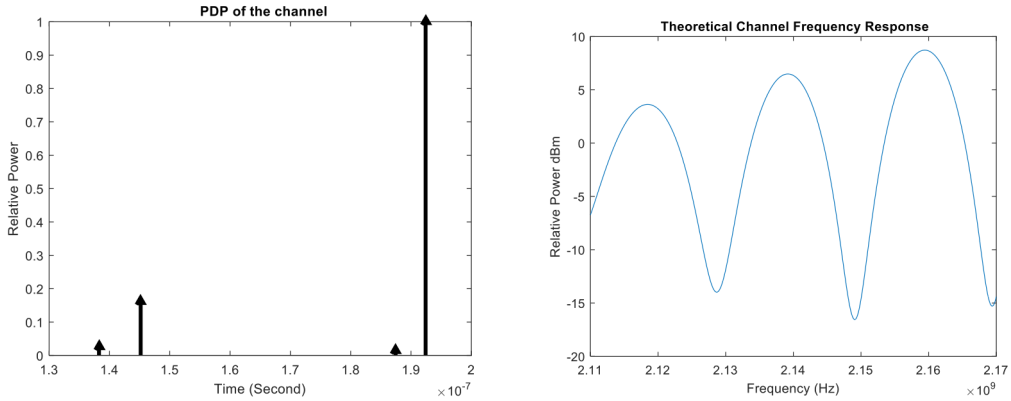

Figure 3-26 PDP and Frequency Response for Point 2

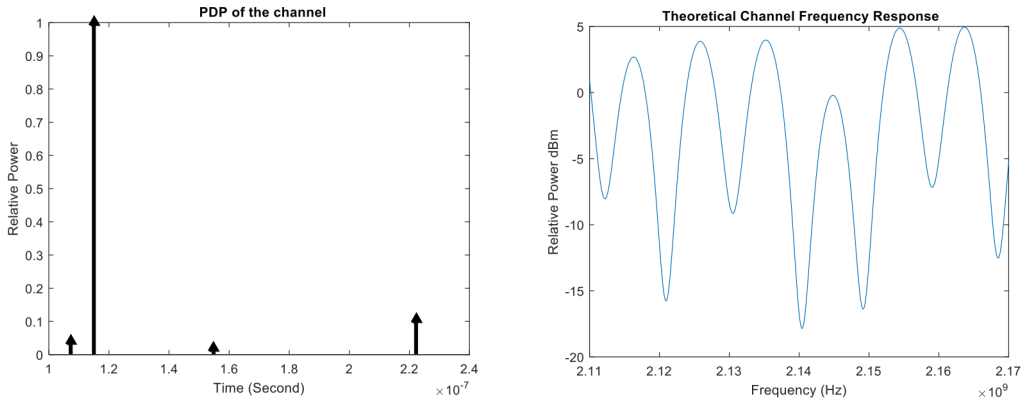

Figure 3-27 PDP and Frequency Response for Point 3

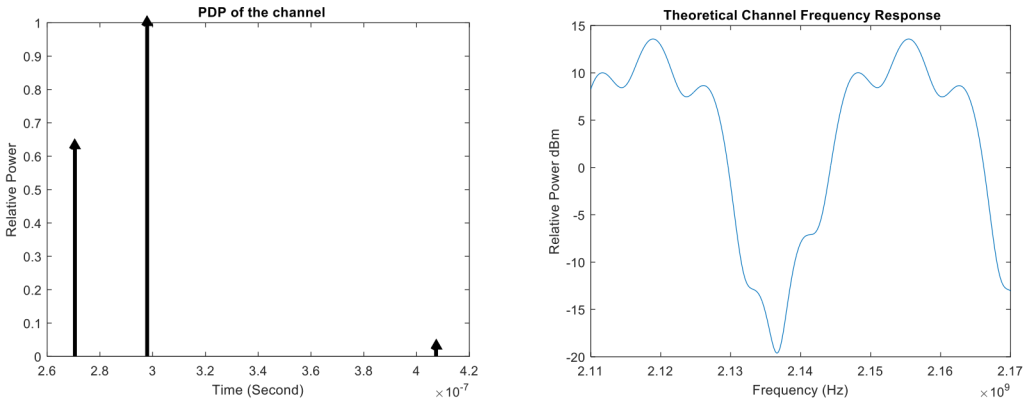

Figure 3-28 PDP and Frequency Response for Point 5

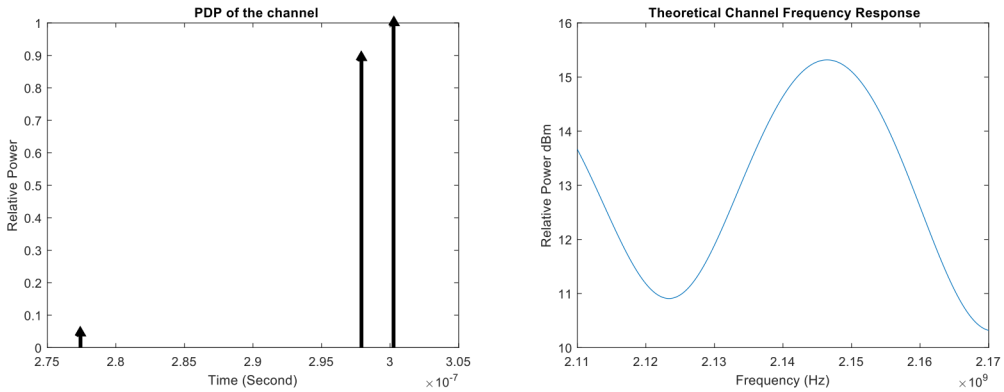

Figure 3-29 PDP and Frequency Response for Point 4

Notes on Multipath Rays: to the best of our knowledge the Ray tracing method implemented in IBwave reports the collective power received at a certain point on the layout without information about the relative delay of these paths. However, the relatively small arrival delay of the first level reflections and the reflection loss make it safe to neglect their effect. For instance, the reflection loss of a ground bounce in the corridor is around 7.5dB delayed by 2.4ns from the direct path at 10m distance from the antenna. The 2.4ns is significantly small compared to the delays caused by DAS. From the PDP and channel response figures, we can conclude that the highest two arrivals have the most significant effect on the frequency response. The third highest component will have a ripple effect on the response according to its relative arrival time and power, which is very clear for point 5 as exhibited in Figure 3-28. The significant factor determining the channel response for an indoor DAS deployment is the DAS delay and power received from simulcasting DAS antenna.

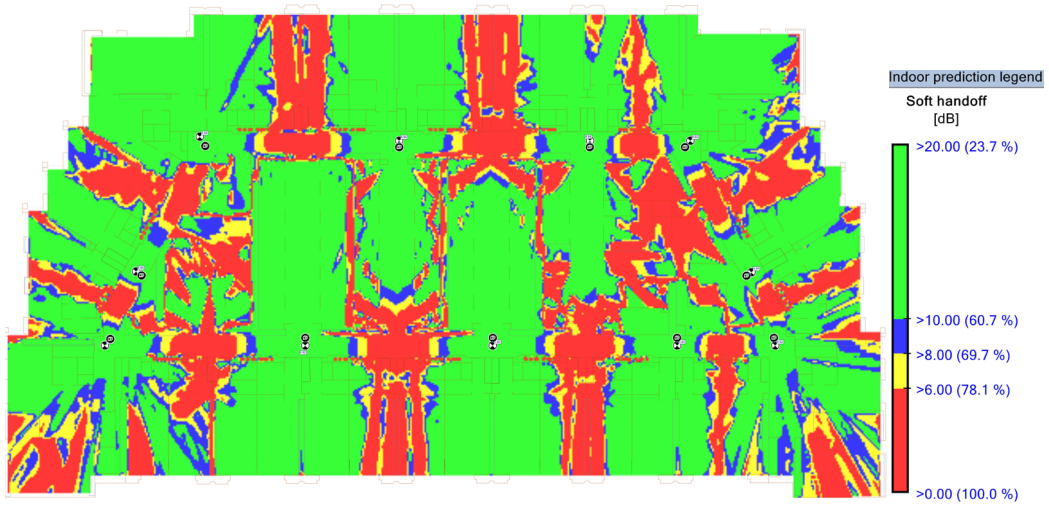

Figure 3-32 Soft HandOff (11-Antenna Design)

Figure 3-30 Service Count Simulation (11-Antenna Design)

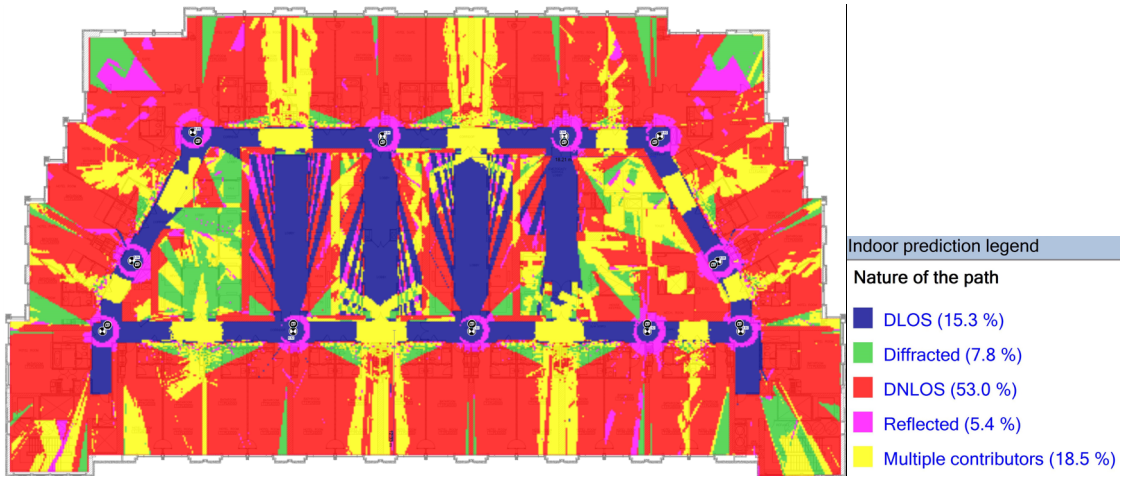

Figure 3-31 Nature of Path Simulation (11-Antenna Design)

3.4.1.2 Effect of Antenna Count

Figure 3-33 and Figure 3-34 display a comparison between two designs comparing the covered area percentage served by a specific number of antenna with signal levels above -90dBm (Figure 3-34), And the percentage of area with certain relative received power (Figure 3-33). It is clear that adding more antennas will reduce the area of single antenna dominance and increase the area of overlap converting them to multiple contribution zones with more dispersive fading effect.

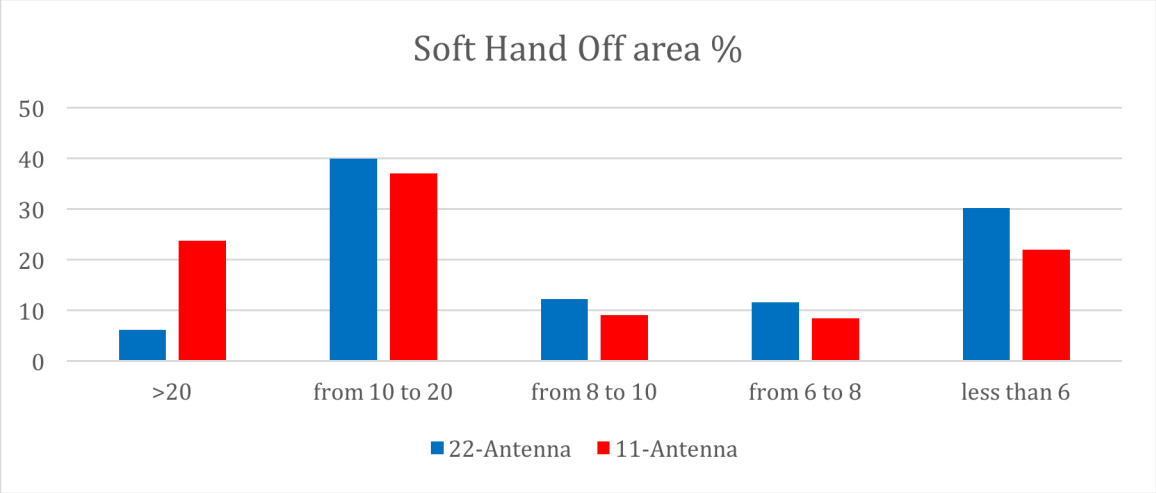

Figure 3-33 Soft-Hand off Area calculations for 2 different designs

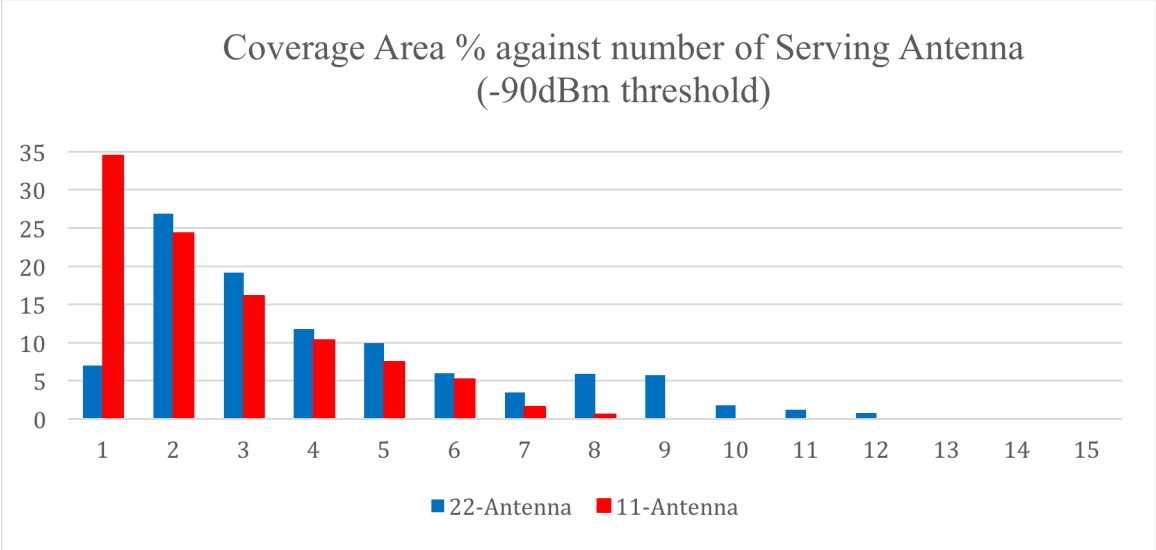

Figure 3-34 Service Count Area calculations for 2 different designs

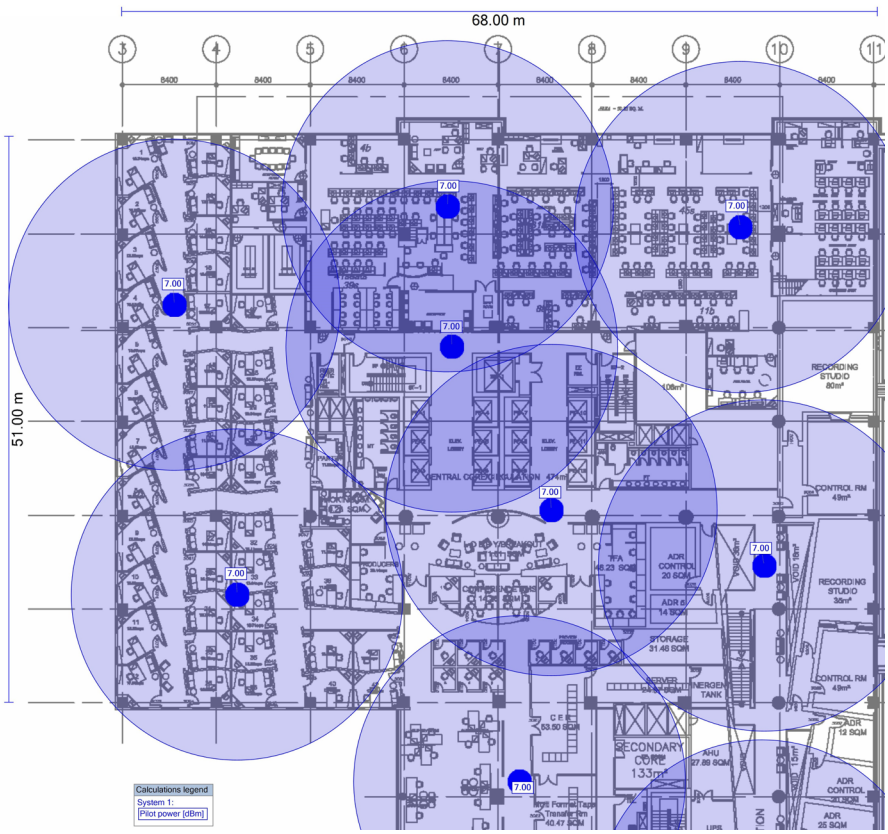

Figure 3-35 Example of an Open office indoor environment

3.4.2 Open office environment

Figure 3-35 shows an Open-office environment with the expected coverage contours of each antenna. Open-Office environment is characterized by low losses and average capacity requirements. Although such environment is considered a simple design problem for an RF engineer, delay effects are most prevalent in this environments. Detailed analysis of delays in an open-office example will be discussed in Chapter 4.

3.4.3 Theater and Stadium Seating

Theaters and Stadiums are high capacity venues with mostly line of sight coverage. Large number of RF sectors are deployed to accommodate the high subscriber density. The stadium design is typically a multi-operator multi-technology with high power

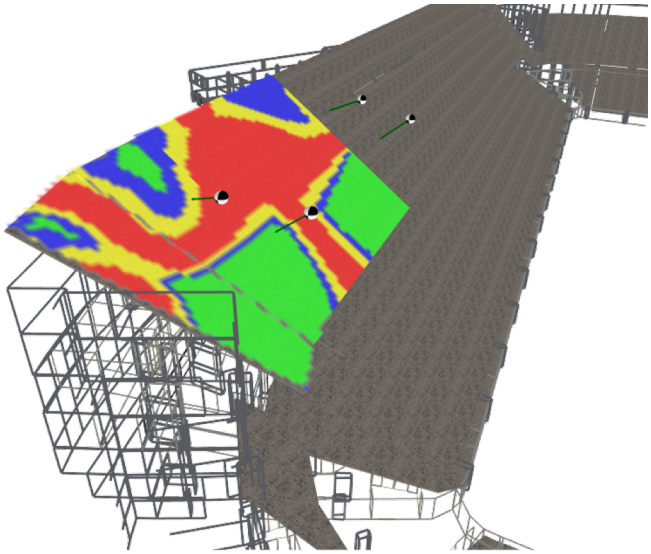

Figure 3-36 Simulcast Coverage Area of a stadium sector covered by 4 Antennas

requirements in cases where dominance is required over high level nearby Macro-Cellular coverage. Obtaining an RF isolation between RF sectors in this open environment is a challenge. RF isolation is typically achieved by using special stadium antenna with high directivity and narrow beam width mounted at a high altitude structures. Or by multiple antenna per sector surrounding the intended coverage area at the seating level. Isolation in the latter case requires placement of directional antenna at the sector borders resulting in a simulcast coverage area in the middle. Figure 3-36 shows an example of the first case with

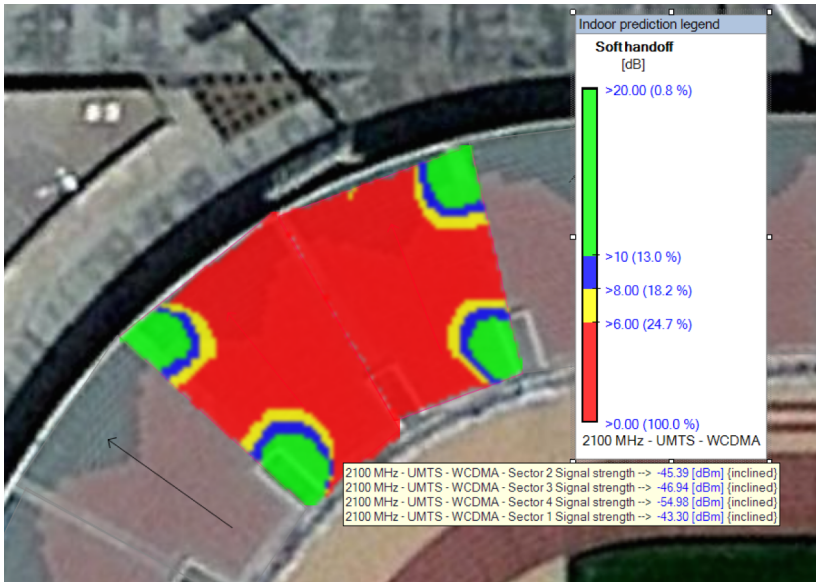

Figure 3-37 Simulcast Coverage Area of a stadium sector covered by antennas on the edges

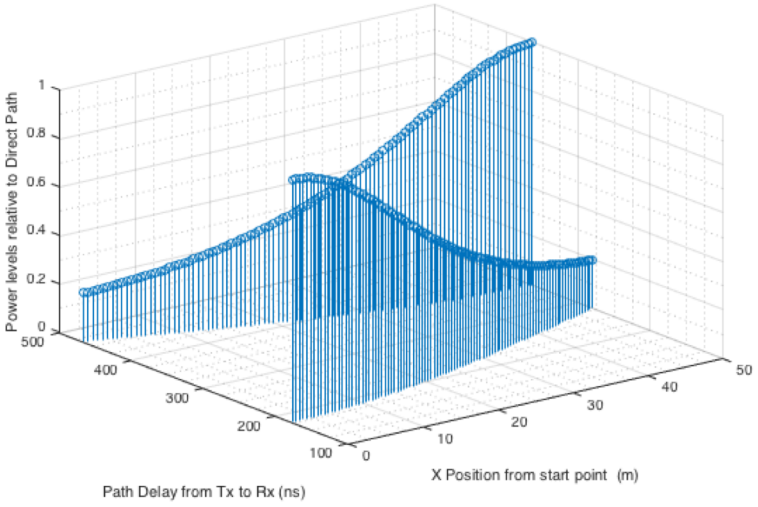

Figure 3-38 PDP of Stadium seating test path

4 antenna mounted on the roof structure (not shown in figure) and Figure 3-37 shows the case of antenna on the edges at the same level of the spectators with more than 70% of the area in simulcast coverage. Simulations for frequency responses and PDP for a test path in the middle of seating from top to bottom is shown in Figure 3-38 and Figure 3-39

Simulations for the RMS delay spread and Coherence bandwidth (calculated here as 20% of the reciprocal of the RMS delay spread) is shown in Figure 3-40. Several simulation results of different combinations of antenna transmit delays were examined. Simulation for the PDP and CIR for the complete seating area was done for a given transmit delay and dimensions with extreme data output size and processing requirements. Some

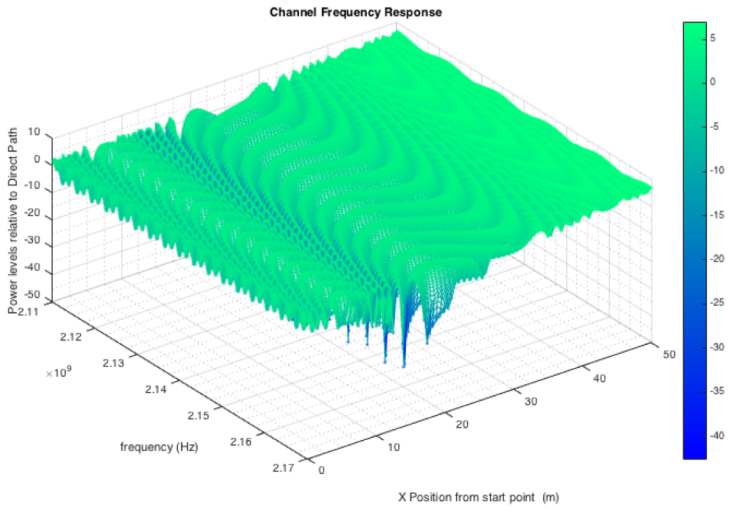

Figure 3-39 Frequency Response of Stadium seating test path

combinations of transmit delays produced better frequency responses for the examined frequency ranges at specific locations. Best RMS delay spread results were achieved by balancing the transmit delay.

It is clear that combining delay measurement results with the ray tracing computations produces detailed channel information and can lead to accurate performance estimation for high capacity DAS sites. It is the author's belief that a more advanced algorithm can be devised to optimize delays to reduce dispersive fading for important venues like stadiums. For instance, since the frequency response is a sum of sinusoids, the transmit delays of the 3-antenna case can be adjusted to produce a frequency response with a relatively large period of null repetition in frequency domain avoiding low coherence bandwidth in areas of interest.

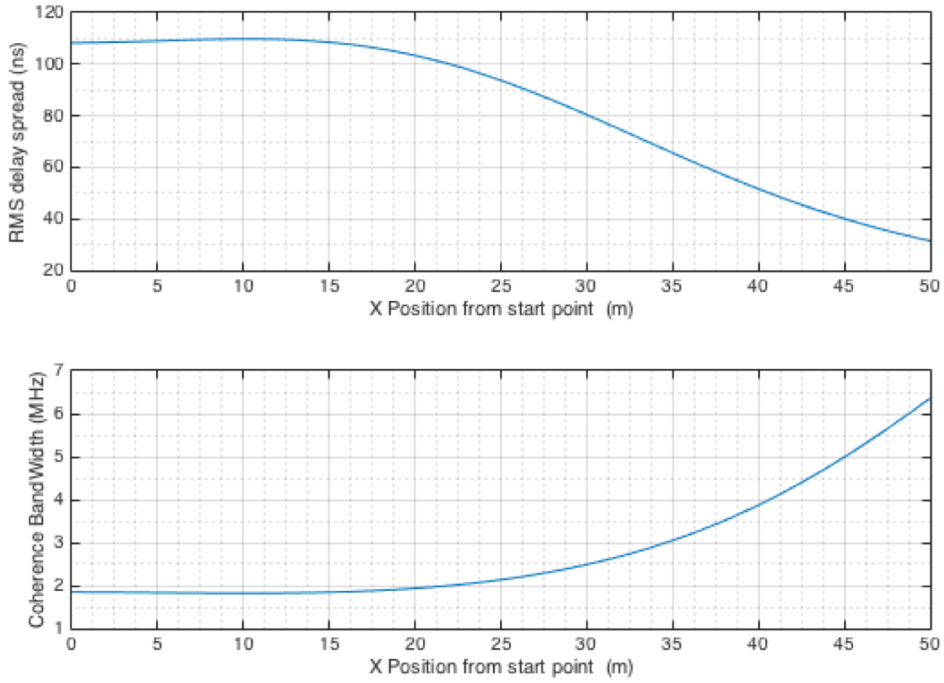

Figure 3-40 RMS delay Spread and Coherence Band Width for Stadium Example

Chapter 4 Engineering DAS delays for Indoor Positioning Application

The U.S. Federal Communication Commission (FCC) Phase-2 E911 emergency positioning requirements mandate that cellular network operators are responsible for positioning wireless terminals with an accuracy of 50m and 150m in 67% and 95% of all positioning attempts respectively for UE-based positioning methods. These values are relaxed to 100m and 300m for 67% and 95% of the attempts respectively for network based methods [2].

The indoor Distributed Antenna Systems are becoming the most effective service delivery method for multi-operators and high-density indoor venues to provide quality voice and Data services. A typical DAS extends the coverage of signal source (BTS, NodeB or an eNodeB) to cover tens of levels of a high-rise building or a multistory shopping mall, all connected to few cellular sectors. Subject to the specific capacity requirement of each site, operators assign a sufficient number of RF sectors to the indoor DAS equipment. Some high traffic sport venue deployments support up to 40 physical sectors covering the seatings and indoor sections of the venue. The very basic information available to position an originating E911 call is the cell ID number (CID). While DAS is used mainly to solve indoor coverage and capacity challenges, it can also provide more reliable location information regarding user equipment (UE) beyond what is provided by the CID. As seen in section 3.2.1, the BTS estimates the UE location by measuring the time of signal propagation or Time of Arrival (TOA) to the UE in a process called Ranging. Detailed implementation of ranging process and TOA measurement varies from one technology to another. TOA can provide average accuracy for outdoor positioning but often complemented by Time Difference of Arrival measurements (TDOA). In a TDOA more than one BTS is involved and complex processing is done in the corresponding location information server. For indoor RBS and DAS sites, only TOA information is provided by the BTS. The challenge is to have a meaningful translation of TOA to a physical location within the coverage area or building. To achieve that, the DAS must be carefully designed with this purpose in mind. In the following section we will observe how propagation delays

of DAS can be engineered to provide information about UE location within a given accuracy based on TOA.

4.1. Distributed Delay DAS concept

In order to avail the optimum location information from DAS and reduce ambiguity, we must insure that all DAS transmitters have a different distinctive propagation delay. We introduce a new Distributed Delay DAS design concept, A Distributed Delay DAS is a distributed antenna system designed to produce uniform and gradual propagation delay to each antenna in a specific deployment, thus assuring a distinctive delay mapping to different physical antenna locations. The basic concept is to utilize the maximum delay range available from the active equipment and distribute it between consecutive RF amplifier devices. For example, a certain head-end device provides the ability to change digital delays to remote-end equipment from 10μs to 24μs and has a maximum of 8 remote-end devices connected. The delays to these types of remotes must be set to 10μs, 12 μs, 14μs and so on up to 24μs for the 8th remote.

For an analog active system where delays are defined by cable lengths, we achieve the same result by utilizing the maximum allowable cable length $\hat{l}_i$ of a given active equipment stage. We define this delay step or separation as

$$\Delta\tau_{p|i} = \frac{(\hat{l}_i - \check{l}_i)\, Pd_i}{(m_i - 1)} \tag{4.1}$$

where

$\hat{l}_i$ is maximum cable length specific to the active equipment in use in stage-*i*,

$\check{l}_i$ is the shortest possible cable length in that specific deployment

m_i is the number of parallel cable branches connected to the *i-1* stage (number of connected equipment of the *i-1* stage)

Note that the only parameter we can control is the amount of equipment in a given stage. While we can utilize all the full capability of the active equipment, we may want to reduce m_i in order to increase time separation between transmitters $\Delta\tau_{p|i}$. For the system in Figure 3-2 and Figure 3-3, m_1 =4 and m_2 =2.

To understand the proposed solution we simulate PDP for the design given in Figure 4-2 and Figure 4-1 where we have 4 omni-directional antenna positioned to give

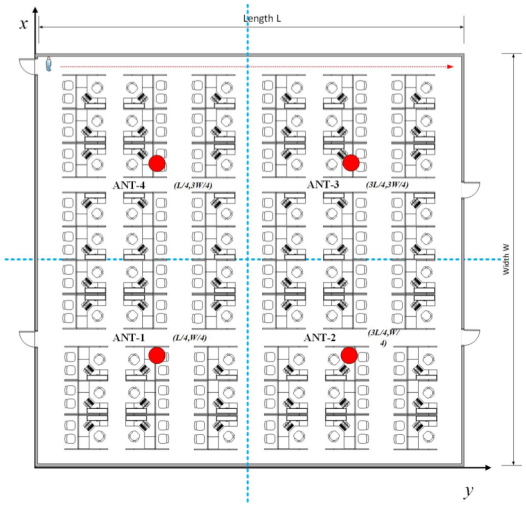

Figure 4-1 Open office with 4 antennas

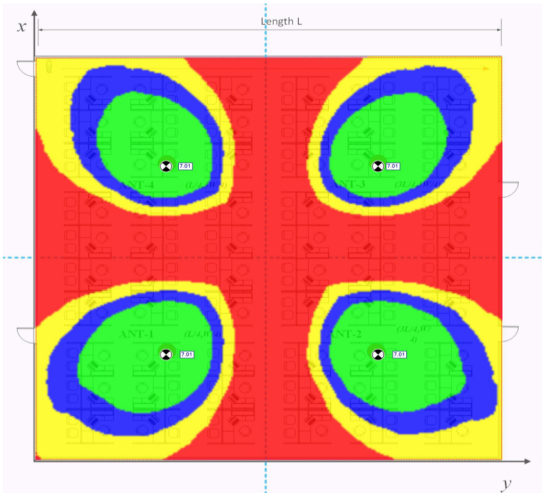

Figure 4-2 Soft Handoff Simulation

symmetrical coverage levels across the square open-office hall (*L=W=40m)*. Each antenna is assumed to cover a circular area of radius $d = \frac{W}{\sqrt{2}}$ with a particular coverage threshold. Antenna-1 is utilized as the time reference. Consecutive antennas will have a $\Delta\tau_{p|i} =$ 260ns transmission delay over the previous antenna. i.e., signal delays are 0, 260ns , 520ns and 780ns for the 4 antennas respectively. The expected PDP profile in coverage dominance area (green area in Figure 4-2) should have 4 peaks separated 260ns with the highest peak corresponding to the dominant antenna at its assigned delay. These peaks are further shifted in time depending on the relative propagation delay of the signal over the air from other antennas. The fundamental concepts for building a DDDAS is to first have the $\Delta\tau_{p|1}$ large enough to eliminate ambiguities of TOA estimation caused by multipath and wall penetration bias. Second, the resultant PDP should be measurable by the deployed technology standard. WCDMA, LTE, CDMA, etc.

Figure 4-3 shows the PDP of 20 points on the test path at the edge of the room (*y=40*). This path is selected as it represents the points of minimum separation of arrivals for the given antenna and delay arrangement and only direct path is considered.

Figure 4-4 shows the relative arrival time with minimum separation at *x=30* around 200ns. Running the simulation for all locations, we can estimate time of arrival window corresponding to each antenna. Since the signal travels in the same path for forward and reverse direction from and to the BTS, it is expected that the PDP is identical for both communication directions for a given location. A BTS with TOA measurement resolution

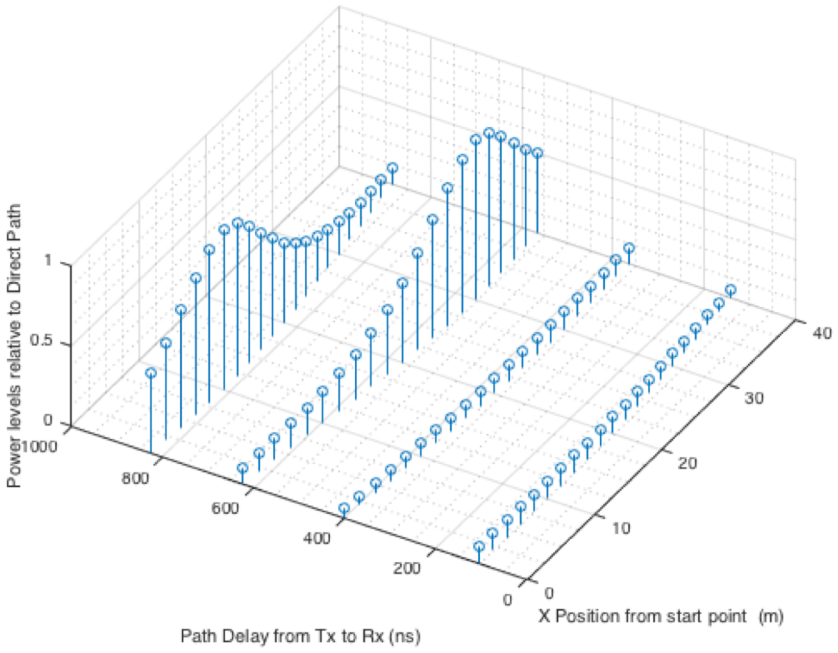

Figure 4-3 PDP of open office along the edge of the room

of 200ns or better can distinguish the location of the peak within the predetermined TOA window which correspond to a specific antenna and hence provide the location information as designed. For receiving points with equal level of power from two or more antenna (e.g., center point of the office) the PDP will have 4 equal peaks received at exactly 260ns apart. Detection of such locations will depend mainly on the complexity of the TOA measurement system. A system that can provide information about first arrival in addition to an indicative measure of successive arrivals will be able to detect the location accurately. An example of such measure is the RMS delay spread or a more complex system that can actually measure the channel PDP. These values of PDP and RMS delay spread can be simulated using ray tracing and verified at deployment stage to form a lookup table of TOA+RMS delay spread values against receiver location. This database can serve as delay-location map for indoor location finding. Figure shows the RMS Delay Spread for the given example. Given the above mentioned assumptions and results we can conclude that a 20m by 20m area resolution or better can be achieved in an open space. This resolution is mainly defined by antenna coverage area provided that time measurement and separation criteria are met. The coverage resolution is improved with dense propagation environments as a

direct result of more antenna and wall isolation. For hotel environment shown in section 3.4.1 each antenna is effectively covering 2 rooms with total area of approximately 200m^2

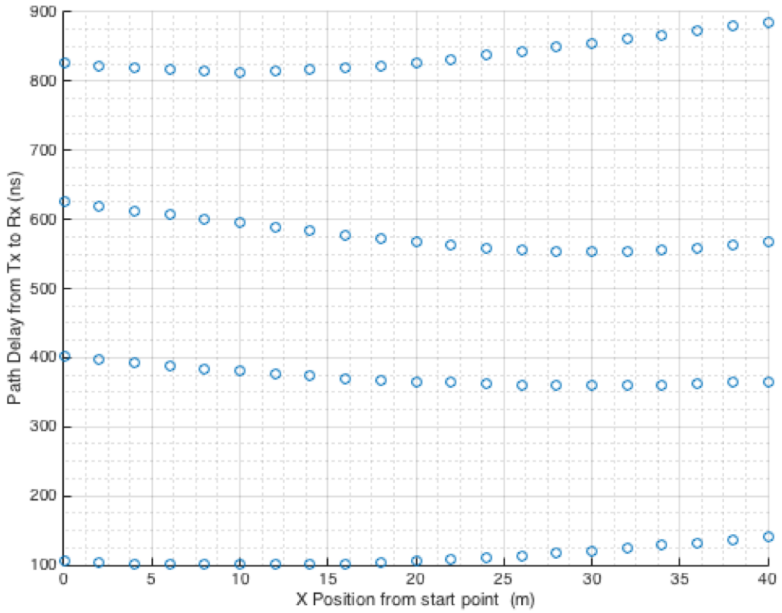

Figure 4-4 Arrival time for direct rays only

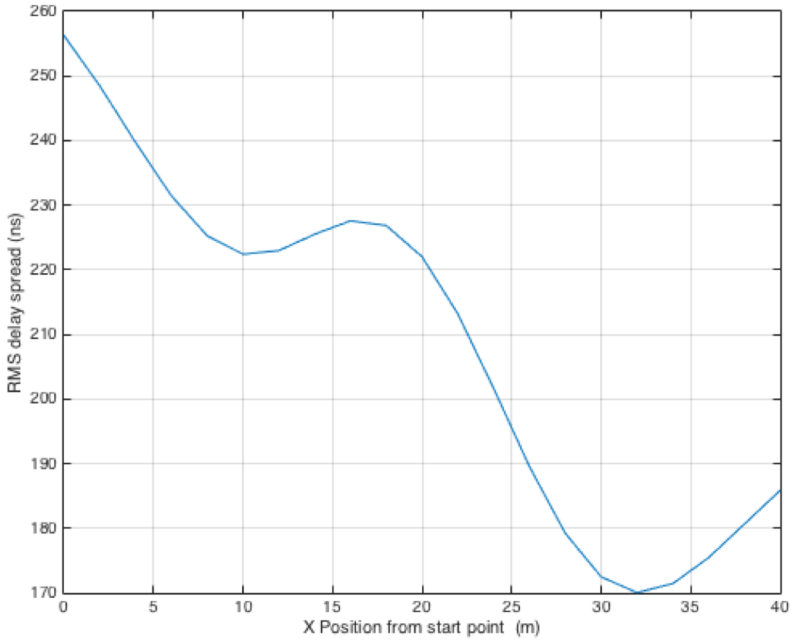

Figure 4-5 RMS Delay Spread of open office along the edge of the room

Figure 4-6 and Figure 4-7 show the previously simulated case with reflections from walls and ground bounce. All wall losses assumed to be 6dB. Although the minimum separation is reduced, only Reflections with significant power levels should be considered in the estimations of required time measurement resolution.

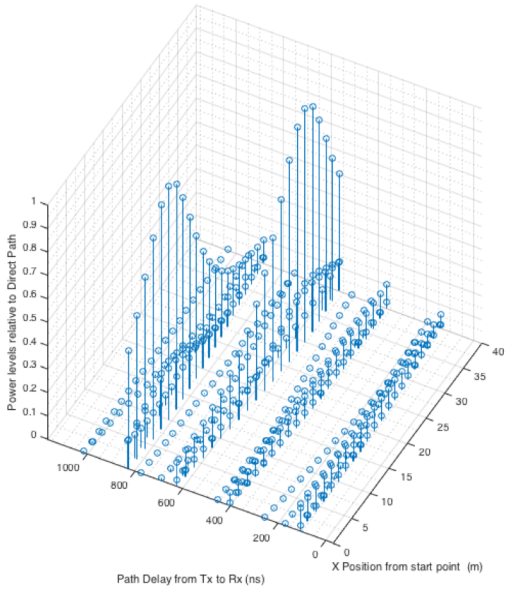

Figure 4-7 PDP of open office along the edge of the room (direct ray + reflections)

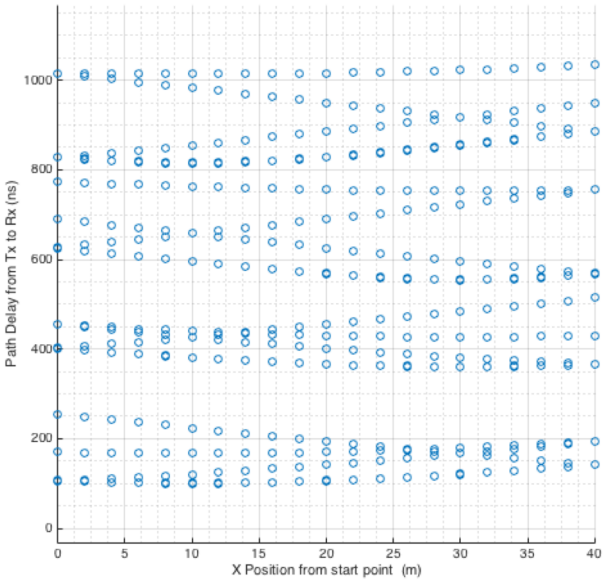

Figure 4-6 Arrival time for direct rays and reflections

4.2. Criteria for Distinctive Mapping and Accurate Ranging

Consider the PDP in Figure 4-8 corresponding to the antenna arrangement of the previous open office example in Figure 4-1. The time access represents the absolute delay or TOA from the BTS. Relative transmission delay between consecutive antennas denoted $\Delta\tau_{01}$, $\Delta\tau_{12}$ and $\Delta\tau_{23}$. The shown peaks are grouped in clusters corresponding to a direct ray and its multipath reflections. The indicated power levels are the maximum expected received power levels from a particular antenna. The actual power levels are scaled according to the location of the receiver. e.g., if a receiver is in the dominant region of antenna-1, only direct ray from antenna-1 and its reflections are present with significant power. A receiver positioned midway between antenna-1 and antenna-4 will receive relatively equal powers from both antenna and hence will have a PDP with the first and last cluster of peaks and the middle clusters will be significantly low. The PDP in Figure 4-7 shows the case where the received power from antenna-1 and antenna-2 are very small compared to antenna-3 and antenna-4. The expected arrival window of the direct ray is shown as a shaded area. The green dotted line indicates the arrival time at a distance *D/2* away from the antenna where *D=W/2* is the distance between the two antennas.

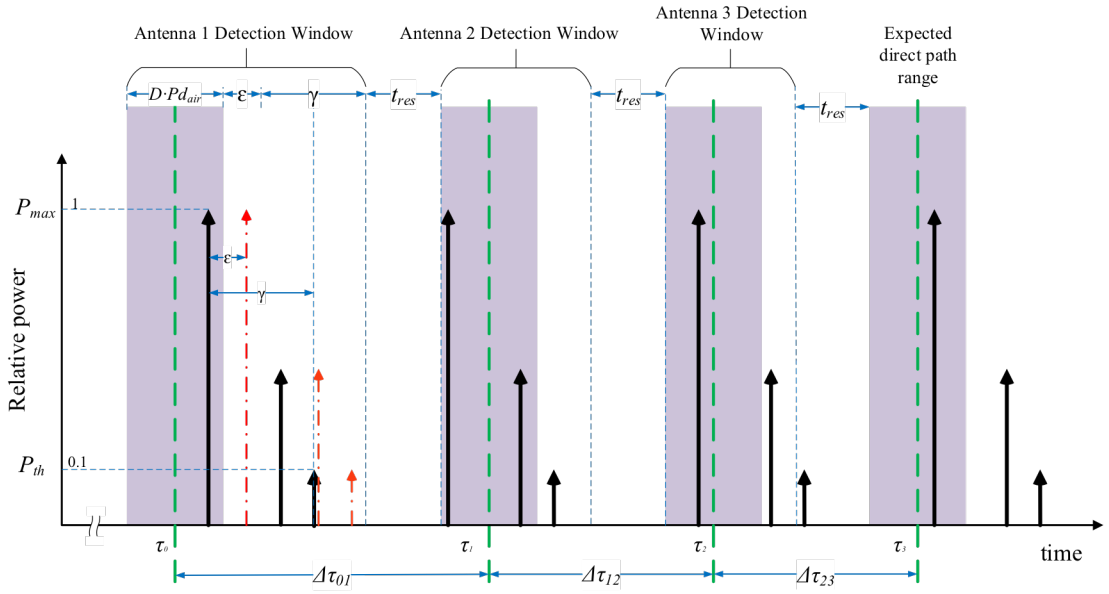

Figure 4-8 Expected PDP for open office example

To avoid ambiguity in ranging, it is required to avoid the overlap of arrivals of consecutive clusters. The selection of the minimum required time offset $\Delta\tau$ should take into account a guard period for multipath and wall delays due to penetrations in the given environment. The measurement system should be able to distinguish between the last significant multipath component and the arrival of the following direct ray. We can define the minimum delay separation required for stage-1 as

$$\Delta\tau_{p|1} \geq \Delta\tau_{p\,min} = \gamma + \varepsilon + t_{res} + D.Pd_{air} \tag{4.2}$$

where t_{res} is the propagation delay measurement resolution of the system, γ is a factor accounting for the indoor multipath at stage-0, ε is a wall bias factor and Pd_{air} is the propagation delay per unit length of free space. The value of ε can be estimated by counting the number of penetrated walls multiplied by the wall penetration time. ε is a characteristic of the propagation environment and can vary from one site to another.

To estimate γ, we assume it corresponds to a ray propagating in free space reflected with no loss off a wall and received with a relative power level above a certain percentage of the direct ray power at the edge of the intended antenna coverage area (center point of Figure 4-1). For a given relative power ratio the assumed reflected ray must have traveled a distance r. The governing relation is

$$relative\ power = \left(\frac{d}{r}\right)^2 \tag{4.3}$$

where d is the direct path length. For threshold of 0.1, $r = \sqrt{10}\,d$ and we can write

$$\gamma = \sqrt{10}\,d \cdot Pd_{air} \tag{4.4}$$

for our example $d \cong \sqrt{2}\,\frac{W}{4}$

To avoid any overlap caused by higher stages, minimum delay separation of the upper stages must be greater than all relative delays in the lower stage. That is

$$\Delta\tau_{p|i+1} \geq (\hat{l}_i \cdot Pd_i) + \Delta\tau_{p|i} \tag{4.5}$$

The better the resolution of measuring propagation delay, the higher the flexibility in designing and planning Distributed Delay DAS. Equating (4.1) with (4.2) we see that m_i and t_{res} are inversely proportional. Having a high t_{res} will limit the number of possible

parallel active equipment in a given stage below the design architecture of the active product and will possibly require additional equipment in the higher stages to achieve the required separation in the delay.

4.3. Measurement Resolution Values for Different Cellular Technologies

There are many techniques implemented to measure signal propagation delay of the signal to the UE. Standards define both mandatory and optional parameters such as Time Advance (TA) for GSM, Round Trip Time (RTT) for WCDMA and Propagation Delay (PD) for LTE, to name a few. The detailed study of measurement techniques and accuracy is beyond our scope. However, we will indicate typical values of current standards.

For CDMA system, the "CDMAServingOneWayDelay2" parameter is reported in multiples of 100ns. Further the standard defines optional resolution of 50ns [11]. For WCDMA, the RTT measurement resolution is one chip [12] and the propagation delay can be calculated by subtracting the time needed for the UE to respond (*RxTx*) type-1, then dividing by 2 [12][13].

For LTE, time advance parameter (T_{ADV}) should be reported with a resolution of 2 time slots T_s which corresponds to approximately 65ns [14]. The resolution of TA in GSM is too low to suit our application. Although these values are the standard parameters, it is believed that radio base station vendors can provide more accurate non-standardized measurements determining the propagation delay and algorithms to reduce the measurement errors due to multipath in the RF stage.

Realistic values of γ and ε require testing on a real site and with access to RBS measurement capabilities and algorithms, which are vendor specific.

DAS product [29] uses low cost 75Ω coaxial cable. Maximum length can go up to $\hat{l}_1$= 280m and a maximum fiber length for stage-2 $\hat{l}_2$= 6000m, with practical assumptions for $\check{l}_1$= 20m. Calculation for the given example yields γ=150ns and wall bias should be zero since we don't have any wall ε =0ns, then substituting into equations (4.1) to (4.5) we get minimum required separation of 266ns , 281ns and 476ns for CDMA, LTE and WCDMA respectively.

We can have a maximum of 4 stage-0 equipment (Remote Antenna Units-RAU) connected to every piece of stage-1 equipment (Expansion Hub). Using a thin coax CATV of *VF*=85%, cable length must be incremented by 86 m for LTE and CDMA. Similarly, for WCDMA, we can have a maximum of 3 RAUs with cables incrementing by 120m. Fiber cables of Stage-2 equipment (Main Hubs) must be incremented by approximately 250ns 253ns and 291ns for CMDA, LTE and WCDMA respectively to maintain condition of equation (4.5). The CDMA and LTE case is depicted in Figure 3-2 and Figure 3-3 with 8 RAU units connected to the system via 2 EH units.

4.4. Distributed Delay Passive DAS for Indoor Positioning

We have explained how to design Distributed Delay DAS to provide accurate location information using Low Power Active DAS (Stage-1 and above). Manipulating DAS delays on a passive DAS (Stage-0) is difficult as it has a direct impact on the RF design and signal EIRP. A passive DAS has high power distributed using splitters with similar Propagation Delays for adjacent antennas. The relative delay between signal transmission from adjacent antenna is too small to apply the previously explained technique. Suggestions to make the problem more easily reconciled include using a different generation of coaxial cables designed with lower Velocity Factors to introduce higher delay and hence more separation in time, or ,using unequal power splitters throughout the Passive Distribution network. This solution, however, adds extra RF losses and cost to the design compared to a standard design.

Implementation of a smart TOA measurement system that rejects multipath combined with an appropriately designed passive DAS narrows the ambiguity to just a couple floors. Complementing this with RF pattern matching techniques further narrows the location estimate to a specific side of the building (e.g., north side or north-west). The concept of optimizing a DAS design for indoor positioning is an under-researched field requiring the cooperation of both BTS and DAS manufacturers to achieve the highest accuracy possible for indoor positioning.

4.5. RF Pattern matching and RF fingerprinting

RF fingerprinting, also called Database correlation method, is a class of algorithms which are often formulated as classification or regression problems in the form of a data mining problem.[19] A fingerprint or a dataset instance is a set of location-dependent signal parameters available in Radio Access network (RAN) [7]; the more observable parameters, the more distinguishable the fingerprint is.

RF fingerprinting usually involve 2 phases, a learning phase and a test and operation phase. The learning phase is the data collection phase where the fingerprint correlation database CDP is built. Pattern matching is performed in the operation phase. Pattern matching is a process of comparing the collected fingerprint with the stored database in the location server to estimate the location

For the case of indoor pattern matching: The learning stage is a strictly a supervised learning where the location of each collected instance of variables is given. It is possible to utilize Fingerprinting for indoor location estimation without a deployed DAS. An advantage of RF fingerprinting is that it does not require additional network equipment but rather employs the available information from the Radio Access Network (RAN). Cell ID, Round Trip Time and received signal strength of neighboring towers are the typical measured parameters. Adding the power delay profile PDP to these parameters for an indoor location will make the fingerprints more unique. Complementing fingerprinting with a DAS, designed using the techniques explained earlier, can narrow down the pattern matching significantly to a very small subset and achieves higher indoor accuracy.

Field measurement for a high power tunnel DAS not optimized for indoor positioning was conducted. The tunnel is located in Dubai Jumairah Palm. It spans approximately 1.4km with 2 DAS remotes installed around one quarter of the length from each end. The DAS head-end units and operators' NodeB are installed in a control room at the end of the tunnel. A second operator is sharing the same Passive Infrastructure without sharing the active DAS (using dedicated fiber-connected NodeB remote radio head collocated at remote locations with similar architecture and power to the high power DAS). Passive radiating cable is used to cover the majority of the tunnel terminated with a high directivity Yagi antenna at both exits and at the center. Figure 4-9 displays the readings of delays along the tunnel from the far end to the NodeB end for CPICH channel. The Delay

is measured in multiples of WCDMA chip period. Absolute delay is shown as a thin line and Delay Spread as a thick line. Delay spread is zero in the center and at the exits where the receiver is in a direct ray from the antenna. Delay spread increases above 5 chips under radiating cable coverage area. This indicates a high multipath environment caused by the radiating cable. The absolute delay is expected to be maximum at the far exit of the tunnel (to the left of the graph) and to decrease as we approach the head-end side. Since each remote is feeding a radiating cable going in both directions of the tunnel, the absolute delay line should have 2 local minima at the remote location (marked red) and increase by adding the additional delay of the cable to the right and left. The shift at the center is attributed to the difference of delays over fiber to the remotes. If these delays were compensated for, the two minima should be at the same absolute delay. However, for location detection optimization, difference in delays is required. Passive DAS presents a similar graph. Figure 4-10 shows the absolute delay for Passive and Active DAS in the same tunnel. It is clear

Figure 4-9 CPICH Delay and Delay Spread for Palm Jumairah Tunnel

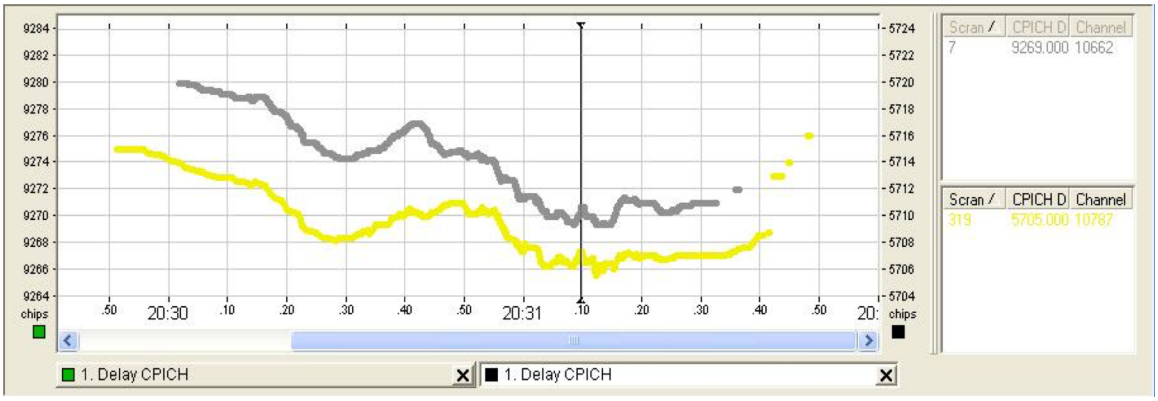

Figure 4-10 Absolute Delay for Active and Passive tunnel DAS

that the remote location on the left experiences higher delay for active than passive which is attributed to different fiber length to the Active remote and the remote radio head (RRH).

It's obvious that an RF fingerprinting learning system and pattern matching can identify the location of user equipment with certain accuracy depending on the measurement system resolution and capabilities. Having the Delays of the DAS optimized too will provide a clear difference in fingerprint pattern. Complementing these two values with the monitoring of neighboring sites will further improve the accuracy.

The same concept when applied to Passive indoor DAS can give produce results. However, for dense indoor locations, a passive DAS will have multiple locations with the same absolute delay values causing ambiguities for pattern matching. These ambiguities can only be resolved by having an increasing gradient of absolute delay values across the building in what we defined as a Distributed Delay DAS. Many practical Design tips and tricks can be developed as a solution to implement this kind of passive DAS design, limited only by the designer's imagination.

Chapter 5 Applications of Channel Sounder for DAS

In this chapter we will discuss possible applications of a channel sounder for DAS commissioning and implementation. An overview of some channel sounding techniques will be presented followed by a proof of concept implementation of a Sliding Correlator Channel Sounder using a Software Defined Radio (SDR) development board. Applications of channel sounding for DAS and a measurement procedure will be introduced for DAS delay optimization.

5.1. Channel Sounding Concept.

Channel sounding is the measurement of the Impulse Response of a wireless channel. Results of the channel sounding are used to obtain parameters of stochastic channel models and to verify the quality of deterministic channel models [20]. It has been in use since the 1950s to measure channel characteristics with different techniques and implementations. A review of channel sounding techniques is presented in [27]. Channel sounding techniques are divided into two major classifications according to the measurement domain, either Frequency-Domain measurement or Time-Domain measurement. The simplest form of a Time-Domain channel sounder is an impulse sounder that generates repetitive pulses from an RF transmitter with power measurement at the receiver in time domain. This technique has limitations related to power amplifier design requirements and peak to average ratio. Correlative channel sounders transmit an RF signal modulated with long duty cycle waveform then perform correlation with the same waveform at the receiver. An example of such waveforms is Chirp signal and Maximal Length Linear Feed Back Shift Register (LFSR) sequence (m-sequence). Appendix D presents additional details about these sequences and the generating polynomials.

Frequency-Domain sounders transmit a constant amplitude swept RF CW signal. The receiver is continuously tuned to the same frequency to plot power levels against frequency. The frequency response is then filtered and post processed to give the Power Delay Profile by Inverse Fourier Transform. Reference [20] provides details of additional modified measurement methods from the basic time and frequency domain techniques.

For the various techniques and implementations of channel sounding, the ability to measure a time varying channel is limited by the time needed to produce a single snapshot of the channel (one full frequency response or impulse response).

While these techniques vary considerably in performance and characteristics, our main priorities in indoor DAS sounding is time measurement resolution rather than the dynamic range. The indoor DAS channel is assumed to be a slowly varying channel in all our analyses. The selection for our prototype sounder technique is the Sliding Correlator Channel Sounder described in [18] due to its ease of implementation on an SDR platform.

5.2. Implementation of SDR Channel Sounder

A software-defined radio can be described as a Radio Communications system that relies in part on its implementation on a software code run on a suitable processing platform. The driving idea behind SDR is to minimize Technology/Modulation specific hardware and replace it with a software code that can be modified if needed to support different applications and technologies to reduce the solution cost and increase the deployment flexibility.

SDR boards USRP B210 and B200 from Ettus Research were selected because of their wide frequency band and the wide options of supported open-source and commercial software tools. The maximum bit rate limitation of the boards for our application is the transfer rate between the board and personal computer where all the signal processing is performed. The sampling speed is restrained by the lowest performing node on the signal path. It can be the processing speed of the CPU or the DATA transfer rate of the universal serial bus (USB) which in turns limits the maximum sustainable sampling rate of the system.

The software development tool in use is GNU-Radio [30]. It is an open-source platform that provides SDR building blocks. Figure 5-1 and Figure 5-2 show a channel sounder transmitter and receiver blocks in a user interface GNU-Radio Companion.

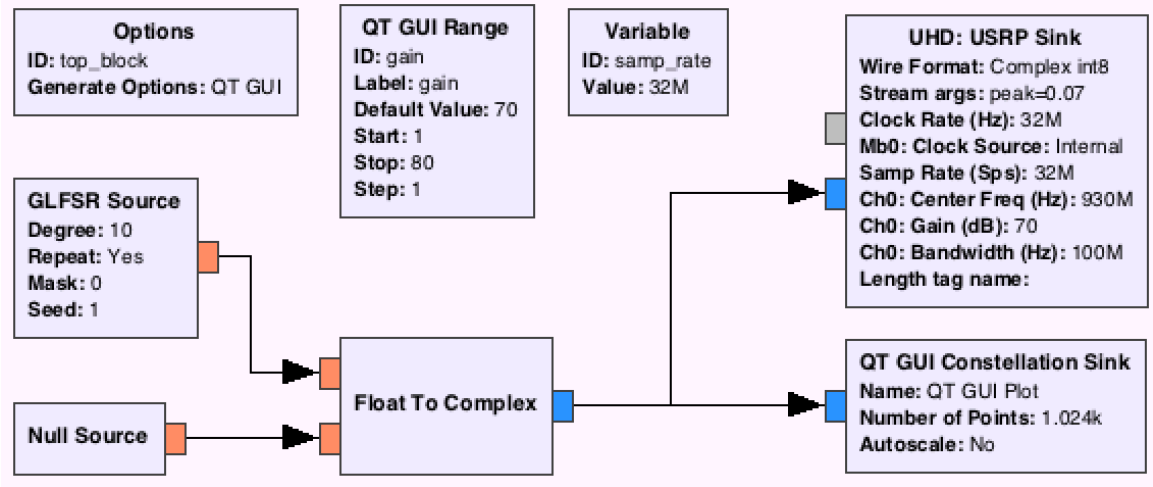

Figure 5-1 GNU-Radio Channel Sounder Transmitter. 32MHz BPSK modulated signal

5.2.1 Sliding Correlator Channel sounder implementation in Gnu-Radio and USRP

Many different topologies were examined to get the maximum stable sampling rate out of the Gnu radio and USRP boards on USB3 interface. A PN sequence is used to directly modulate the real part of USRP sink. The master clock rate of the board was adjusted to match the desired sampling rate instead of using the default 32MHz sampling rate of the board. Running the USRP board with the same clock rate as the software sampling rate eliminates up-sampling (interpolation) processing inside the USRP board. Data transfer mode over the USB was reduced to complex 8-bit integer sample representation in order to reduce the USB throughput requirement and have a stable stream feeding the USRP. A stable rate of 32MHz was achieved at both the transmitter and receiver after removing baseband filtering of the PN sequence. The filtering is necessary to limit bandwidth of the modulating signal, Hence, the RF signal, but it presents extra processing cost.

At the receiver side, the main goal is to eliminate any post-processing requirement and exhibit a live display of the PDP achieved by sampling the signal with the exact sampling rate. Following which, we performed a sliding window correlation with the PN sequence and displayed the output with time for a window equal to or greater than double the code length to provide a better view of the repetitions as in Figure 5-3.

The implemented Channel Sounder characteristics is listed in Table 5-1

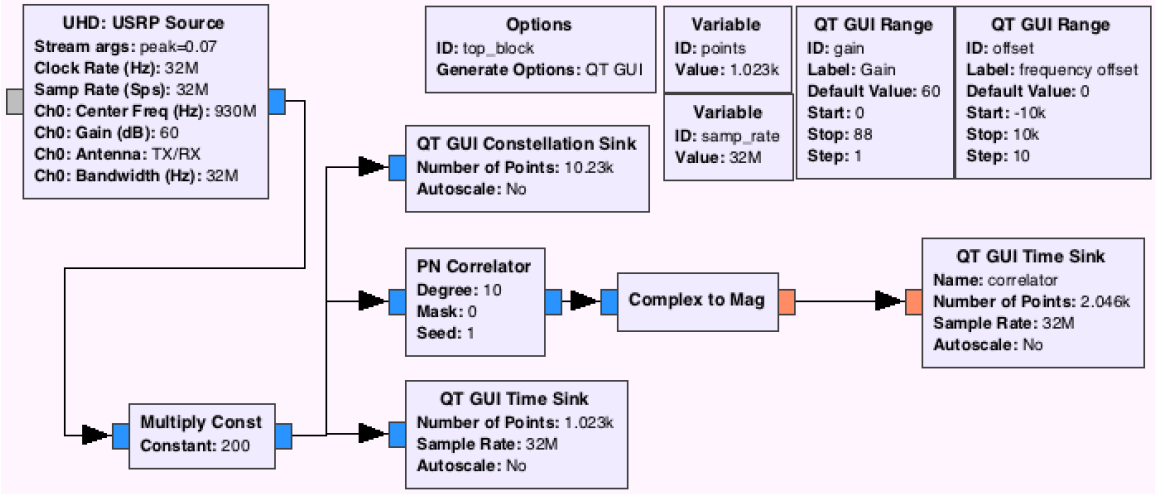

Figure 5-2 GNU-Radio Sliding Correlator Channel Sounder Receiver

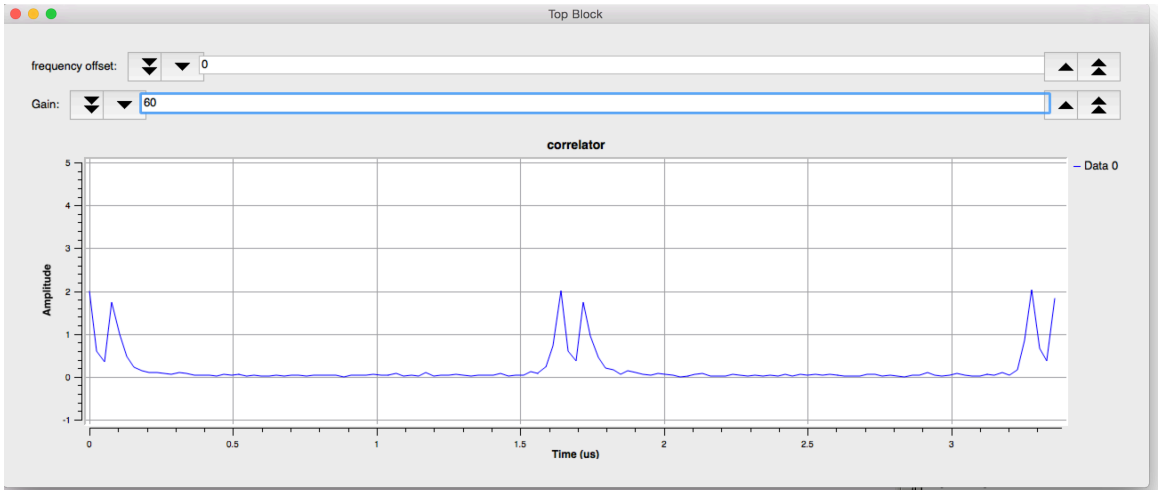

Figure 5-3 Sliding Correlator Output for a two path emulated channel

Code length (N)	Variable, N =1023 for outdoor and N= 63 for indoor
Sampling rate	Up to 38.4MHz. 32MHz stable
Resolution	31.25ns
Frequency Range	70MHz to 6000MHz
Power Output	-10dBm at maximum gain.

Table 5-1 SDR Sounder Charecteristics

5.3. Frequency domain channel sounding

Information regarding the channel can also be extracted from the analysis of the frequency response of the channel under a flat wide band excitation. The resultant spectrum should be the frequency response of the channel assuming the channel is slowly varying or static for the measurement period. The previously described channel sounder transmitter generates a wide band noise like signal in frequency domain that can be transmitted and measured at the receiver by a spectrum analyzer. Figure 3-15 and Figure 3-19 show the responses measured with a spectrum analyzer. Applying hanning window and inverse Fourier Transform on spectrum readings should return the impulse response of the channel. For the 2 ray case, the time difference is simply the inverse of the null separations. A spectrum analyzer is a tool that assists in identifying this simple delay case for DAS deployment in the field.

5.4. Channel Sounding for DAS

While a channel sounder has been a very important tool for researchers to characterize indoor and outdoor channels, so far it hasn't been used as a test tool for commercial deployments of indoor communication systems. A Channel sounder can be very useful in optimizing indoor DAS for location estimation as discussed in Chapter 4. To be able to estimate a location, wall bias and multipath delay values should be verified for the particular propagation environment in question. $\gamma + \varepsilon$ in equation (4.2) can be estimated using channel sounding procedures explained below.

5.4.1 Channel Sounding with Distributed Receiver's Antenna

In this proposed technique we measure the channel response to a mobile transmitter as seen by a single sounder receiver attached to a spatially distributed receiving antenna to produce the DAS reverse delay profile in Figure 4-8. i.e., the measurement is done in reverse direction with the transmitter positioned at several key locations in the intended coverage area. This proposed modification on standard channel sounding technique identifies the TOA and Multipath delays of the indoor DAS when at full traffic relative to the TOA below the closest antenna (multiple subscribers at different locations). If necessary, an iterative measurement and delay adjustment procedure should be performed

to optimize the minimum delay between antennas. This procedure is ideally performed at DAS design stage, but can be performed after DAS deployment provided that DAS delays can be modified if necessary. Figure 5-4 depicts the proposed process for optimizing the DAS delays.

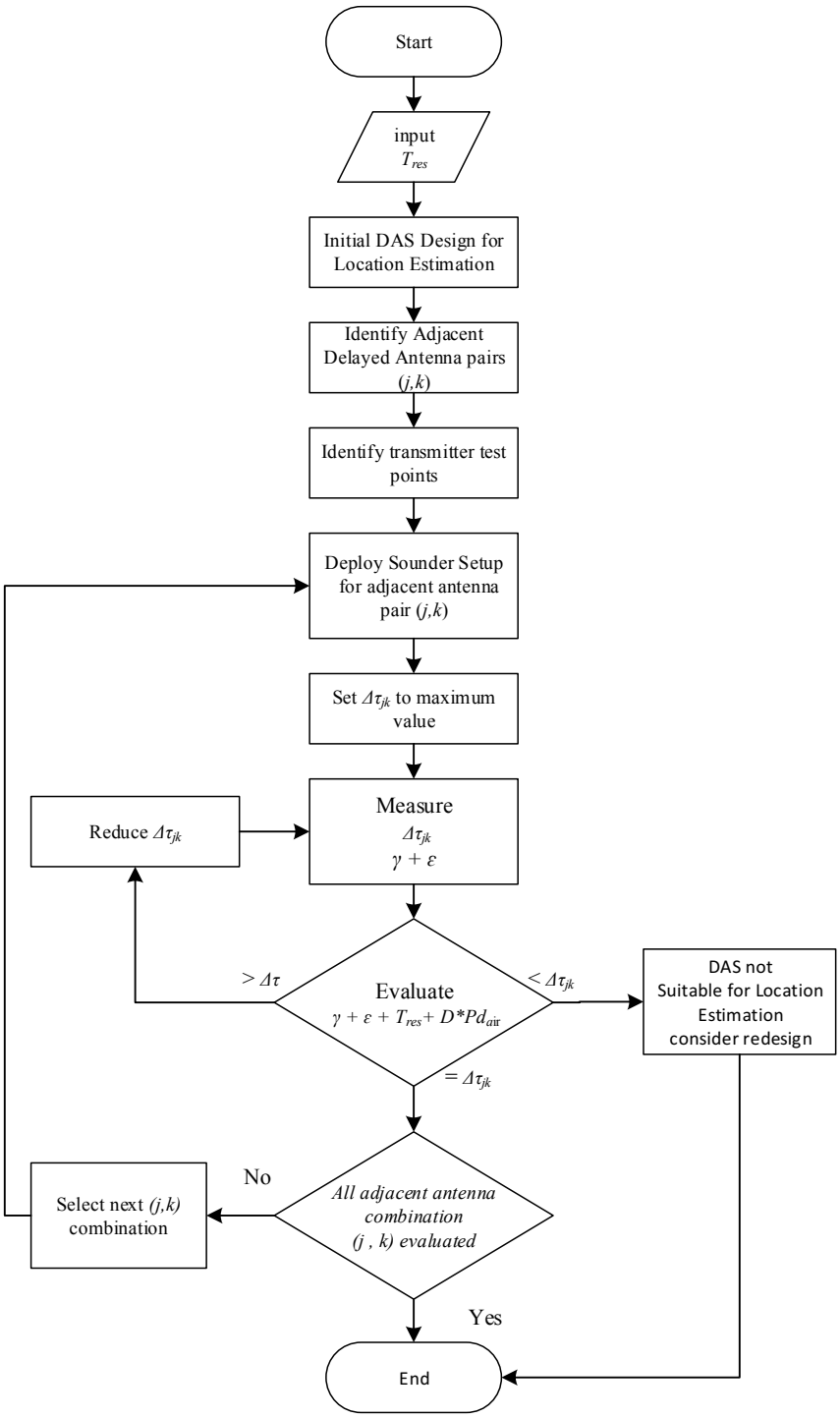

Figure 5-4 DAS delay Optimization Process

Chapter 6 Conclusion

6.1. Accomplishment and contribution

In this paper, the author demonstrated the effects of the DAS delays on indoor channel characteristics. A general DAS model and Delay map that can be used as a general DAS description convention was described to identify nodes, visualize and map delays for any DAS type. Additionally, the author introduced a Distributed Delay DAS design concept to optimize location estimation for indoor DAS deployment. The results of evaluations proved that indoor localization accuracy achieved mandated accuracy levels for indoors without the need of additional equipment. Moreover, the same holds true when utilizing RF fingerprinting by observation of DAS delays for Passive and active DAS. A new channel sounding procedure utilizing "distributed receiver antenna" was demonstrated to measure the collective delay profile of a given DAS design or deployment for all locations.

6.2. Future work

The research conducted in this paper should provide a basis for deeper researches on the following points.

- Improve indoor prediction tools to produce channel responses and estimating data performance with comparison to Channel Sounding and real deployments,
- Revisit indoor location positioning techniques with DAS utilizing ranging with Distributed Delay DAS designs and RF fingerprinting,
- Research the negative effects of DDDAS on channel performance to understand its limitations under channel equalization techniques,
- Deeper research of Telecom Vendors implementations of TOA techniques and ways to improve them to be able to accurately range Mobiles in a Distributed Delay DAS,
- Research innovative techniques to manipulate passive DAS delays.

6.3. Closing

This research is the focus of the author's vocational experience. Through the course of this study, I have learned that there is more to achieve in this particular field. It is the author's hope to uncover an area of research that might not be the state of art of scientific research but felt it is an important point that needs more attention to close the gap between Design, Prediction, implementation and optimization of an indoor site. A research point that needs a collaboration of BTS vendors and DAS manufacturers to achieve the highest accuracy in DAS predictions and benefit out of a DAS deployment.

Bibliography

[1] M. Tolstrup, *Indoor radio planning*. Chichester, U.K.: Wiley, 2011.

[2] 'Wireless E911 Location Accuracy Requirements, PS Docket 07-114, Second Report and Order, FCC 10-176, 25 FCC Rcd 18909 (2010).', 2015.

[3] H. Anderson, *Fixed broadband wireless system design*. Chichester, West Sussex, England: John Wiley & Sons, 2003.

[4] D. Ferreira and R. Caldeirinha, 'DEVELOPMENT AND PERFORMANCE ASSESSMENT OF A REAL TIME HIGH-RESOLUTION RF CHANNEL SOUNDER', *IGARSS*, 2011.

[5] D. Cox, 'Delay Doppler characteristics of multipath propagation at 910 MHz in a suburban mobile radio environment', *IEEE Transactions on Antennas and Propagation*, vol. 20, no. 5, pp. 625-635, 1972.

[6] D. Pu and A. Wyglinski, *Digital communication systems engineering with software-defined radio*. .

[7] S. Zekavat and R. Buehrer, *Handbook of position location*. .

[8] M. Pourkhaatoun and S. Zekavat, 'A REVIEW ON TOA ESTIMATION TECHNIQUES AND COMPARISON', 1st ed., S. Zekavat and R. Buehrer, Ed. 2014.

[9] N. Alsindi, X. Li and K. Pahlavan, 'Analysis of Time of Arrival Estimation Using Wideband Measurements of Indoor Radio Propagations', *IEEE Trans. Instrum. Meas.*, vol. 56, no. 5, pp. 1537-1545, 2007.

[10] N. Alsindi, Z. Chaloupka and J. Aweya, 'Entropy-based non-line of sight identification for wireless positioning systems', *2014 Ubiquitous Positioning Indoor Navigation and Location Based Service (UPINLBS)*, 2014.

[11] TELECOMMUNICATIONS INDUSTRY ASSOCIATION, 'Joint Standard J-STD-036-A. Enhanced Wireless 9-1-1 Phase 2', 2002.

[12] 'UMTS Requirements for support of radio resource management (FDD), 3GPP TS 25.133 rel 12 v(12.7.0)', 2015.

[13] J. Wennervirta and T. Wigren, 'RTT Positioning Field Performance', *IEEE Transactions on Vehicular Technology*, vol. 59, no. 7, pp. 3656-3661, 2010.

[14] 'Evolved Universal Terrestrial Radio Access (E-UTRA); Requirements for support of radio resource management (3GPP TS 36.133 version 12.7.0 Release 12)', 2015.

[15] National Public Safety Telecommunications Council (NPSTC) In- Building Working Group, 'Best Practices for In-Building Communications', 2007.

[16] M. Rumney, *LTE and the evolution to 4G wireless*. .

[17] K. Kaiser, *Transmission lines, matching, and crosstalk*. Boca Raton: Taylor & Francis, 2006.

[18] M. Islam, B. Kim, P. Henry and E. Rozner, 'A wireless channel sounding system for rapid propagation measurements', *2013 IEEE International Conference on Communications (ICC)*, 2013.

[19] M. Werner, *Indoor location-based services*. .

[20] A. Molisch, *Wireless communications*. Chichester, West Sussex, U.K.: Wiley, 2011.

[21] R. Pirkl and G. Durgin, 'Optimal Sliding Correlator Channel Sounder Design', *IEEE Transactions on Wireless Communications*, vol. 7, no. 9, pp. 3488-3497, 2008.

[22] K. Kitao, K. Saito, Y. Okano, T. Imai and J. Hagiwara, 'Basic study on spatio-temporal dynamic channel properties based on channel sounder measurements', *2009 Asia Pacific Microwave Conference*, 2009.
[23] J. Conrat, P. Pajusco and J. Thiriet, 'A Multibands Wideband Propagation Channel Sounder from 2 to 60 GHz', *2006 IEEE Instrumentation and Measurement Technology Conference Proceedings*, 2006.
[24] R. Pirkl and G. Durgin, 'How to build an optimal broadband channel sounder', *2007 IEEE Antennas and Propagation International Symposium*, 2007.
[25] C. R. Anderson, 'Design and Implementation of an Ultrabroadband Millimeter-Wavelength Vector Sliding Correlator Channel Sounder and In-Building Multipath Measurements at 2.5 & 60 GHz', 2015.
[26] A. Shahid, A. Ghafoor and M. Riaz, 'Wall Parameter Estimation Using Propagation Time Delay', *IET International Radar Conference 2013*, 2013.
[27] D. Demery, J. Parsons and A. Turkmani, 'Sounding techniques for wideband mobile radio channels: a review', *IEE Proc. I Commun. Speech Vis.*, vol. 138, no. 5, p. 437, 1991.
[28] 'USRP B210/B200 Datasheet', 2015. [Online]. Available: http://www.ettus.com/content/files/b200-b210_spec_sheet.pdf. [Accessed: 20- Aug- 2015].
[29] 'Interreach Fusion For Business Brochure', 2015. [Online]. Available: HTTP://WWW.TE.COM/CONTENT/DAM/TE-COM/DOCUMENTS/BROADBAND-NETWORK-SOLUTIONS/GLOBAL/DAS/BROCHURES/DAS-BROCHURE-INTERREACH-FUSION-320259AE.PDF. [Accessed: 20- Aug- 2015].
[30] Gnuradio.org, 2015. [Online]. Available: http://gnuradio.org/. [Accessed: 21- Aug- 2015].
[31] 'FlexWave Prism Brochure', 2015. [Online]. Available: http://www.te.com/content/dam/te-com/documents/broadband-network-solutions/global/das/brochures/das-brochure-flexwave-prism-106969ae.pdf. [Accessed: 22- Aug- 2015].
[32] Ibwave.com, 'In-Building Wireless Network Solutions | iBwave |', 2015. [Online]. Available: http://www.ibwave.com. [Accessed: 24- Aug- 2015].
[33] Consultix-egypt.com, 'Consultix |CW & WCDMA Test Transmitters', 2015. [Online]. Available: http://consultix-egypt.com/our-products/cw-wcdma-test-transmitters/. [Accessed: 01- Sep- 2015].
[34] Rohde-schwarz.com, 'R&S®FSH Handheld Spectrum Analyzer - Overview', 2015. [Online]. Available: https://www.rohde-schwarz.com/en/product/fsh-productstartpage_63493-8180.html. [Accessed: 01- Sep- 2015].

Appendix A **MATLAB codes**

two antenna in corridor

```
% simulates 2 antenna in a corridore or a tunnel. of Width =W length =L
% TxLoc is the TX location matrix.
% Rx Loc is the receiver locaiton matrix.
%
clear All
%% data input
TxCount=2;
W=3;
L=20;
TxLoc=[3 W/2 hT;17  W/2 hT];
hT=2.5; % transmiter hieght
hR=1; % receiver hieght
f=(2110e6:0.1e6:2170e6); %frequency of simulation
GroundLoss=-6; % ground reflection loss
WallLoss=-6; % wall reflection loss
PdAir=3.33564095198152; %propagation delay of Air
PdCable=PdAir/0.89; %propagation delay of cable connecting the two antenna
resolution= 1; % calculation step in meters
cableLength=0;% define cable length between two antnna
x=(0:resolution:L)';
offset=PdCable*cableLength; % 2nd antenna tranmsit offset based on cable delay
%y=(0:resolution:W)'; for one direction along Y=constant comment this line.
pwr=zeros(1,TxCount*4);%
%TxLoc=zeros(TxCount,3);
%%

%corridor images
image1 =[TxLoc(:,1) , -TxLoc(:,2) , TxLoc(:,3)];% mirror on Y axis ( side wall)
image2=[TxLoc(:,1) , TxLoc(:,2).*-1+2*W , TxLoc(:,3)];% mirror on Y=W axis (opposite side wall)
image3=[TxLoc(:,1) , TxLoc(:,2) , -TxLoc(:,3)];% mirror on z axis for ground reflection
images=[TxLoc;image1;image2;image3];% all images in one matrix
%% path length calculations along a direct line of points
% z is constant, y is constant, x is variable
RxLoc=zeros(length(x),3);
RxLoc(:,3)=hR;
RxLoc(:,2)=W/2; % middle of corridor
RxLoc(:,1)=x;


distance=zeros(length(images),length(RxLoc));
for k=1:length(RxLoc);
   for n=1:length(images); % n is the image or transmitter index
      distance(n,k)=sqrt((images(n,1)-RxLoc(k,1))^2+(images(n,2)-RxLoc(k,2))^2+(images(n,3)-RxLoc(k,3))^2);
   end
end
%% calculate air propagation delay
delays=distance.*PdAir;
minPath=(min(distance(:)));
relPower_dB=-20*log10(distance./minPath);% based on free air propagation path loss exponent of 2

%% wall losses calculations
[a  b]=size(TxLoc);
for k=1:a
relPower_dB(k+a,:)=relPower_dB(k+a,:)+WallLoss; %account for Wall loss
relPower_dB(k+2*a,:)=relPower_dB(k+2*a,:)+WallLoss; %account for Wall loss
relPower_dB(k+3*a,:)=relPower_dB(k+3*a,:)+GroundLoss;%account for ground loss
end
%% offset transmit delays of antenna
for k=1:4
delays(2*k,:)=delays(2*k,:)+offset;
end
relPower=10.^(relPower_dB/10);
%% Plot Frequency Responses and PDP for each point of RX loc
```

```
FreqResponse=zeros(length(RxLoc),length(f));
[c d]=size(images);
t=zeros(c,1);
a=zeros(c,1);

for k=1:length(RxLoc)
   for q=1:c;
         t(q)=delays(q,k);
         a(q)=relPower(q,k);
    end
   % frequency response is only ploted for 2 antenna with ground and side
   % wall reflections
   FreqResponse(k,:)=((abs(a(1)*exp(-2i*t(1)*pi.*f)+a(2)*exp(-2i*t(2)*pi.*f) ...
   +a(3)*exp(-2i*t(3)*pi.*f) ...
   +a(4)*exp(-2i*t(4)*pi.*f) ...
   +a(5)*exp(-2i*t(5)*pi.*f) ...
   +a(6)*exp(-2i*t(6)*pi.*f) ...
   +a(7)*exp(-2i*t(7)*pi.*f) ...
   +a(8)*exp(-2i*t(8)*pi.*f))).^2);
   % plot PDP and freq response figure
   figure
   subplot(2,1,1);
   plot(f,10*log10(FreqResponse(k,:)));
   xlabel('Frequency (Hz)')
   ylabel('Relative Power dBm')
   title('{\bf Theoretical Channel Frequency Response}')
   subplot(2,1,2);
   stem(delays(:,k),relPower(:,k),'MarkerSize',4,'Marker','^','LineWidth',3,'Color',[0 0 0]);% Real Power Delay
profile as
   xlabel('Time (ns)');
   ylabel('Relative Power');
   title('{\bf  PDP of the channel}');
end

%% plot 3D PDP
X=[x,x,x,x,x,x,x,x]';
figure
stem3(X,delays,relPower);
xlabel('X Position from start point  (m)');
ylabel('Path Delay from Tx to Rx (ns)');
zlabel('Power levels relative to Direct Path');
%% Plot 3D freq response and box plot
figure
FreqResponse_dB=10*log10(FreqResponse);
boxplot(FreqResponse_dB',x);
xlabel('X Position from start point  (m)');
ylabel('Power levels relative to Direct Path');
title('{\bf  Power Levels Statistics across channel spectrum}');
figure;
waterfall(f,x,FreqResponse_dB);
xlabel('frequency (Hz)');
ylabel('X Position from start point  (m)');
zlabel('Power levels relative to Direct Path');
title('{\bf  Channel Frequency Response}');

%% calculation of Moments and RMS delay
%allign delays matrix to calculate delay from first arrival.
[a b]=size(delays);
minDelay = min(delays,[],1);
for k=1:a
   excessDelays(k,:)=delays(k,:)-minDelay;
   end
firstMoment=sum((relPower.*excessDelays),1)./sum(relPower,1);
secondMoment=sum((relPower.*(excessDelays.^2)),1)./sum(relPower,1);
RMSdelaySpread2=sqrt(secondMoment-(firstMoment).^2);
figure
plot(x,RMSdelaySpread2)
```

```
xlabel('X Position from start point  (m)');
ylabel('RMS delay spread (ns)');
```

four antenna in an open room with reflections

```
%calculatesPDP along a test path from 4 antenna located in TxLoc.
%test path defined in RxLoc
clear all
%% Data Input
TxCount=4;
timeOffset=[0;260;260*2;260*3];% time offset of antenna tansmission
W=40;
L=40;
TxLoc=[L/4 W/4 2.5;(3*L/4) W/4 2.5;(3*L/4) (3*W/4) 2.5;L/4 (3*W/4) 2.5];
hT=2.5; % transmiter hieght
hR=1.5; % receiver hieght
f=(2110e6:0.01e6:2170e6);%frequency of simulation
PdAir=3.33564095198152;%propagation delay of Air
PdCable=PdAir/0.89; %propagation delay of cable connecting the two antenna
GroundLoss=-6; % ground bounce loss
WallLoss=-6; % wall reflection loss

resolution= 2; % calculation step in meters
x=(0:resolution:L)';
pwr=zeros(1,TxCount*6);

%% corridor images location calculation
image1 =[TxLoc(:,1) , -TxLoc(:,2) , TxLoc(:,3)];% mirror on Y axis ( side wall)
image2=[TxLoc(:,1) , TxLoc(:,2).*-1+2*W , TxLoc(:,3)];% mirror on Y=W axis (opposite side wall)
image3=[TxLoc(:,1) , TxLoc(:,2) , -TxLoc(:,3)];% mirror on z axis for ground reflection
image4=[-TxLoc(:,1) , TxLoc(:,2) , TxLoc(:,3)];% mirror on X axis ( side wall)
image5=[TxLoc(:,1).*-1+2*L , TxLoc(:,2) , TxLoc(:,3)];% mirror on X=L axis ( side wall)
images=[TxLoc;image1;image2;image3;image4;image5];% all images in one matrix

%% path length calculations along a direct line of points
% z is constant, y is constant, x is variable
RxLoc=zeros(length(x),3);
RxLoc(:,3)=hR;
RxLoc(:,2)=W/2; % middle of corridor
RxLoc(:,1)=x;

distance=zeros(length(images),length(RxLoc));
for k=1:length(RxLoc);
   for n=1:length(images); % n is the image or transmitter index
      distance(n,k)=sqrt((images(n,1)-RxLoc(k,1))^2+(images(n,2)-RxLoc(k,2))^2+(images(n,3)-RxLoc(k,3))^2);
   end
end
%% calculate air propagation delay
delays=distance.*PdAir;
minPath=(min(distance(:)));
relPower_dB=-20*log10(distance./minPath);% based on free air propagation path loss exponent of 2
%% offset transmit delays of antenna
offset=[timeOffset;timeOffset;timeOffset;timeOffset;timeOffset;timeOffset];
for k=1:length(x)
delays(:,k)=delays(:,k)+offset;
end

%% wall losses calculations
[a  b]=size(TxLoc);
for k=1:a
relPower_dB(k+a,:)=relPower_dB(k+a,:)+WallLoss; %account for Wall loss
relPower_dB(k+2*a,:)=relPower_dB(k+2*a,:)+WallLoss; %account for Wall loss
relPower_dB(k+3*a,:)=relPower_dB(k+3*a,:)+GroundLoss;%account for ground loss
relPower_dB(k+4*a,:)=relPower_dB(k+4*a,:)+WallLoss;%account for ground loss
relPower_dB(k+5*a,:)=relPower_dB(k+5*a,:)+WallLoss;%account for ground loss
end
relPower=10.^(relPower_dB/10);
FreqResponse=zeros(length(RxLoc),length(f));
[c d]=size(images);
t=zeros(c,1);
a=zeros(c,1);
```

```
%% Plot Frequency Responses and PDP for each point of RX loc
for k=1:length(RxLoc)
    for q=1:c;
        t(q)=delays(q,k);
        a(q)=relPower(q,k);
    end
    FreqResponse(k,:)=((abs(a(1)*exp(-2i*t(1)*pi.*f)+a(2)*exp(-2i*t(2)*pi.*f) ...
    +a(3)*exp(-2i*t(3)*pi.*f) ...
    +a(4)*exp(-2i*t(4)*pi.*f) ...
    +a(5)*exp(-2i*t(5)*pi.*f) ...
    +a(6)*exp(-2i*t(6)*pi.*f) ...
    +a(7)*exp(-2i*t(7)*pi.*f) ...
    +a(8)*exp(-2i*t(8)*pi.*f) ...
    +a(9)*exp(-2i*t(9)*pi.*f) ...
    +a(10)*exp(-2i*t(10)*pi.*f) ...
    +a(11)*exp(-2i*t(11)*pi.*f) ...
    +a(12)*exp(-2i*t(12)*pi.*f) ...
    +a(13)*exp(-2i*t(13)*pi.*f) ...
    +a(14)*exp(-2i*t(14)*pi.*f) ...
    +a(15)*exp(-2i*t(15)*pi.*f) ...
    +a(16)*exp(-2i*t(16)*pi.*f) ...
    +a(17)*exp(-2i*t(17)*pi.*f) ...
    +a(18)*exp(-2i*t(18)*pi.*f) ...
    +a(19)*exp(-2i*t(19)*pi.*f) ...
    +a(20)*exp(-2i*t(20)*pi.*f) ...
    +a(21)*exp(-2i*t(21)*pi.*f) ...
    +a(22)*exp(-2i*t(22)*pi.*f) ...
    +a(23)*exp(-2i*t(23)*pi.*f) ...
    +a(24)*exp(-2i*t(24)*pi.*f))).^2);

    figure
    subplot(2,1,1);
    plot(f,10*log10(FreqResponse(k,:)));
    xlabel('Frequency (Hz)')
    ylabel('Relative Power dBm')
    title('{\bf Theoretical Channel Frequency Response}')
    grid on;grid minor;
    subplot(2,1,2);
    stem(delays(:,k),relPower(:,k),'MarkerSize',4,'Marker','^','LineWidth',3,'Color',[0 0 0]);% Real Power Delay
profile as
    grid on;grid minor;
    xlabel('Time (ns)');
    ylabel('Relative Power');
    title('{\bf  PDP of the channel}');
end
%% plot 3D PDP
X=[x,x,x,x,x,x,x,x,x,x,x,x,x,x,x,x,x,x,x,x,x,x,x,x,x]';
X1 = [x,x,x,x]';, X2 = X1;X3=X1; X4=X1;X5=X1;X6=X1;
delay1=delays(1:4,:); delay2=delays(5:8,:);
delay3=delays(9:12,:);delay4=delays(13:16,:);
delay5=delays(17:20,:);delay6=delays(21:24,:);
relPower1=relPower(1:4,:); relPower2=relPower(5:8,:);
relPower3=relPower(9:12,:);relPower4=relPower(13:16,:);
relPower5=relPower(17:20,:);relPower6=relPower(21:24,:);
figure
stem3(X1,delay1,relPower1);
xlabel('X Position from start point  (m)');
ylabel('Path Delay from Tx to Rx (ns)');
zlabel('Power levels relative to Direct Path');
grid on;grid minor;
%% Plot 3D freq response and box plot
figure
stem3(X,delays,relPower);
xlabel('X Position from start point  (m)');
ylabel('Path Delay from Tx to Rx (ns)');
zlabel('Power levels relative to Direct Path');
grid on;grid minor;
figure
```

```
FreqResponse_dB=10*log10(FreqResponse);
boxplot(FreqResponse_dB',x);
xlabel('X Position from start point  (m)');
ylabel('Power levels relative to Direct Path');
title('{\bf  Power Levels Statistics across channel spectrum}');
grid on;grid minor;
figure;
waterfall(f,x,FreqResponse_dB);
xlabel('frequency (Hz)');
ylabel('X Position from start point  (m)');
zlabel('Power levels relative to Direct Path');
title('{\bf  Channel Frequency Response}');
grid on;grid minor;

%% calculation of Moments and RMS delay

[a b]=size(delays);
minDelay = min(delays,[],1);
for k=1:a
   excessDelays(k,:)=delays(k,:)-minDelay;
   end
firstMoment=sum((relPower.*excessDelays),1)./sum(relPower,1);
secondMoment=sum((relPower.*(excessDelays.^2)),1)./sum(relPower,1);
RMSdelaySpread2=sqrt(secondMoment-(firstMoment).^2);
figure
plot(x,RMSdelaySpread2)
xlabel('X Position from start point  (m)');
ylabel('RMS delay spread (ns)');
grid on;grid minor;
```

four antenna in an open area with Direct Path only in 2D

```
% calculates PDP along a test path from 4 antenna located in TxLoc.
% test path defined in RxLoc. for 2D simulations multiple test pathes are
% used but will generate large output data
clear all

%% Data Input
TxCount=4;
W=50;
L=50;
hT=2.5; % transmiter hieght
hR=1.5; % receiver hieght
TxLoc=[0 0 hT;L 0 hT;L W hT;0 W hT];
f=(2110:0.1:2170)*1e6;%frequency of simulation in MHz
PdAir=3.33564095198152;%propagation delay of Air
PdCable=PdAir/0.89; %propagation delay of cable connecting the two antenna
resolution=0.5; % calculation step in meters
x=(0:resolution:L)';
pwr=zeros(1,TxCount);
%timeOffset=[0;0;0;0]
timeOffset=[25*PdCable;75*PdCable;75*PdCable;25*PdCable];% time offset of antenna tansmission
images=TxLoc;% all images in one matrix
Y=6; % number of test pathes along the X direction.
for y=0:Y
%% path length calculations along a direct line of points
% z is constant, y is constant, x is variable
RxLoc=zeros(length(x),3);
RxLoc(:,3)=hR;
RxLoc(:,2)=y*W/Y;
RxLoc(:,1)=x;

distance=zeros(length(images),length(RxLoc));
for k=1:length(RxLoc);
   for n=1:length(images); % n is the image or transmitter index
      distance(n,k)=sqrt((images(n,1)-RxLoc(k,1))^2+(images(n,2)-RxLoc(k,2))^2+(images(n,3)-RxLoc(k,3))^2);
   end
end
%% calculate air propagation delay
delays=distance.*PdAir;
minPath=(min(distance(:)));% returns the minimum path between any antenna and the receiver at all locations. this will
be the reference of calculation relative power
relPower_dB=-20*log10(distance./minPath);% based on free air propagation path loss exponent of 2
%% offset transmit delays of antenna
offset=timeOffset;
for k=1:length(x)
delays(:,k)=delays(:,k)+offset;
end

%% rel power calculation
relPower=10.^(relPower_dB/10);
FreqResponse=zeros(length(RxLoc),length(f));
[c d]=size(images);
t=zeros(c,1);
a=zeros(c,1);
%% Plot Frequency Responses and PDP for each point of RX loc
for k=1:length(RxLoc)
   for q=1:c;
      t(q)=1e-9*delays(q,k);
      a(q)=relPower(q,k);
   end
   FreqResponse(k,:)=((abs(a(1)*exp(-2i*t(1)*pi.*f)+a(2)*exp(-2i*t(2)*pi.*f) ...
   +a(3)*exp(-2i*t(3)*pi.*f))).^2);

end
%% plot 3D PDP and box plots
X=[x,x,x,x]';
% 3D pdp Plot only direct rays
figure
stem3(X,delays,relPower);
xlabel('X Position from start point  (m)');
ylabel('Path Delay from Tx to Rx (ns)');
zlabel('Power levels relative to Direct Path');
```

```
grid on;grid minor;

%% Plot 3D freq response and box plot
FreqResponse_dB=10*log10(FreqResponse);
% plot boxplot
figure
boxplot(FreqResponse_dB',x);
xlabel('X Position from start point  (m)');
ylabel('Power levels relative to Direct Path');
title('{\bf  Power Levels Statistics across channel spectrum}');
grid on;grid minor;
% plot mesh frequency response
figure1 = figure;
colormap('winter');
% Create axes
axes1 = axes('Parent',figure1);
view(axes1,[145.5 58]);
grid(axes1,'on');
hold(axes1,'on');
% Create mesh
mesh(f,x,FreqResponse_dB,'Parent',axes1,'Marker','.','LineStyle',':');
% Create colorbar
colorbar('peer',axes1);
xlabel('frequency (Hz)');
ylabel('X Position from start point  (m)');
zlabel('Power levels relative to Direct Path');
title('{\bf  Channel Frequency Response}');
grid on;grid minor;

%% calculation of Moments and RMS delay
[a b]=size(delays);
minDelay = min(delays,[],1);
for k=1:a
   excessDelays(k,:)=delays(k,:)-minDelay;
   end
firstMoment=sum((relPower.*excessDelays),1)./sum(relPower,1);
secondMoment=sum((relPower.*(excessDelays.^2)),1)./sum(relPower,1);
RMSdelaySpread2=sqrt(secondMoment-(firstMoment).^2);
figure
subplot(2,1,1);
plot(x,RMSdelaySpread2)
xlabel('X Position from start point  (m)');
ylabel('RMS delay spread (ns)');
grid on;grid minor;
subplot(2,1,2);
plot(x,200./(RMSdelaySpread2))
xlabel('X Position from start point  (m)');
ylabel('Coherence BandWidth (MHz)');
grid on;grid minor;
end
```

```
% This program generates maximal lenght PN sequences according to
% 'GenPoly' add multiple delayed versions of the signal to simulate
% multipath environment as seen by a sliding correlator channel sounder
% chip rate not necessarly the sample rate.
% upsampling will multiply the impulse respone by
% sync function and will cause unneeded effect in DFFT results
% for sampling rate equal to chip rate the resolution of delay reading is
% multiples of the sampling time ts. errors corresponding to this
% sampling error will cause errors in defining the impulse response of
% the channel compared to the time domain method.

% input frequency range , sampling rate,
% if power delay profile is known enter delays and power in dBm at
% receive(5-tabs pdp)

% point. otherwise uncomment the random generated delay and power code line
%% Generate pn Sequence matrix sampled at K samples per chip
% input is the polynomial type to pn1
h = commsrc.pn('GenPoly' , [9 5 0], ...% generates PN seq from plonomial
'initialstates', [0 0 0 0 0 0 0 0 1], ...
'CurrentStates', [0 0 0 0 0 0 0 0 1], ...
'NumBitsOut', 511);
h.reset
set(h, 'NumBitsOut', 511);
pn0=h.generate;     % first PN sequence
pn0=2*(pn0-0.5);    % pn sequence in bipolar form
K=1;                        % number of samples per chip upsampling
L=5;                        % number of multipath components used for random generation of multipath
HWSampleRate=32e6; % maximum sustanable hardware sampling rate of USRP connected to a PC through a
USB3 port
ts=1/HWSampleRate;
pn=upsample(pn0,K); %generate an upsampled version of the pn code
for n=1:K-1% upsampling the pn code.
    pn=pn+upsample(pn0,K,n);
end
Chiprate=HWSampleRate/K;
Tchip=1/Chiprate;
pn0=pn;
%% Data input
f=(2110e6:0.05e6:2170e6);% Frequency simulation range
N=length(pn0);
% comment for random generation of delay and power
%AntennaTransmitDelay=   [100,300,320,100,0];  % in (ns) delay caused by stage-1 and upwards
%PathDelay=          [0,0,0,0,0]; %(ns) if known and estimated manually
%PowerIndB=              [-45.39,-46.94,-54.98,-43.3,-100000];% measuered Rx power.
%amp= sqrt(0.001*50.*(10.^(PowerIndB./10)));% power to volt
%DelayInTime =   PathDelay + AntennaTransmitDelay;

DelayInTime=random('unid',N,1,L); % uncomment to generate random unifor delays, can be changed widh
different pd
DelayInChips=   round((1e-9*DelayInTime)/ts);

amp=random('unif',0,1,1,L); %uncomment to generate random power levels
amp=amp./max(amp);

pn=zeros(N,L);
for m=1:L
    pn(1:N,m)=amp(m).*circshift(pn0,DelayInChips(m)); % generate the multipath version of Rx PN sequence
end
 %% Normalize the amplitude
Rx=zeros(N,1);
for m=1:L
    Rx=pn(1:N,m)+Rx;
end
Rx=Rx./(max(Rx));% normalize
%% DFT
fs = HWSampleRate;  %
```

```
t = 0:1/fs:((length(Rx)-1)/fs);
N = length(Rx);         % Window length
y = fft(Rx);
y= fftshift(y);
f1 = (-N/2:N/2-1)*(fs/N);
%f = (0:N-1)*(fs/N);    % Frequency range
power =10*log10( y.*conj(y)/N);   % Power of the DFT
figure;
plot(f1,power)
xlabel('Frequency (Hz)')
ylabel('Power in dBm')
title('{\bf Frequency Response}')

%% cross Correlation
c=xcorr(Rx,pn0);
% reformat the result to reflect the dealy values of a
s1 =c(1:N-1);
s1=[0;s1];
s2=c(N:end);
s3=s1+s2;
Y0=s3/max(s3);%normalize power delay profile as should be detected by CH sounder
figure;
stem (t,Y0,'MarkerSize',1,'Marker','diamond','LineWidth',2,'Color',[0 0 0]);
xlabel('Time (Second)');
ylabel('Relative Amplitude');
title('{\bf  PDP of the channel}');
figure;
stem(DelayInTime,amp.^2,'MarkerSize',4,'Marker','^','LineWidth',3,'Color',[0 0 0]);% Real Power Delay profile as
xlabel('Time (ns)');
ylabel('Relative Power');
title('{\bf  PDP of the channel}');
%% plot channel in time domain

t1=1e-9*DelayInTime(1);t2=1e-9*DelayInTime(2);
t3=1e-9*DelayInTime(3);t4=1e-9*DelayInTime(4);
t5=1e-9*DelayInTime(5);
tErr1=ts*DelayInChips(1);tErr2=ts*DelayInChips(2);
tErr3=ts*DelayInChips(3);tErr4=ts*DelayInChips(4);
tErr5=ts*DelayInChips(5);
a1=amp(1);a2=amp(2);
a3=amp(3);a4=amp(4);
a5=amp(5);
FreqResponse1=(abs(a1*exp(-2i*t1*pi.*f)+a2*exp(-2i*t2*pi.*f)+a3*exp(-2i*t3*pi.*f)+a4*exp(-
2i*t4*pi.*f)+a5*exp(-2i*t5*pi.*f))).^2;
FreqResponse2=(abs(a1*exp(-2i*tErr1*pi.*f)+a2*exp(-2i*tErr2*pi.*f)+a3*exp(-2i*tErr3*pi.*f)+a4*exp(-
2i*tErr4*pi.*f)+a5*exp(-2i*tErr5*pi.*f))).^2;

figure
subplot(2,1,1);
plot(f,10*log10(FreqResponse1));
xlabel('Frequency (Hz)')
ylabel('Relative Power dBm')
title('{\bf Theoretical Channel Frequency Response}')
subplot(2,1,2);
plot(f,10*log10(FreqResponse2));
xlabel('Frequency (Hz)')
ylabel('Relative Power dBm')
title('{\bf Estimated Channel Frequency Response using Channel Sounder information}')
%% calculate RMS delay spread
minDelay = min(DelayInTime,[],2);
excessDelays=DelayInTime-minDelay;
relPower=amp.^2;
firstMoment=sum((relPower.*excessDelays),2)./sum(relPower,2);
secondMoment=sum((relPower.*(excessDelays.^2)),2)./sum(relPower,2);
RMSdelaySpread1=sqrt(secondMoment-(firstMoment).^2)
```

Appendix B **LFSR generating polynomial**

GNU-Radio's implementation of Maximal length Linear Feedback Shift register sequence

			Maximum Path Delay (ns)			
# of bits	Feed Back Polynomial		Fs=3.84	Fs=10MHz	Fs=16MHz	Fs=38MHz
		1	260.4	100	62.5	26.3
2	$x^2 + x + 1$	3	781.3	300	187.5	78.9
3	$x^3 + x^2 + 1$	7	1822.9	700	437.5	184.2
4	$x^4 + x^3 + 1$	15	3906.3	1500	937.5	394.7
5	$x^5 + x^3 + 1$	31	8072.9	3100	1937.5	815.8
6	$x^6 + x^5 + 1$	63	16406.3	6300	3937.5	1657.9
7	$x^7 + x^6 + 1$	127	33072.9	12700	7937.5	3342.1
8	$x^8 + x^6 + x^5 + x^4 + 1$	255	66406.3	25500	15937.5	6710.5
9	$x^9 + x^5 + 1$	511	133072.9	51100	31937.5	13447.4
10	$x^{10} + x^7 + 1$	1023	266406.3	102300	63937.5	26921.0

Table B-1 maximal length LFSR Generating Polynomial

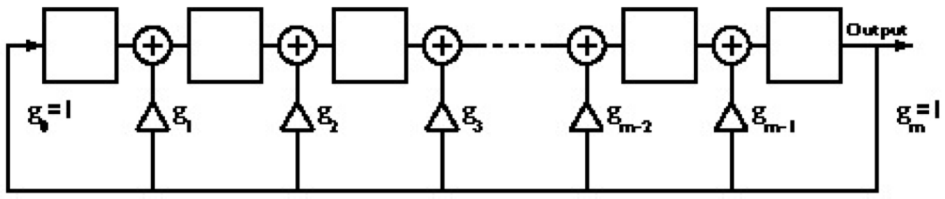

Figure B-1 Galois Implementation of LFSR used in GNU-Radio

Appendix C **IBwave Simulations**

Comment on Soft Hand-Off simulations: Soft Hand-Off simulation are used to indicate the antenna coverage overlap within the same sector. The soft handoff is intended, originally, to predict overlap between different sectors. However, with the assignment of a different RF sector to each antenna in the simulation we can use it to predict overlap within the same sector

Figure C-1 Typical floor layout of Hi-Rise Hotel

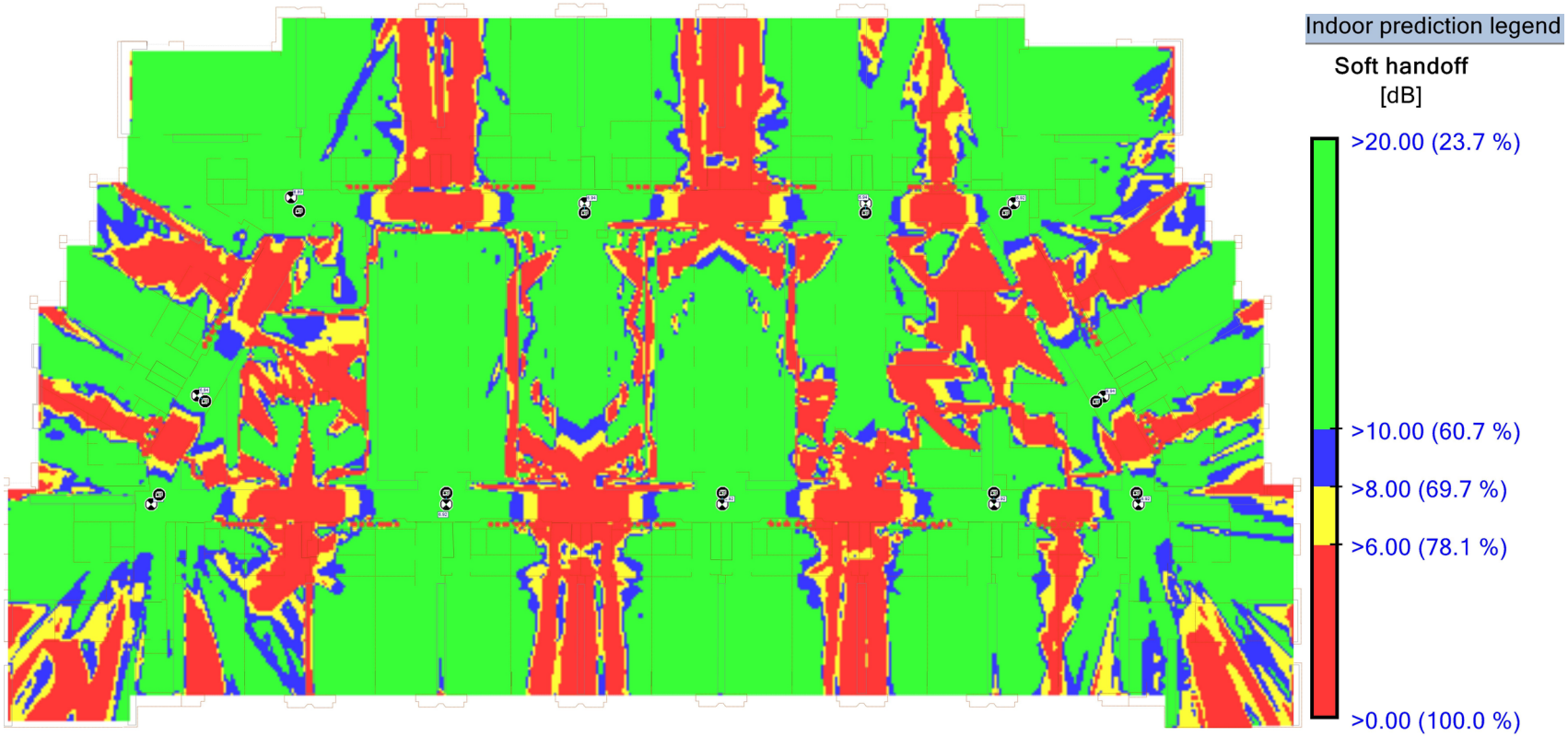

Figure C-2 Soft Hand-Off Simulation (11-Antenna Design)

Figure C-3 Service Count Simulation (11-Antenna Design)

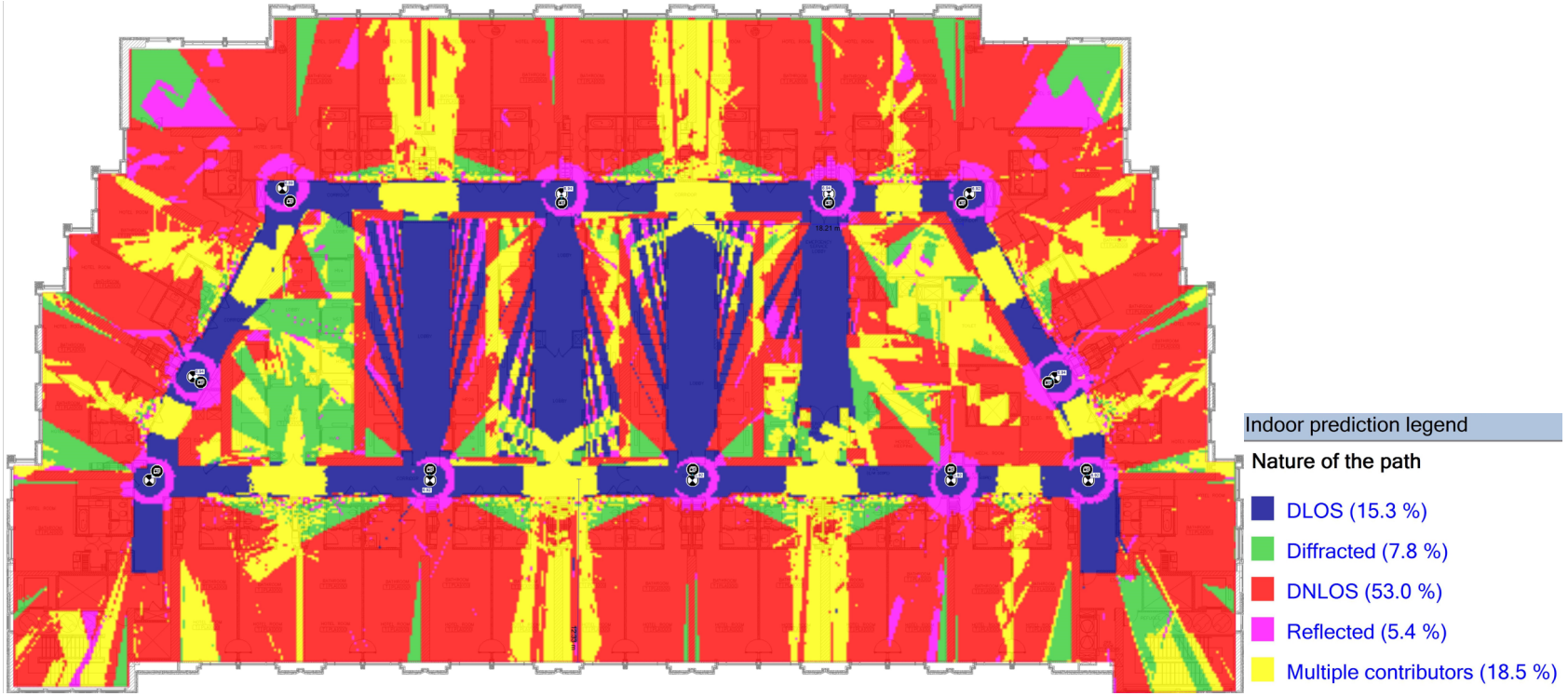

Figure C-4 Nature of Path Simulation (11-Antenna Design)

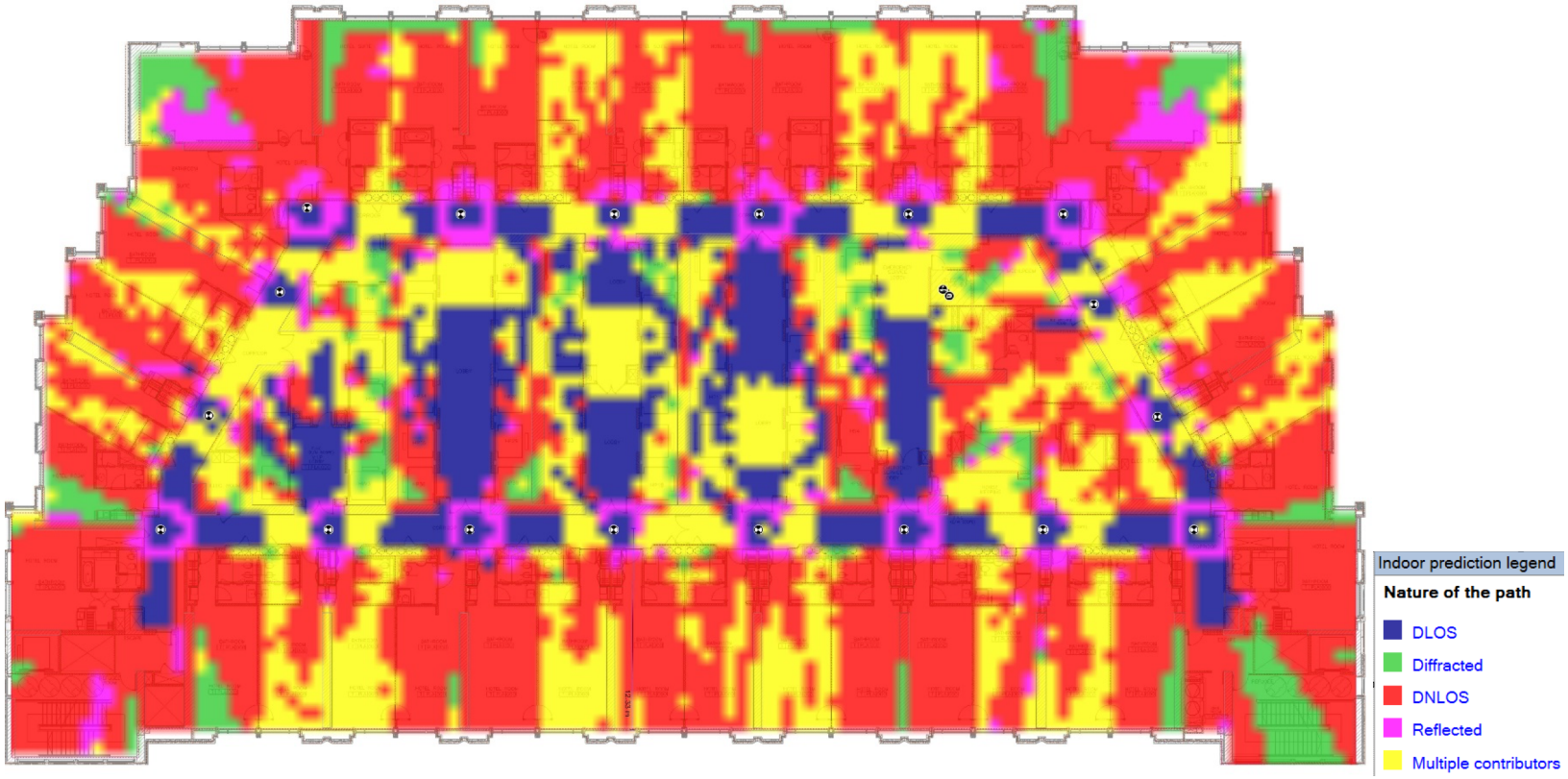

Figure C-5 Nature of Path Simulation (22-Antenna Design)

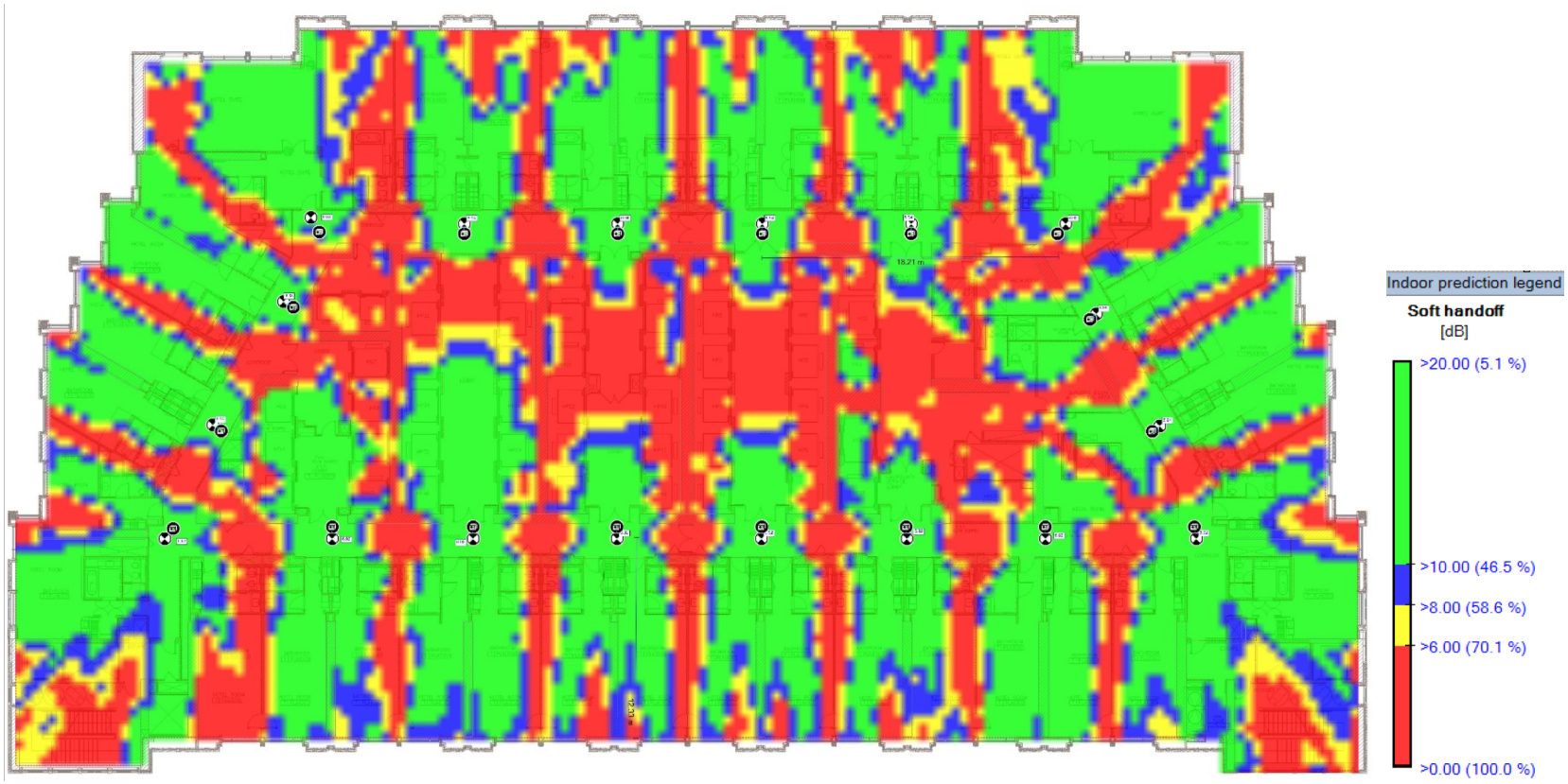

Figure C-6 Soft Hand-Off Simulation (22-Antenna Design)

Appendix D **2-Ray Dispersive Fading Null Charts**

2-Ray Dispersive Nulls Charts against Relative Delay at Rx location can be used as a quick way to identify the result of a specific DAS deployment. The Time axis can be replaced with the equivalent cable length difference feeding the 2 antenna in Simulcast.

A vertical line intercepts the curves at the exact location of dispersive fading nulls of the frequency response of the channel.

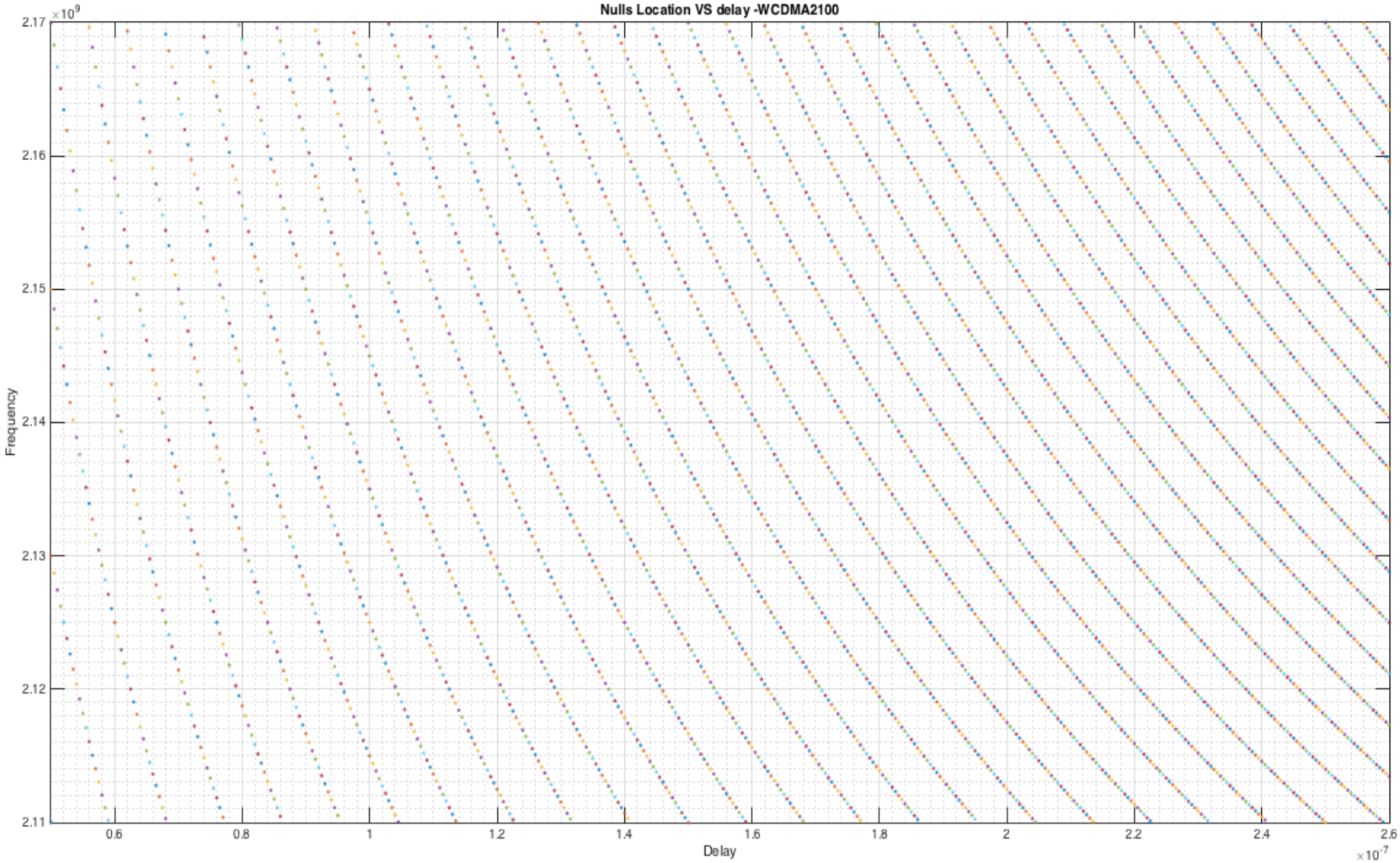

Figure D-1 Dispersive fading nulls for 2100MHz Ban

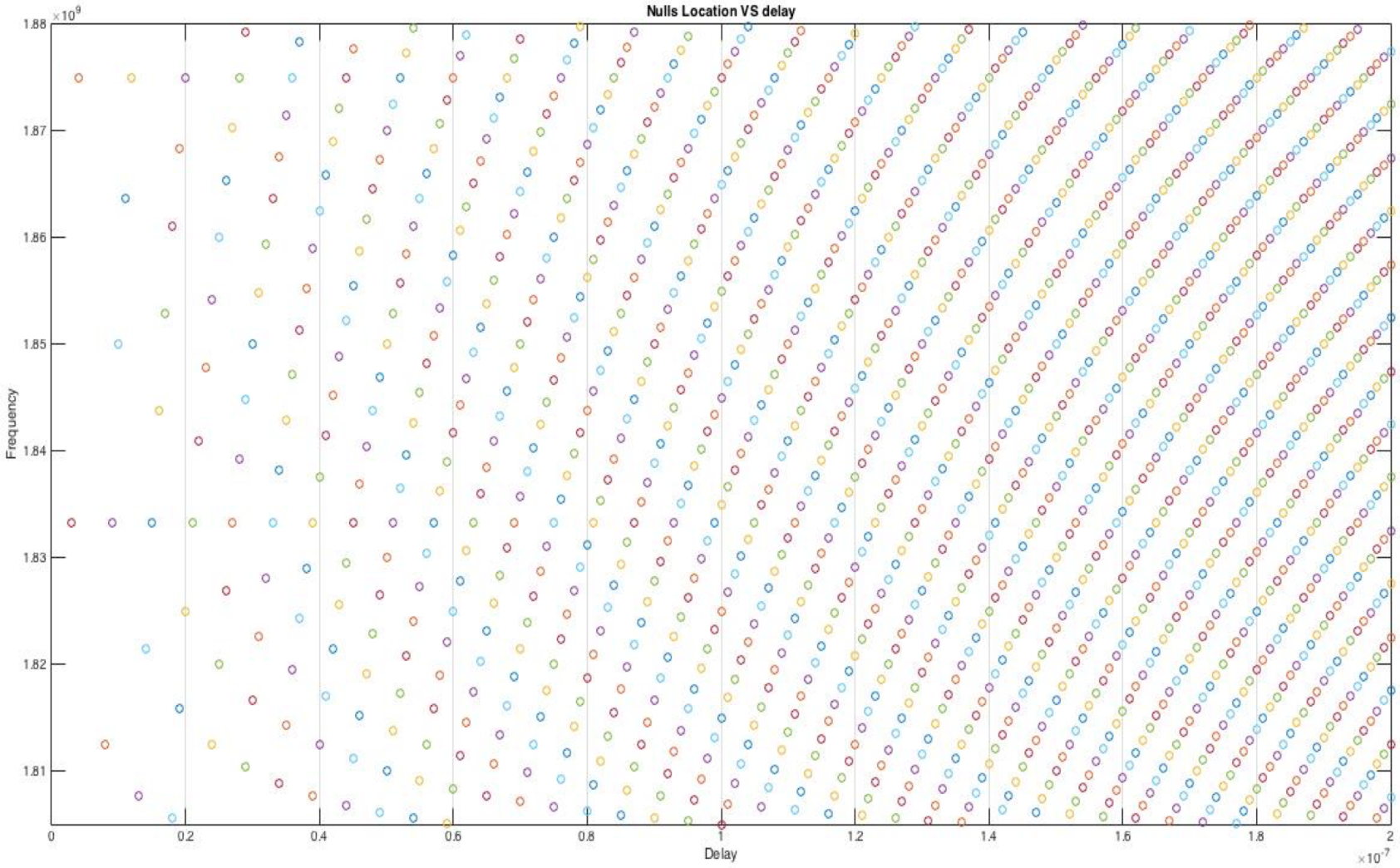

Figure D-2 Dispersive fading nulls for 1800MHz Band

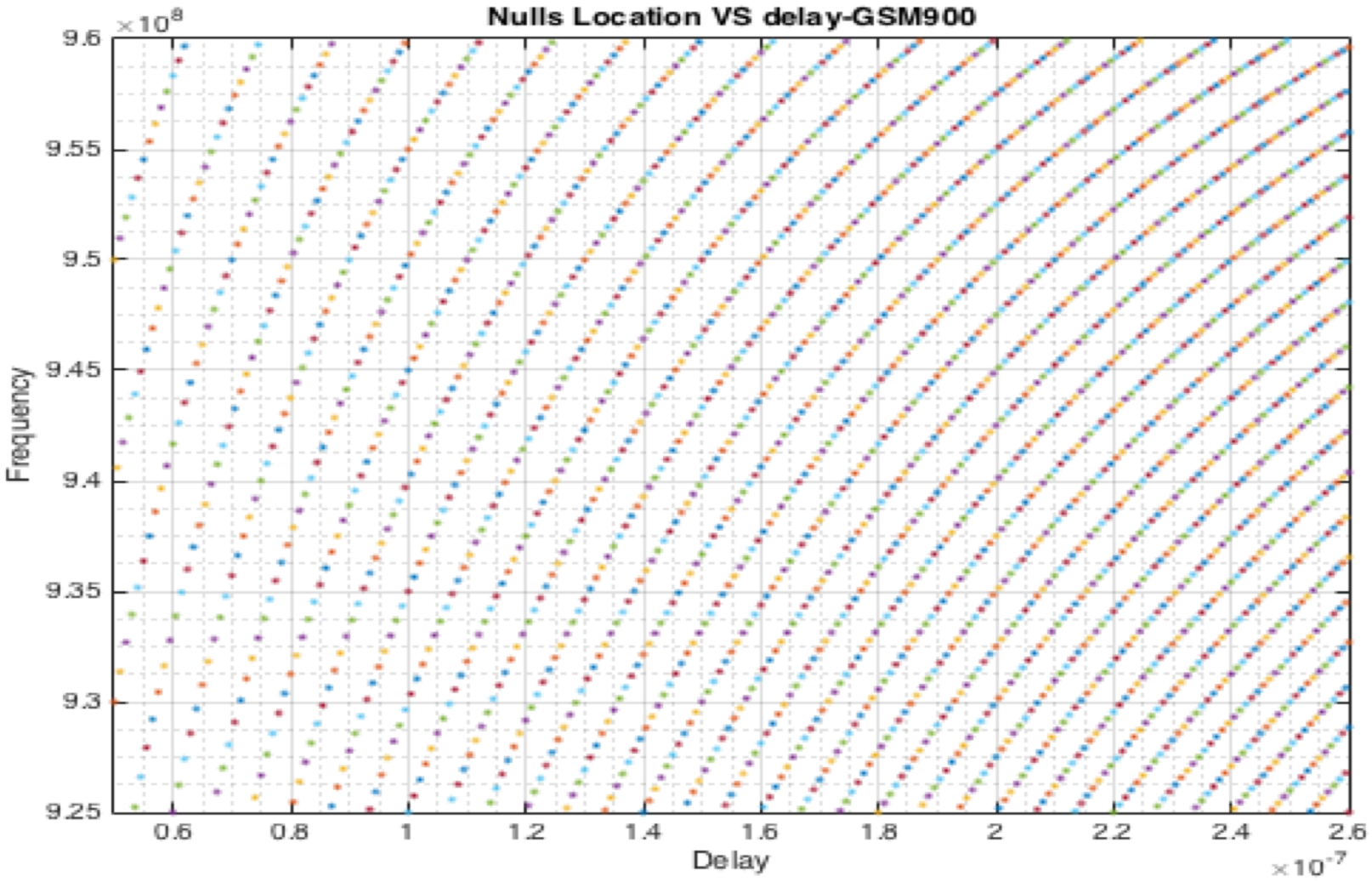

Figure D-3 Dispersive fading nulls for 900MHz Band

Appendix E **Simulations and Measurement**

E.1. Tunnel Delay Measurement details.

Delay Measurement was done using a WCDMA pilot scanning receiver from PCtel with a GPS option to estimate CPICH chip delay. A PC with Nemo Outdoor 4 software package (from Anite.com) was used to plot and interpret the results. The scanning receiver was connected to vehicle mounted antenna with a gain value approximately equal to the cable loss. The drive test was conducted four times (two in each direction) times with vehicle speed fixed at 40km/h producing consistent results of Delay Spread and CPICH delay

E.2. Simulcast Channel Test-Bench

The general configuration of the test bench is shown in Figure E-1 Simulcast Channel Test-Bench Setup. A 3-way or a 2-way splitter and combiner are used for the corresponding 3-antenna and 2-antenna cases. Variable attenuators are used to balance the signal power at the receiver port. Once the signal is balanced a frequency sweep is generated and plotted on a spectrum analyzer. The results are then post processed to read the null separation values and calculate the time delay difference and cable length. Alternatively a wideband signal can be generated with the SDR board instead of sweeping the transmitter frequency.

Additionally, with the WCDMA pilot signal generator [33], the CPICH is transmitted and the digital demodulator option of the spectrum analyzer [34] is used to measure the Error Victor Magnitude (EVM) of the received signal.

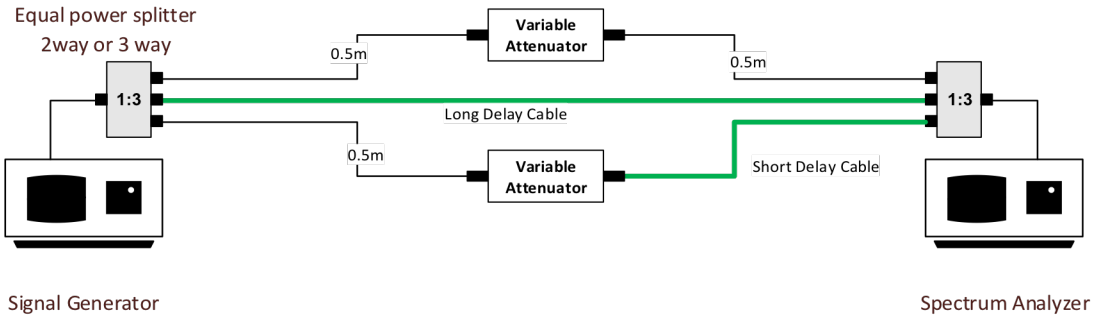

Figure E-1 Simulcast Channel Test-Bench Setup